

# 000 001 002 003 004 005 006 007 008 009 010 011 012 013 014 015 016 017 018 019 020 021 022 023 024 025 026 027 028 029 030 031 032 033 034 035 036 037 038 039 040 041 042 043 044 045 046 047 048 049 050 051 052 053 COMPLEXITY ANALYSIS OF NORMALIZING CONSTANT ESTIMATION: FROM JARZYNSKI EQUALITY TO AN- NEALED IMPORTANCE SAMPLING AND BEYOND

Anonymous authors

Paper under double-blind review

## ABSTRACT

Given an unnormalized probability density  $\pi \propto e^{-V}$ , estimating its normalizing constant  $Z = \int_{\mathbb{R}^d} e^{-V(x)} dx$  or free energy  $F = -\log Z$  is a crucial problem in Bayesian statistics, statistical mechanics, and machine learning. It is challenging especially in high dimensions or when  $\pi$  is multimodal. To mitigate the high variance of conventional importance sampling estimators, annealing-based methods such as Jarzynski equality and annealed importance sampling are commonly adopted, yet their quantitative complexity guarantees remain largely unexplored. We take a first step toward a non-asymptotic analysis of annealed importance sampling. In particular, we derive an oracle complexity of  $\tilde{O}(d\beta^2 \mathcal{A}^2/\varepsilon^4)$  for estimating  $Z$  within  $\varepsilon$  relative error with high probability, where  $\beta$  is the smoothness of  $V$  and  $\mathcal{A}$  denotes the action of a curve of probability measures interpolating  $\pi$  and a tractable reference distribution. Our analysis, leveraging Girsanov's theorem and optimal transport, does not explicitly require isoperimetric assumptions on the target distribution. Finally, to tackle the large action of the widely used geometric interpolation, we propose a new algorithm based on reverse diffusion samplers, establish a framework for analyzing its complexity, and empirically demonstrate its efficiency in tackling multimodality.

## 1 INTRODUCTION

We study the problem of estimating the normalizing constant  $Z = \int_{\mathbb{R}^d} \hat{\pi}(x) dx$  of an unnormalized probability density function (p.d.f.)  $\pi \propto \hat{\pi} := e^{-V}$  on  $\mathbb{R}^d$ , so that  $\pi(x) = \hat{\pi}(x)/Z$ . The normalizing constant appears in various fields: in Bayesian statistics, when  $\hat{\pi}$  is the product of likelihood and prior,  $Z$  is also referred to as the marginal likelihood or evidence (Gelman et al., 2013); in statistical mechanics, when  $V$  is the Hamiltonian,<sup>1</sup>  $Z$  is known as the partition function, and  $F := -\log Z$  is called the free energy (Chipot & Pohorille, 2007; Lelièvre et al., 2010; Pohorille et al., 2010). The task of normalizing constant estimation has numerous applications, including computing log-likelihoods in probabilistic models (Sohl-Dickstein & Culpepper, 2012), estimating free energy differences (Lelièvre et al., 2010), and training energy-based models in generative modeling (Song & Kingma, 2021; Carbone et al., 2023; Sander et al., 2025).

Estimating normalizing constants is challenging in high dimensions or when  $\pi$  is multimodal (i.e.,  $V$  has a complex landscape). Conventional approaches based on importance sampling (Meng & Wong, 1996) are widely adopted to tackle this problem, but they suffer from high variance due to the mismatch between the proposal and the target when  $\pi$  is complicated (Chatterjee & Diaconis, 2018). To alleviate this issue, the technique of *annealing* tries constructing a sequence of intermediate distributions that bridge these two distributions, which motivates several popular methods including path sampling (Chen & Shao, 1997; Gelman & Meng, 1998), annealed importance sampling (AIS, Neal (2001)), and sequential Monte Carlo (SMC, Doucet et al. (2000); Del Moral et al. (2006); Syed et al. (2024)) in statistics literature, as well as thermodynamic integration (TI, Kirkwood (1935)) and Jarzynski equality (JE, Jarzynski (1997); Ge & Jiang (2008); Hartmann et al. (2019)) in statistical mechanics literature. In particular, JE points out the connection between the free energy difference

<sup>1</sup>Up to a multiplicative constant  $\beta = 1/k_B T$  known as the thermodynamic beta, where  $k_B$  is the Boltzmann constant and  $T$  is the temperature. When borrowing physical terminologies, we ignore this for simplicity.

054 between two states and the work done over a series of trajectories linking these two states, while  
 055 AIS constructs a sequence of intermediate distributions and estimates the normalizing constant by  
 056 importance sampling over these distributions. These two methods are our primary focus in this paper.  
 057

058 Despite the empirical success of annealing-based methods (Ma et al., 2013; Krause et al., 2020;  
 059 Mazzanti & Romero, 2020; Yasuda & Takahashi, 2022; Chen & Ying, 2024; Schönle et al., 2025),  
 060 the theoretical understanding of their performance is still limited. Existing works for importance  
 061 sampling mainly focus on the **asymptotic** bias and variance of the estimator (Meng & Wong, 1996;  
 062 Gelman & Meng, 1998), while works on JE usually simplify the problem by assuming the work  
 063 follows simple distributions (e.g., Gaussian or gamma) (Echeverria & Amzel, 2012; Arrar et al., 2019).  
 064 Moreover, only analyses asymptotic in the number of particles derived from central limit theorem  
 065 exist (Lelièvre et al., 2010, Sec. 4.1). This paper aims to establish a rigorous **non-asymptotic** analysis  
 066 of estimators based on JE and AIS, while introducing minimal assumptions on the target distribution.  
 067 We also propose a new algorithm based on reverse diffusion samplers to tackle a shortcoming of AIS.

068 **Contributions.** **1.** We discover a novel strategy for analyzing the complexity of normalizing constant  
 069 estimation, applicable to a wide range of target distributions (Assumps. 1 and 2) that may not satisfy  
 070 isoperimetric conditions such as log-concavity. **2.** In Sec. 3, we study JE and prove an upper bound on  
 071 the time required for running the annealed Langevin dynamics to estimate the normalizing constant  
 072 within  $\varepsilon$  relative error with high probability. The final bound depends on the action (the integral of the  
 073 squared metric derivative in Wasserstein-2 distance) of the curve. **3.** Building on the insights from this  
 074 analysis of the continuous dynamics, in Sec. 4 we establish the first non-asymptotic oracle complexity  
 075 bound for AIS, representing the first analysis of normalizing constant estimation algorithms without  
 076 assuming a log-concave target distribution. **4.** Finally, in Sec. 5, we first point out a potential  
 077 limitation of the commonly used geometric interpolation, which provides a quantitative explanation  
 078 of the mass teleportation phenomenon. We then propose a series of new algorithms based on reverse  
 079 diffusion samplers and formalize a framework for analyzing its oracle complexity. Our experimental  
 080 results demonstrate the superiority of the proposed algorithm over AIS in overcoming multimodality.

081 **Related Works.** Below, we summarize the related works in four aspects.

082 **I. Methods for normalizing constant estimation.** We mainly discuss two classes of methods here.  
 083 First, the *equilibrium* methods, such as TI (Kirkwood, 1935) and its variants (Brosse et al., 2018;  
 084 Ge et al., 2020; Chehab et al., 2023; Kook & Vempala, 2025), which involve sampling sequentially  
 085 from a series of equilibrium Markov transition kernels. Second, the *non-equilibrium* methods, such  
 086 as AIS (Neal, 2001), which samples from a non-equilibrium stochastic process that gradually evolves  
 087 from a prior distribution to the target distributions. In App. H.1, we show that TI is a special case  
 088 of AIS using the “perfect” transition kernels. Recent years have also witnessed the emergence of  
 089 *learning-based* non-equilibrium methods, which are typically byproducts of neural samplers (Nüsken  
 090 & Richter, 2021; Zhang & Chen, 2022; Máté & Fleuret, 2023; Richter & Berner, 2024; Sun et al.,  
 091 2024; Vargas et al., 2024; Máté et al., 2024; Albergo & Vanden-Eijnden, 2025; Blessing et al., 2025;  
 092 Chen et al., 2025; Havens et al., 2025; Du et al., 2025). Finally, there are also methods based on  
 093 particle filtering (Kostov & Whiteley, 2017; Jasra et al., 2018; Ruzayqat et al., 2022).

094 **II. Variance reduction in JE and AIS.** Our proof methodology focuses on the discrepancy between  
 095 the sampling path measure and the reference path measure, which is related to the variance reduction  
 096 technique in applying JE and AIS. For example, Vaikuntanathan & Jarzynski (2008) introduced  
 097 the idea of escorted simulation, Hartmann et al. (2017) proposed a method for learning the optimal  
 098 control protocol in JE through the variational characterization of free energy, and Doucet et al. (2022)  
 099 leveraged score-based generative model to learn the optimal backward kernel. Quantifying the  
 100 discrepancy between path measures is the core of our analysis.

101 **III. Complexity analysis for normalizing constant estimation.** Chehab et al. (2023) studied the  
 102 asymptotic statistical efficiency of the curve for TI measured by the asymptotic mean-squared error,  
 103 and highlighted the advantage of the geometric interpolation. In terms of non-asymptotic analysis,  
 104 existing works mainly rely on the isoperimetry of the target distribution. For instance, Andrieu et al.  
 105 (2016) derived bounds of bias and variance for TI under Poincaré inequality (PI), Brosse et al. (2018)  
 106 provided complexity guarantees for TI under both strong and weak log-concavity conditions, while  
 107 Ge et al. (2020) improved the complexity under strong log-concavity using multilevel Monte Carlo.

108 **IV. Complexity analysis of sampling beyond isoperimetry.** Our analysis of estimating normalizing  
 109 constants of non-log-concave distributions is also closely related to the study of sampling beyond

108 log-concavity. In general, such problems are NP hard (Ge et al., 2018; He & Zhang, 2025). Existing  
 109 works providing convergence guarantees have leveraged more general isoperimetric inequalities  
 110 such as weak PI (Mousavi-Hosseini et al., 2023), tried to establish convergence in weaker notions  
 111 (Balasubramanian et al., 2022; Cheng et al., 2023), or utilized denoising diffusion models (Huang  
 112 et al., 2024a; He et al., 2024). We highlight Guo et al. (2025) that this paper mainly draws inspiration  
 113 from, which introduced the action of a curve in quantifying the convergence of annealed sampling.  
 114 While they focused on sampling and presented cases where annealing works, we extend the analysis  
 115 to a conceptually different task, and further establish lower bounds on the action of the commonly  
 116 used geometric interpolation, motivating a new algorithm based on reverse diffusion samplers.

117 **Notations and Definitions.** For  $a, b \in \mathbb{R}$ , let  $\llbracket a, b \rrbracket := [a, b] \cap \mathbb{Z}$ ,  $a \wedge b := \min(a, b)$ , and  $a \vee b :=$   
 118  $\max(a, b)$ . For  $a, b > 0$ , the notations  $a \lesssim b$ ,  $b \gtrsim a$ ,  $a = O(b)$ ,  $b = \Omega(a)$  indicate that  $a \leq Cb$  for  
 119 some universal absolute constant  $C > 0$ , and the notations  $a \asymp b$ ,  $a = \Theta(b)$  stand for  $a \lesssim b \lesssim a$ .  
 120  $\tilde{O}(\cdot)$ ,  $\tilde{\Theta}(\cdot)$  hide logarithmic dependence in  $O(\cdot)$ ,  $\Theta(\cdot)$ . A function  $U \in C^2(\mathbb{R}^d)$  is  $\alpha(> 0)$ -strongly-  
 121 convex if  $\nabla^2 U \succeq \alpha I$ , and is  $\beta(> 0)$ -smooth if  $-\beta I \preceq \nabla^2 U \preceq \beta I$ . We do not distinguish  
 122 probability measures on  $\mathbb{R}^d$  from their Lebesgue densities. For two probability measures  $\mu, \nu$ , the  
 123 total-variation (TV) distance is  $\text{TV}(\mu, \nu) = \sup_{\text{measurable } A} |\mu(A) - \nu(A)|$ , and the Kullback-Leibler  
 124 (KL) divergence is  $\text{KL}(\mu \parallel \nu) = \int \log \frac{d\mu}{d\nu} d\mu$ . Finally, a function  $T : \mathbb{R}^d \times \mathbb{R}^d \rightarrow [0, +\infty)$  is a  
 125 transition kernel if for any  $x$ ,  $T(x, \cdot)$  is a p.d.f. Throughout this paper,  $(B_t)$  and  $(W_t)$  represent  
 126 standard Brownian motions (BM) on  $\mathbb{R}^d$ .

127 **Preliminaries.** For brevity, we integrate the required background information into the main text, with  
 128 a detailed exposition available in App. A.

## 130 2 PRELIMINARIES AND PROBLEM SETTING

132 To motivate the study of normalizing constant estimation, we first present several examples.

133 **Example 1.** [Free energy difference.] In many statistical physics problems (Lelièvre et al., 2010),  
 134 given two energy functions  $U_0, U_1$  (possibly linked through some thermodynamic process), one is  
 135 often interested in estimating the free energy difference  $\Delta F := -1/\beta \log(\int e^{-\beta U_1} dx / \int e^{-\beta U_0} dx)$ ,  
 136 which is related with the normalizing constant of the distributions  $\pi_i \propto e^{-\beta U_i}$ .

138 **Example 2.** [Likelihood in latent variable models.] In latent variable models such as variational  
 139 autoencoders (Kingma & Welling, 2013), a common evaluation metric is the marginal likelihood of a  
 140 data point  $x$ ,  $p_\theta(x) = \int p_\theta(x|z)p(z)dz$ . This is nothing but the normalizing constant of the posterior  
 141 distribution of the latent variable  $z$  given data  $x$ ,  $p_\theta(z|x) \propto_z p_\theta(x|z)p(z)$ .

142 **Example 3.** [Volume of convex bodies.] In theoretical computer science, a classical problem is to  
 143 estimate the volume of a convex body  $\mathcal{K}$  (Dyer et al., 1991; Cousins & Vempala, 2018; Kook et al.,  
 144 2024), which is equivalent to the normalizing constant of the uniform distribution on  $\mathcal{K}$ ,  $\pi \propto 1_{\mathcal{K}}$ .

145 Building on prior theoretical results (Brosse et al., 2018; Ge et al., 2020), we study the oracle  
 146 complexity of estimating the normalizing constant of a density under the following criterion:

148 **Aim:** Given a density  $\pi \propto \hat{\pi} := e^{-V}$  on  $\mathbb{R}^d$ , bound the complexity of obtaining an estimator  $\hat{Z}$  of  
 149  $Z = \int_{\mathbb{R}^d} \hat{\pi}(x)dx$  such that with constant probability, the relative error is within  $\varepsilon (\ll 1)$ :

$$151 \quad \Pr \left( \left| \frac{\hat{Z}}{Z} - 1 \right| \leq \varepsilon \right) \geq \frac{3}{4}. \quad (1)$$

154 **Remark 1.** We make two remarks regarding (1). First, similar to how taking the mean of i.i.d.  
 155 estimates reduces variance, we show in Lem. 10 that the probability above can be boosted to  $1 - \zeta$ ,  
 156  $\forall \zeta \in (0, 1/4)$  using the median trick: obtaining  $O(\log 1/\zeta)$  i.i.d. estimates satisfying (1) and taking  
 157 their median. Therefore, we focus on the task of obtaining a single estimate satisfying (1) hereafter.  
 158 Second, (1) also allows us to quantify the complexity of estimating the free energy  $F = -\log Z$ ,  
 159 which is often of greater interest in statistical mechanics than the partition function  $Z$ . We show in  
 160 App. G that estimating  $Z$  with  $O(\varepsilon)$  relative error and estimating  $F$  with  $O(\varepsilon)$  absolute error share  
 161 the same complexity up to constants. Further discussion of this guarantee, including a literature  
 review and the comparison with bias and variance, is deferred to App. G.

162 A straightforward method for estimating  $Z$  is through *importance sampling*, i.e.,  $Z = \mathbb{E}_{\pi_0} \hat{\pi}/\pi_0$  for  
 163 some tractable proposal distribution  $\pi_0$ , yet its variance can be large due to the mismatch between  $\pi_0$   
 164 and  $\pi$ . The rationale behind **annealing** involves a gradual transition from  $\pi_0$  to  $\pi_1 = \pi$ . Throughout  
 165 this paper, we consider a curve of probability measures denoted as

$$166 \quad 167 \quad 168 \quad \left( \pi_\theta = \frac{1}{Z_\theta} e^{-V_\theta} \right)_{\theta \in [0,1]},$$

169 where  $V_1 = V$  is the potential of  $\pi$ , and  $Z_1 = Z$  is what we need to estimate. We do not specify the  
 170 exact form of this curve now, but only introduce the following mild regularity assumption on the  
 171 curve, as assumed in classical textbooks such as Ambrosio et al. (2008; 2021); Santambrogio (2015):

172 **Assumption 1.** *The potential  $[0, 1] \times \mathbb{R}^d \ni (\theta, x) \mapsto V_\theta(x) \in \mathbb{R}$  is jointly  $C^1$ , and the curve  
 173  $(\pi_\theta)_{\theta \in [0,1]}$  is absolute continuous with finite action  $\mathcal{A} := \int_0^1 |\dot{\pi}|_\theta^2 d\theta$ .*

174 Here,  $|\dot{\pi}|_\theta := \lim_{\delta \rightarrow 0} \frac{W_2(\pi_{\theta+\delta}, \pi_\theta)}{|\delta|}$  is the Wasserstein-2 ( $W_2$ ) **metric derivative** of the curve  
 175  $(\pi_\theta)_{\theta \in [0,1]}$  at  $\theta$ , which measures the “speed” of the curve in the space of probability distributions, and  
 176 **absolute continuity** means the above limit exists and is finite for all  $\theta \in [0, 1]$ . A curve having a  
 177 finite action is a weaker condition than requiring each  $\pi_\theta$  to satisfy isoperimetric inequalities (e.g.,  
 178 Poincaré or log-Sobolev). We refer readers to App. A.2 for details of optimal transport (OT), and  
 179 in particular, we highlight the connection between the metric derivative and the continuity equation  
 180 (Lem. 4), which will serve as a key tool in our analysis.

181 For the purpose of non-asymptotic analysis, we further introduce the following mild assumption:

182 **Assumption 2.**  *$V$  is  $\beta$ -smooth,  $\nabla V(0) = 0$ , and  $m := \sqrt{\mathbb{E}_\pi \|\cdot\|^2} < +\infty$ .*

183 **Remark 2.** *One can always find a stationary point  $x_*$  of (possibly non-convex)  $V$  using optimization  
 184 methods within negligible cost compared with the complexity for estimating  $Z$ . By considering the  
 185 translated distribution  $\pi(\cdot - x_*)$ , we assume 0 is a stationary point without loss of generality.*

186 Equipped with this fundamental setup, we now proceed to introduce the JE and AIS, and establish an  
 187 analysis for their complexity.

### 192 3 ANALYSIS OF THE JARZYNSKI EQUALITY

193 To elucidate how annealing works in the task of normalizing constant estimation, we first consider  
 194 **annealed Langevin diffusion (ALD)**, which runs **Langevin diffusion (LD)** with a dynamically  
 195 changing target distribution. Recall that the LD with target distribution is the stochastic differential  
 196 equation (SDE)  $dX_t = \nabla \log \pi(X_t) dt + \sqrt{2} dB_t$ , which converges to  $\pi$  as  $t \rightarrow \infty$ . To define  
 197 ALD, we introduce a reparameterized curve  $(\tilde{\pi}_t = \pi_{t/T})_{t \in [0, T]}$  for some large time duration  $T$  to be  
 198 determined later, and consider the following SDE:

$$201 \quad dX_t = \nabla \log \tilde{\pi}_t(X_t) dt + \sqrt{2} dB_t, \quad t \in [0, T]; \quad X_0 \sim \tilde{\pi}_0. \quad (2)$$

202 The following Jarzynski equality provides a connection between the work functional and the free  
 203 energy difference, which naturally yields an estimator of normalizing constant.

204 **Theorem 1** (Jarzynski equality (Jarzynski, 1997)). *Let  $\mathbb{P}^\rightarrow$  be the path measure of (2). Then the work  
 205 functional  $W$  and the free energy difference  $\Delta F$  have the following relation:*

$$206 \quad \mathbb{E}_{\mathbb{P}^\rightarrow} e^{-W} = e^{-\Delta F}, \quad \text{where } W(X) := \frac{1}{T} \int_0^T \partial_\theta V_\theta|_{\theta=\frac{t}{T}}(X_t) dt \text{ and } \Delta F := -\log \frac{Z_1}{Z_0}.$$

207 Below, we sketch the proof from Vargas et al. (2024, Prop. 3.3), which offers a crucial aspect for our  
 208 analysis: the forward and backward SDEs. See App. A.1 for a detailed introduction.

210 **Sketch of Proof** Let  $\mathbb{P}^\leftarrow$  be the path measure of the following backward SDE with time-reversed  
 211 Brownian motion (BM)  $(B_t^\leftarrow)_{t \in [0, T]}$  (i.e.,  $(t \mapsto B_{T-t}^\leftarrow)_{t \in [0, T]}$  is a standard BM, see Def. 1):

$$212 \quad dX_t = -\nabla \log \tilde{\pi}_t(X_t) dt + \sqrt{2} dB_t^\leftarrow, \quad t \in [0, T]; \quad X_T \sim \tilde{\pi}_T. \quad (3)$$

216 **Intuitively, this is running the ALD backward in time from  $T$  to 0, targeting distribution  $\tilde{\pi}_t$  at time**  
 217  **$t$ .** Leveraging the Girsanov’s theorem (Lem. 1) and Itô’s formula, one can establish the following  
 218 **identity of the Radon-Nikodým (RN) derivative between the forward and backward path measures,**  
 219 **known as the *Crooks fluctuation theorem* (Crooks, 1998; 1999):**

$$221 \quad \log \frac{d\mathbb{P}^{\rightarrow}}{d\mathbb{P}^{\leftarrow}}(X) = - \int_0^T (\partial_t \log \tilde{\pi}_t)(X_t) dt = W(X) - \Delta F, \quad \text{a.s. } X \sim \mathbb{P}^{\rightarrow}, \quad (4)$$

224 which implies JE by the identity  $\mathbb{E}_{\mathbb{P}^{\rightarrow}} d\mathbb{P}^{\leftarrow} / d\mathbb{P}^{\rightarrow} = 1$ . Complete proof can be found in App. C.1.  $\square$

225 Under the *ideal* setting where (i)  $Z_0$  is known, (ii) the ALD in (2) can be simulated exactly, and  
 226 (iii) the work functional  $W(X)$  can be computed precisely, Thm. 1 provides an unbiased estimator  
 227  $\hat{Z} := Z_0 e^{-W(X)}$  for  $Z = Z_0 e^{-\Delta F}$ . Despite its dominant use (Chipot & Pohorille, 2007; Lelièvre  
 228 et al., 2010), the statistical efficiency of this estimator is not well understood. While it is known that  
 229 the variance of  $\hat{Z}$  can be large, *non-asymptotic* analyses quantifying its efficiency is lacking. We  
 230 address this gap by establishing an upper bound on the time  $T$  required for the ALD to satisfy the  
 231 accuracy criterion (1) in the following theorem, whose proof is detailed in App. C.2.

233 **Theorem 2.** *Under Assump. 1, it suffices to choose  $T = 32\mathcal{A}/\varepsilon^2$  to obtain  $\Pr(|\hat{Z}/Z - 1| \leq \varepsilon) \geq 3/4$ .*

235 We first observe that our bound aligns with the decay rate of the variance of the work in Mazonka  
 236 & Jarzynski (1999) (see also Lelièvre et al. (2010, Chap. 4.1.4)), which considered a special case  
 237  $\pi_\theta = \mathcal{N}(\theta L, 1/K)$ . They showed that  $W \sim \mathcal{N}(B_T, 2B_T)$  with  $B_T = L^2/T (1 - (1 - e^{-KT})/KT)$ ,  
 238 and hence the *normalized variance*  $\text{Var}_{\mathbb{P}^{\rightarrow}} \hat{Z}/Z = e^{2B_T} - 1$  is **asymptotically  $O(1/T)$**  as  $T \rightarrow \infty$ .  
 239 Our bound, under a different criterion (1), is  $O(1/T)$  for **all**  $T > 0$ .

240 To illustrate the proof idea of Thm. 2, note that while the ALD (2) targets the distribution  $\tilde{\pi}_t$  at time  
 241  $t$ , there is always a lag between  $\tilde{\pi}_t$  and the actual law of  $X_t$ . Similarly, the same lag exists in the  
 242 backward ALD (3). This lag turns out to be the source of the error in the estimator  $\hat{Z}$ .

243 In practice, to alleviate the issue of high variance in estimating free energy differences, Vaikuntanathan  
 244 & Jarzynski (2008) proposed adding a compensatory drift term  $v_t(X_t)$  to the ALD (2). Ideally, the  
 245 optimal choice would eliminate the lag entirely, ensuring  $X_t \sim \tilde{\pi}_t$  for all  $t \in [0, T]$ . Inspired by  
 246 this, we compare the path measure of ALD  $\mathbb{P}^{\rightarrow}$  to the SDE having the perfect compensatory drift  
 247 term, whose path measure  $\mathbb{P}$  has marginal distribution  $\tilde{\pi}_t$  at time  $t$ . To make possible the perfect  
 248 match, it turns out that  $v_t$  must satisfy the Fokker-Planck equation with  $\tilde{\pi}_t$ . The Girsanov’s theorem  
 249 (Lem. 1) enables the computation of  $\text{KL}(\mathbb{P} \parallel \mathbb{P}^{\rightarrow})$  and  $\text{KL}(\mathbb{P} \parallel \mathbb{P}^{\leftarrow})$ , which are related to  $\|v_t\|_{L^2(\tilde{\pi}_t)}^2$ .  
 250 Finally, among all admissible drift terms  $v_t$ , Lem. 4 suggests an optimal choice of  $v_t^*$  to minimize  
 251 this norm, thereby leading to the metric derivative  $|\dot{\tilde{\pi}}|_t$  and the action  $\mathcal{A}$ . This way avoids the explicit  
 252 dependence of isoperimetric assumptions in our bound.

253 A similar connection between free energy and action integral was discovered in stochastic thermodynamics (Sekimoto, 2010; Seifert, 2012), one paradigm for non-equilibrium thermodynamics. By the  
 254 second law of thermodynamics, the averaged dissipated work, defined as the averaged work minus  
 255 the free energy difference, i.e.,  $\mathcal{W}_{\text{diss}} := \mathcal{W} - \Delta F := \mathbb{E}_{\mathbb{P}^{\rightarrow}} W - \Delta F$ , is non-negative. When the  
 256 underlying process is modeled by an overdamped LD,  $\mathcal{W}_{\text{diss}}$  can be quantified by an action integral  
 257 divided by the time duration (Aurell et al., 2011; Chen et al., 2020). This follows from the observation  
 258 that  $\mathcal{W}_{\text{diss}} = \text{KL}(\mathbb{P}^{\rightarrow} \parallel \mathbb{P}^{\leftarrow})$  and then a similar argument to that above. This connection provides a  
 259 finer description of the second law of thermodynamics (Aurell et al., 2012) over a finite time horizon.

261 Finally, we place Thm. 2 within the broader theme of **sampling v.s. normalizing constant estimation**  
 262 by comparing Thm. 2 with the complexity of non-log-concave sampling. Guo et al. (2025) proved  
 263 that under the same assumptions, the ALD (2) can draw a sample within  $\varepsilon^2$ -error in  $\text{KL}(\pi \parallel \cdot)$  with the  
 264 same order of time  $T \asymp \mathcal{A}/\varepsilon^2$ . While the classical work Jerrum et al. (1986) proved the existence of a  
 265 polynomial-time algorithm for sampling and a polynomial-time algorithm for estimating normalizing  
 266 constant imply each other in the *discrete* settings, we establish a similar quantitative connection  
 267 between the complexities of these two tasks in the *continuous* settings *without* log-concavity, opening  
 268 a new avenue of research on understanding their relationship. Though reaching similar results, the  
 269 proof strategies are different: Guo et al. (2025) is a direct application of Girsanov’s theorem between  
 $\mathbb{P}^{\rightarrow}$  and  $\mathbb{P}$ , while Thm. 2 involves more complicated backward SDE arguments.

270 4 ANALYSIS OF THE ANNEALED IMPORTANCE SAMPLING  
271

272 In practice, it is not feasible to simulate the ALD precisely, nor is it possible to evaluate the exact  
273 value of the work  $W(X)$ . Therefore, discretization and approximation are required. To address this,  
274 we first outline the following annealed importance sampling (AIS) equality akin to JE.

275 **Theorem 3** (Annealed importance sampling equality (Neal, 2001)). *Suppose we have probability  
276 distributions  $\pi_\ell = f_\ell/Z_\ell$ ,  $\ell \in \llbracket 0, M \rrbracket$  and transition kernels  $F_\ell(x, \cdot)$ ,  $\ell \in \llbracket 1, M \rrbracket$ , and assume that  
277 each  $\pi_\ell$  is an invariant distribution of  $F_\ell$ ,  $\ell \in \llbracket 1, M \rrbracket$ . Define the path measure*

$$279 \mathbb{P}^{\rightarrow}(x_{0:M}) = \pi_0(x_0) \prod_{\ell=1}^M F_\ell(x_{\ell-1}, x_\ell). \quad (5)$$

282 Then the same relation between the work function  $W$  and free energy difference  $\Delta F$  holds:

$$284 \mathbb{E}_{\mathbb{P}^{\rightarrow}} e^{-W} = e^{-\Delta F}, \quad \text{where } W(x_{0:M}) := \log \prod_{\ell=0}^{M-1} \frac{f_\ell(x_\ell)}{f_{\ell+1}(x_\ell)} \text{ and } \Delta F := -\log \frac{Z_M}{Z_0}.$$

288 *Proof.* Since  $\pi_\ell$  is invariant for  $F_\ell$ , the following backward transition kernels are well-defined:

$$289 \quad 290 \quad 291 B_\ell(x, x') = \frac{\pi_\ell(x')}{\pi_\ell(x)} F_\ell(x', x), \quad \ell \in \llbracket 1, M \rrbracket.$$

292 By applying these backward transition kernels sequentially, we define the backward path measure

$$294 \mathbb{P}^{\leftarrow}(x_{0:M}) = \pi_M(x_M) \prod_{\ell=1}^M B_\ell(x_\ell, x_{\ell-1}). \quad (6)$$

297 It can be easily demonstrated, as in (4), that  $\log \frac{d\mathbb{P}^{\rightarrow}}{d\mathbb{P}^{\leftarrow}}(x_{0:M}) = W(x_{0:M}) - \Delta F$ . Consequently,  
298 the identity  $\mathbb{E}_{\mathbb{P}^{\rightarrow}} \frac{d\mathbb{P}^{\leftarrow}}{d\mathbb{P}^{\rightarrow}} = 1$  implies the desired equality.  $\square$

300 While the frameworks of JE and AIS hold for *general* curves of interpolation, for the study of  
301 non-asymptotic complexity guarantees, we focus on a widely used curve in theoretical analysis  
302 (Brosse et al., 2018; Ge et al., 2020), which we refer to as the **geometric interpolation**:<sup>2</sup>

$$303 \quad 304 \quad 305 \pi_\theta = \frac{1}{Z_\theta} f_\theta = \frac{1}{Z_\theta} \exp \left( -V - \frac{\lambda(\theta)}{2} \|\cdot\|^2 \right), \quad \theta \in [0, 1], \quad (7)$$

306 where  $\lambda(\cdot)$  is a decreasing function with  $\lambda(0) = 2\beta$  and  $\lambda(1) = 0$ , referred to as the *annealing  
307 schedule*. With this choice of  $\lambda(0)$ , by Assump. 2, the potential of  $\pi_0$  is  $\beta$ -strongly-convex and  
308  $3\beta$ -smooth, making sampling and normalizing constant estimation relatively easy. To estimate  
309  $Z_0$ , we use the **thermodynamic integration (TI)** algorithm from Ge et al. (2020), which requires  
310  $\tilde{O}(d^{4/3}/\varepsilon^2)$  gradient oracle calls. In a nutshell, TI is an equilibrium method that constructs a series  
311 of intermediate distributions and estimates adjacent normalizing constant ratios via expectation  
312 under these intermediate distributions, realized through MCMC sampling from each intermediate  
313 distribution. As TI is peripheral to our primary focus, we defer its full description, **including the  
314 choice of hyperparameters and complexity bound**, to App. H.1.

315 Given (7), we introduce time points  $0 = \theta_0 < \theta_1 < \dots < \theta_M = 1$  to be specified later, and adopt  
316 the framework outlined in Thm. 3 by setting  $\pi_\ell = f_\ell/Z_\ell$  to correspond to  $\pi_{\theta_\ell} = f_{\theta_\ell}/Z_{\theta_\ell}$ , albeit with a  
317 slight abuse of notation. To estimate the normalizing constant, we need to sample from the forward  
318 path measure  $\mathbb{P}^{\rightarrow}$  and compute the work function along the trajectory. Since  $\pi_{\theta_\ell}$  must be an invariant  
319 distribution of the transition kernel  $F_\ell$  in  $\mathbb{P}^{\rightarrow}$ , we define  $F_\ell$  via running LD targeting  $\pi_{\theta_\ell}$  for a short  
320 time  $T_\ell$ , i.e.,  $F_\ell(x, \cdot)$  is given by the law of  $X_{T_\ell}$  in the following SDE initialized at  $X_0 = x$ :

$$321 \quad 322 dX_t = \nabla \log \pi_{\theta_\ell}(X_t) dt + \sqrt{2} dB_t, \quad t \in [0, T_\ell]. \quad (8)$$

323 <sup>2</sup>(7) differs slightly from a widely used curve in applications (Gelman & Meng, 1998; Neal, 2001):  $\pi_\theta \propto \pi^{1-\lambda(\theta)} \phi^{\lambda(\theta)}$ , where  $\phi$  is a prior distribution (typically Gaussian). We refer to both as *geometric interpolation*.

In this setting, AIS can be interpreted as a discretization of JE (Lelièvre et al., 2010, Rmk. 4.5). However, in practice, exact samples from  $\pi_0$  are often unavailable, and the simulation of LD cannot be performed perfectly.<sup>3</sup> To capture these considerations, we define the following path measure:

$$\hat{\mathbb{P}}^{\rightarrow}(x_{0:M}) = \hat{\pi}_0(x_0) \prod_{\ell=1}^M \hat{F}_\ell(x_{\ell-1}, x_\ell), \quad (9)$$

where  $\hat{\pi}_0$  is the law of an approximate sample from  $\pi_0$ , and the transition kernel  $\hat{F}_\ell$  is a discretization of the LD in  $F_\ell$ , defined as running *one step* of **annealed Langevin Monte Carlo (ALMC)** using the exponential integrator discretization scheme (Zhang & Chen, 2023; Zhang et al., 2023b;a) with step size  $T_\ell$ . Formally,  $\hat{F}_\ell(x, \cdot)$  is the law of  $X_{T_\ell}$  in the following SDE initialized at  $X_0 = x$ :

$$dX_t = - \left( \nabla V(X_0) + \lambda \left( \theta_{\ell-1} + \frac{t}{T_\ell} (\theta_\ell - \theta_{\ell-1}) \right) X_t \right) dt + \sqrt{2} dB_t, \quad t \in [0, T_\ell]. \quad (10)$$

Here, instead of simply setting  $\hat{F}_\ell$  as one step of LMC targeting  $\pi_{\theta_\ell}$ , the dynamically changing  $\lambda(\cdot)$  helps reduce the discretization error, as will be shown in our proof. Furthermore, with a sufficiently small step size, the overall discretization error can also be minimized, motivating us to apply just one update step in each transition kernel.

We refer readers to Alg. 1 in App. B for a summary of the detailed implementation of our proposed AIS algorithm, including the TI procedure and the update rules in (10). The following theorem delineates the oracle complexity of the algorithm required to obtain an estimate  $\hat{Z}$  meeting the desired accuracy criterion (1), whose detailed proof can be located in App. D. **The required values of hyperparameters  $M$ , and  $T_\ell$  can be found at the end of the proof.**

**Theorem 4.** *Let  $\hat{Z}$  be the AIS estimator described as in Alg. 1, i.e.,  $\hat{Z} := \hat{Z}_0 e^{-W(x_{0:M})}$  where  $\hat{Z}_0$  is estimated by TI and  $x_{0:M} \sim \hat{\mathbb{P}}^{\rightarrow}$ . Under Assumps. 1 and 2, consider the annealing schedule  $\lambda(\theta) = 2\beta(1-\theta)^r$  for some  $1 \leq r \lesssim 1$ . Use  $\mathcal{A}_r$  to denote the action of  $(\pi_\theta)_{\theta \in [0,1]}$  to emphasize the dependence on  $r$ . Then, the oracle complexity for obtaining an estimate  $\hat{Z}$  that satisfies (1) is*

$$\tilde{O} \left( \frac{d^{\frac{4}{3}}}{\varepsilon^2} \vee \frac{m\beta\mathcal{A}_r^{\frac{1}{2}}}{\varepsilon^2} \vee \frac{d\beta^2\mathcal{A}_r^2}{\varepsilon^4} \right). \quad (11)$$

We present a high-level proof sketch using Fig. 1. The continuous dynamics, comprising the forward path  $\mathbb{P}^{\rightarrow}$ , the backward path  $\mathbb{P}^{\leftarrow}$ , and the reference path  $\mathbb{P}$ , are depicted as three black curves. To address discretization error, the  $\ell$ -th red (purple) arrow proceeding from left to right represents the transition kernel  $\hat{F}_\ell(B_\ell)$ , whose composition forms  $\hat{\mathbb{P}}^{\rightarrow}(\mathbb{P}^{\leftarrow})$ .

**(I)** Analogously to the analysis of JE (Thm. 2), define the reference path measure  $\mathbb{P}$  with transition kernels  $F_\ell^*$  such that  $x_\ell \sim \pi_{\theta_\ell}$ . Given the sampling path measure  $\hat{\mathbb{P}}^{\rightarrow}$ , define  $\bar{\mathbb{P}}^{\rightarrow}$  as the version of  $\hat{\mathbb{P}}^{\rightarrow}$  without the initialization error, i.e., by replacing  $\hat{\pi}_0$  with  $\pi_0$  in (9).

**(II)** Show that it suffices to obtain an accurate estimate  $\hat{Z}_0$  and initialization distribution  $\hat{\pi}_0$ , together with sufficiently small KL divergences  $\text{KL}(\mathbb{P} \parallel \mathbb{P}^{\leftarrow})$  and  $\text{KL}(\mathbb{P} \parallel \bar{\mathbb{P}}^{\rightarrow})$ , which quantify the closeness between the continuous dynamics and the discretization error in implementation, respectively.

**(III)** Using the chain rule, decompose  $\text{KL}(\mathbb{P} \parallel \mathbb{P}^{\leftarrow})$  into the sum of KL divergences between each pair of transition kernels  $F_\ell$  and  $F_\ell^*$  (i.e., green “distances”). As in Thm. 2,  $F_\ell^*$ , a transition kernel from  $\pi_{\theta_{\ell-1}}$  to  $\pi_{\theta_\ell}$ , is realized by ALD with a compensatory vector field, ensuring the SDE exactly follows

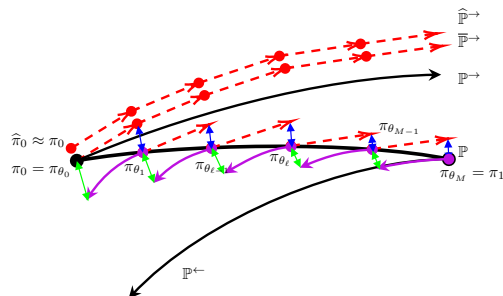


Figure 1: Illustration of the proof idea for Thm. 4.

<sup>3</sup>Recall that we need  $F_\ell$  to have invariant distribution  $\pi_\ell$  in Thm. 3.

378 the trajectory  $(\pi_\theta)_{\theta \in [\theta_{\ell-1}, \theta_\ell]}$ . Similarly, by applying the chain rule and Girsanov’s theorem, we can  
 379 express  $\text{KL}(\mathbb{P} \parallel \overrightarrow{\mathbb{P}})$  as the sum of the blue “distances”, allowing for a similar analysis.  
 380

381 **(IV)** Finally, derive three necessary conditions on the time steps  $\theta_\ell$  to control both  $\text{KL}(\mathbb{P} \parallel \mathbb{P}^\leftarrow)$  and  
 382  $\text{KL}(\mathbb{P} \parallel \overrightarrow{\mathbb{P}})$ . Choosing a proper schedule yields the desired complexity bound.

383 Our proposed algorithm consists of two phases: first, estimating  $Z_0$  by TI, which is provably efficient  
 384 for well-conditioned distributions, and second, estimating  $Z$  by AIS, which is better suited for  
 385 handling non-log-concave distributions. The three terms in (11) arise from (i) ensuring the accuracy  
 386 of  $\widehat{Z}_0$ , (ii) controlling  $\text{KL}(\mathbb{P} \parallel \mathbb{P}^\leftarrow)$ , and (iii) controlling  $\text{KL}(\mathbb{P} \parallel \overrightarrow{\mathbb{P}})$ , respectively, as discussed in **(III)**  
 387 above. Due to the non-log-concavity of  $\pi$ , the action  $\mathcal{A}$  is typically large, making (iii), the cost for  
 388 controlling the discretization error, the dominant complexity. The  $\varepsilon$ -dependence can be interpreted  
 389 as the total duration  $T = \Theta(1/\varepsilon^2)$  required for the continuous dynamics to converge (as in Thm. 2)  
 390 divided by the step size  $\tilde{\Theta}(\varepsilon^2)$  to control the discretization error. Finally, we remark that although  
 391 Thm. 4 is only proved for geometric interpolation, the proof strategy can be generalized to any curve  
 392 of distributions  $(\pi_\theta)_{\theta \in [0,1]}$  satisfying weak regularity conditions, and possibly with an additional  
 393 compensatory drift term, as long as we know the expression of the score  $\nabla \log \pi_\theta$ , and also the  
 394 Lipschitz constants of the score and the drift term for controlling the discretization error.

395

## 396 5 NORMALIZING CONSTANT ESTIMATION VIA DENOISING DIFFUSION

397

398 **Disadvantage of Geometric Interpolation.** From the analysis of JE and AIS (Thms. 2 and 4), the  
 399 choice of the interpolation curve  $(\pi_\theta)_{\theta \in [0,1]}$  is crucial for the complexity. The geometric interpolation  
 400 (7) is widely adopted due to the availability of closed-form scores of the intermediate distributions  $\pi_\theta$ ,  
 401 and for certain structured non-log-concave distributions, the associated action is polynomially large,  
 402 enabling efficient AIS. For instance, Guo et al. (2025, Ex. 2) analyzed a Gaussian mixture target  
 403 distribution with identical covariance, means having the same norm, and arbitrary weights. However,  
 404 for general target distributions, the action of the related curve can grow prohibitively large. We now  
 405 establish an exponential lower bound on the action of a curve starting from a Gaussian mixture,  
 406 highlighting the potential inefficiency of AIS under geometric interpolation.

407 **Proposition 1.** Consider the Gaussian mixture target distribution  $\pi = \frac{1}{2}\mathcal{N}(0, 1) + \frac{1}{2}\mathcal{N}(m, 1)$   
 408 on  $\mathbb{R}$  for some sufficiently large  $m \gtrsim 1$ , whose potential is  $m^2/2$ -smooth. Under the setting in AIS  
 409 (Thm. 4), define  $\pi_\theta(x) \propto \pi(x)e^{-\lambda(\theta)x^2/2}$ ,  $\theta \in [0, 1]$ , where  $\lambda(\theta) = m^2(1-\theta)^r$  for some  $r \geq 1$ . Then,  
 410 the action of the curve  $(\pi_\theta)_{\theta \in [0,1]}$ ,  $\mathcal{A}_r$ , is lower bounded by  $\mathcal{A}_r \gtrsim m^4 e^{m^2/40}$ .

411

412 The full proof is in App. E.1. The key technical tool is a closed-form expression of the  $W_2$  distance  
 413 in  $\mathbb{R}$  expressed by the inverse cumulative distribution functions (c.d.f.s) of the involved distributions,  
 414 and we lower bound the metric derivative near the target distribution, where the curve changes the  
 415 most drastically. This observation provides a novel perspective on the quantitative description of  
 416 the **mass teleportation** or **mode switching** phenomenon (Woodard et al., 2009; Tawn et al., 2020;  
 417 Syed et al., 2021; Chemseddine et al., 2025), motivating us to explore alternative curves that can  
 418 potentially yield smaller action, thereby enhancing the efficiency of normalizing constant estimation.  
 419 Intuitively, during the annealing process, the probability mass needs to be transported from one mode  
 420 of the distribution to another well-separated mode in a short period of time (e.g., through the change  
 421 of weights in both modes), which leads to torpid mixing for many samplers.

421

422 **Reverse Diffusion Samplers.** Inspired by score-based generative models (Song et al., 2021), recent  
 423 advancements have led to the development of multimodal samplers based on reversing the Ornstein-  
 424 Uhlenbeck (OU) process, such as reverse diffusion Monte Carlo (RDMC, Huang et al. (2024a)),  
 425 recursive score diffusion-based Monte Carlo (RSDMC, Huang et al. (2024b)), zeroth-order diffusion  
 426 Monte Carlo (ZODMC, He et al. (2024)), and self-normalized diffusion Monte Carlo<sup>4</sup> (SNDMC,  
 427 Vacher et al. (2025)). We collectively refer to these methods as the **reverse diffusion samplers**  
 428 (**RDS**). The key idea is to simulate the time reversal of the following OU process, which transforms  
 429 any target distribution  $\pi$  into  $\phi := \mathcal{N}(0, I)$  as  $T \rightarrow \infty$ :

430

431

$$dY_t = -Y_t dt + \sqrt{2} dB_t, \quad t \in [0, T]; \quad Y_0 \sim \pi. \quad (12)$$

<sup>4</sup>This name is introduced by us as the original paper did not provide a name for the proposed algorithm.

432 Let  $Y_t \sim \bar{\pi}_t$ . The time-reversal  $(Y_t^\leftarrow := Y_{T-t} \sim \bar{\pi}_{T-t})_{t \in [0, T]}$  satisfies the SDE  
 433

$$434 \quad dY_t^\leftarrow = (Y_t^\leftarrow + 2\nabla \log \bar{\pi}_{T-t}(Y_t^\leftarrow))dt + \sqrt{2}dW_t, \quad t \in [0, T]; \quad Y_0^\leftarrow \sim \bar{\pi}_T(\approx \phi). \quad (13)$$

436 Hence, to draw samples  $Y_0^\leftarrow \sim \pi$ , it suffices to approximate the scores  $\nabla \log \bar{\pi}_t$  and discretize (13),  
 437 which can be implemented in various *learning-free (non-parametric) ways in the literature of RDS*  
 438 *mentioned above*. See App. E.5 for a detailed review.

439 **RDS-based Normalizing Constant Estimation.** We now propose to leverage  $(\bar{\pi}_{T-t})_{t \in [0, T]}$  in  
 440 AIS. To support this idea, we first present the following proposition. *We remark that the result can*  
 441 *be generalized to a bound on the Wasserstein gradient flow for the KL divergence to any target*  
 442 *distribution with weak regularity condition, not necessary the standard normal distribution. See the*  
 443 *proof in App. E.2 for details.*

444 **Proposition 2.** *Define  $\bar{\pi}_t$  as the law of  $Y_t$  in the OU process (12) initialized from  $Y_0 \sim \pi \propto e^{-V}$ ,*  
 445 *where  $V$  is  $\beta$ -smooth. Let  $m^2 := \mathbb{E}_\pi \|\cdot\|^2 < \infty$ . Then,  $\int_0^\infty |\dot{\bar{\pi}}_t|^2 dt \leq d\beta + m^2$ .*

446 Prop. 2 shows that under fairly weak conditions on the target distribution, the action of the curve along  
 447 the OU process,  $(\bar{\pi}_{T-t})_{t \in [0, T]}$ , behaves much better than (7). Hence, our analysis of JE (Thm. 2)  
 448 suggests that this curve is likely to yield more efficient normalizing constant estimation. Furthermore,  
 449 recall that in our earlier proof, we introduced a compensatory drift term  $v_t$  to eliminate the lag in  
 450 JE. The same principle applies here: ensuring  $X_t$  precisely following the reference trajectory is  
 451 advantageous, which results in the time-reversal of OU process (13). Building on this insight, we  
 452 propose an RDS-based algorithm for normalizing constant estimation, and establish a framework for  
 453 analyzing its oracle complexity. See App. E.3 for the proof.

454 **Theorem 5.** *Assume a total time duration  $T$ , an early stopping time  $\delta \geq 0$ , and discrete time points*  
 455  *$0 = t_0 < t_1 < \dots < t_N = T - \delta \leq T$ . For  $t \in [0, T - \delta]$ , let  $t_-$  denote  $t_k$  if  $t \in [t_k, t_{k+1})$ . Let*  
 456  *$s_- \approx \nabla \log \bar{\pi}_-$  be a score estimator, and  $\phi = \mathcal{N}(0, I)$ . Consider the following two SDEs on  $[0, T - \delta]$*   
 457 *representing the sampling trajectory and the time-reversed OU process, respectively:*

$$459 \quad \mathbb{Q}^\dagger : \quad dX_t = (X_t + 2s_{T-t_-}(X_{t_-}))dt + \sqrt{2}dB_t, \quad X_0 \sim \phi; \quad (14)$$

$$460 \quad \mathbb{Q} : \quad dX_t = (X_t + 2\nabla \log \bar{\pi}_{T-t}(X_t))dt + \sqrt{2}dB_t, \quad X_0 \sim \bar{\pi}_T.$$

462 Let  $\hat{Z} := e^{-W(X)}$ ,  $X \sim \mathbb{Q}^\dagger$  be the estimator of  $Z$ , where the functional  $X \mapsto W(X)$  is defined as  
 463

$$464 \quad \log \phi(X_0) + V(X_{T-\delta}) - (T - \delta)d + \int_0^{T-\delta} \left( \|s_{T-t_-}(X_{t_-})\|^2 dt + \sqrt{2} \langle s_{T-t_-}(X_{t_-}), dB_t \rangle \right).$$

466 Then, to ensure  $\hat{Z}$  satisfies (1), it suffices that  $\text{KL}(\mathbb{Q} \|\mathbb{Q}^\dagger) \lesssim \varepsilon^2$  and  $\text{TV}(\pi, \bar{\pi}_\delta) \lesssim \varepsilon$ .  
 467

468 For detailed implementation of the update rule in (14) and the computation of  $W(X)$ , see Alg. 2.  
 469 To determine the overall complexity, we can leverage existing results for RDS to derive the oracle  
 470 complexity to achieve  $\text{KL}(\mathbb{Q} \|\mathbb{Q}^\dagger) \lesssim \varepsilon^2$ . When early stopping is needed (i.e.,  $\delta > 0$ ), we prove in  
 471 Lem. 7 that choosing  $\delta \asymp \varepsilon^2/\beta^2 d^2$  suffices to ensure  $\varepsilon$ -closeness in TV distance between  $\bar{\pi}_\delta$  and  $\pi$ ,  
 472 under weak assumptions similar to Assump. 2. For RDMC, RSDMC, ZODMC, and SNDMC, the  
 473 total complexities are, respectively,  $O(\text{poly}(d, 1/\varepsilon) \exp(1/\varepsilon)^{O(n)})$ ,  $\exp(\beta^3 \log^3 \text{poly}(\beta, d, m^2, 1/\varepsilon))$ ,  
 474  $\exp(\tilde{O}(d) \log \beta \log 1/\varepsilon)$ , and  $O((\beta(m^2 \vee d)/\varepsilon)^{O(d)})$ .<sup>5</sup> The full analysis can be found in App. E.5.  
 475

476 As discussed, RDS can be viewed as an *optimally compensated* ALD using the OU process as  
 477 the trajectory. We conclude this section by contrasting these two approaches. On the one hand,  
 478 analytically-tractable curves such as the geometric interpolation offer closed-form drift terms at all  
 479 time points, but may exhibit poor action properties (Prop. 1) or bad isoperimetric constants (Chehab  
 480 et al., 2025), making annealed sampling challenging. On the other hand, alternative curves like  
 481 the OU process may have better properties in action and isoperimetric constants, but their drift  
 482 terms, often related to the scores of the intermediate distributions, lack closed-form expressions,  
 483 and estimating these terms is also non-trivial. This highlights a fundamental trade-off between the  
 484 complexity of the drift term estimation and the property of the interpolation curve.

485 <sup>5</sup>In RDMC, one assumes there exists  $n, c > 0$  such that  $\forall r > 0$ ,  $V + r \|\cdot\|^2$  is convex for all  $\|x\| \geq \frac{c}{r^n}$ . In  
 RDMC and RSDMC,  $\zeta$  is the probability threshold that the estimator may fail to achieve the desired accuracy  $\varepsilon$ .

**Experiments.** We now compare the performance of the methods of normalizing constant estimation for non-log-concave distributions that have been discussed in the paper, including TI, AIS, and the four RDS-based methods. We consider two multimodal target distributions: a modified Müller Brown (MMB) distribution and Gaussian mixture (GM) with 4 components, both in  $\mathbb{R}^2$ . The quantitative results are summarized in Tab. 1, where we report the relative error of  $\hat{Z}$  and, for GM, the maximum mean discrepancy (MMD) and  $W_2$  distance between the generated samples  $\hat{\pi}_{\text{samp}}$  and ground truth samples from  $\pi$ . All RDS-based methods provide accurate estimates of the normalizing constant and high quality samples, while TI and AIS (based on geometric annealing) produce seriously biased estimates due to lack of mode coverage. Further details are presented in App. I.

Table 1: Quantitative results of normalizing constant estimation (mean  $\pm$  std), best in **bold**.

Target	Metric	TI	AIS	RDMC	RSDMC	ZODMC	SNDMC
MMB	$\hat{Z}/Z$	0.7527 $\pm$ 0.0086	2.9740 $\pm$ 7.6705	0.9829 $\pm$ 0.2116	1.2885 $\pm$ 12.7843	0.9878 $\pm$ 0.1154	<b>1.0053 <math>\pm</math> 0.1192</b>
	$\hat{Z}/Z$	0.2427 $\pm$ 0.0016	0.2042 $\pm$ 0.0008	<b>1.0001 <math>\pm</math> 0.0850</b>	0.9202 $\pm$ 1.0276	0.9766 $\pm$ 0.2835	0.9973 $\pm$ 0.0834
	MMD( $\hat{\pi}_{\text{samp}}, \pi$ )	2.5407 $\pm$ 0.0281	2.4618 $\pm$ 0.0270	0.3581 $\pm$ 0.0366	0.3124 $\pm$ 0.0395	0.2591 $\pm$ 0.0381	<b>0.1576 <math>\pm</math> 0.0279</b>
GM	$W_2(\hat{\pi}_{\text{samp}}, \pi)$	10.5602 $\pm$ 0.0794	10.4842 $\pm$ 0.0851	7.0242 $\pm$ 0.9104	2.6012 $\pm$ 0.2482	2.4506 $\pm$ 0.2963	<b>1.5494 <math>\pm</math> 0.6820</b>

## 6 CONCLUSION, LIMITATIONS, AND FUTURE DIRECTIONS

This paper investigates the complexity of normalizing constant estimation using JE, AIS, and RDS, and takes a first step in establishing non-asymptotic convergence guarantees based on insights from continuous-time analysis. Our analysis of JE (Thm. 2) applies to general interpolations without explicit dependence of isoperimetry, thereby substantially extending prior work limited to log-concave distributions. Several limitations remain: the tightness of our upper bounds (Thms. 2 and 4) are unknown; the lower bound on the action in Prop. 1 does not directly imply that JE needs exponentially long time to converge; though the action provides a clean analysis of the statistical efficiency of annealing—which isoperimetric inequalities cannot deal with—its practical interpretability is not well understood. Finally, we conjecture that our proof techniques can extend to samplers beyond overdamped LD (e.g., Hamiltonian or underdamped LD (Sohl-Dickstein & Culpepper, 2012)), and may also apply to estimating normalizing constants of compactly supported distributions on  $\mathbb{R}^d$  (e.g., convex bodies volume estimation (Cousins & Vempala, 2018)) or discrete distributions (e.g., Ising model and restricted Boltzmann machines (Huber, 2015; Krause et al., 2020)) via the Poisson stochastic integral framework (Ren et al., 2025a;b), which we leave as a direction for future research.

## REFERENCES

Michael Samuel Albergo and Eric Vanden-Eijnden. NETS: A non-equilibrium transport sampler. In *Forty-second International Conference on Machine Learning*, 2025. URL <https://openreview.net/forum?id=QqGw9StPbQ>.

Luigi Ambrosio, Nicola Gigli, and Giuseppe Savaré. *Gradient Flows: In Metric Spaces and in the Space of Probability Measures*. Lectures in Mathematics. ETH Zürich. Birkhäuser Basel, 2 edition, 2008. doi: 10.1007/978-3-7643-8722-8.

Luigi Ambrosio, Elia Brué, and Daniele Semola. *Lectures on optimal transport*, volume 130 of *UNITEXT*. Springer Cham, 2021. doi: 10.1007/978-3-030-72162-6. URL <https://link.springer.com/book/10.1007/978-3-030-72162-6>.

Brian D.O. Anderson. Reverse-time diffusion equation models. *Stochastic Processes and their Applications*, 12(3):313–326, 1982. ISSN 0304-4149. doi: 10.1016/0304-4149(82)90051-5. URL <https://www.sciencedirect.com/science/article/pii/0304414982900515>.

Christophe Andrieu, James Ridgway, and Nick Whiteley. Sampling normalizing constants in high dimensions using inhomogeneous diffusions. *arXiv preprint arXiv:1612.07583*, 2016.

Mehrnoosh Arrar, Fernando Martín Boubeta, María Eugenia Szretter, Mariela Sued, Leonardo Boechi, and Daniela Rodriguez. On the accurate estimation of free energies using the Jarzynski equality. *Journal of Computational Chemistry*, 40(4):688–696, 2019. doi: 10.1002/jcc.25754. URL <https://onlinelibrary.wiley.com/doi/10.1002/jcc.25754>.

540 Erik Aurell, Carlos Mej  -Monasterio, and Paolo Muratore-Ginanneschi. Optimal protocols  
 541 and optimal transport in stochastic thermodynamics. *Phys. Rev. Lett.*, 106:250601, Jun 2011.  
 542 doi: 10.1103/PhysRevLett.106.250601. URL <https://link.aps.org/doi/10.1103/PhysRevLett.106.250601>.

543

544 Erik Aurell, Krzysztof Gaw  dzki, Carlos Mej  -Monasterio, Roya Mohayaee, and Paolo Muratore-  
 545 Ginanneschi. Refined second law of thermodynamics for fast random processes. *Journal of  
 546 statistical physics*, 147:487–505, 2012. doi: 10.1007/s10955-012-0478-x.

547

548 Dominique Bakry, Ivan Gentil, and Michel Ledoux. *Analysis and geometry of Markov diffusion  
 549 operators*, volume 103 of *Grundlehren der mathematischen Wissenschaften*. Springer Cham, 1  
 550 edition, 2014. doi: 10.1007/978-3-319-00227-9.

551

552 Krishna Balasubramanian, Sinho Chewi, Murat A Erdogdu, Adil Salim, and Shunshi Zhang. To-  
 553 wards a theory of non-log-concave sampling: First-order stationarity guarantees for Langevin  
 554 Monte Carlo. In Po-Ling Loh and Maxim Raginsky (eds.), *Proceedings of Thirty Fifth Con-  
 555 ference on Learning Theory*, volume 178 of *Proceedings of Machine Learning Research*, pp.  
 556 2896–2923. PMLR, 02–05 Jul 2022. URL <https://proceedings.mlr.press/v178/balasubramanian22a.html>.

557

558 Denis Blessing, Julius Berner, Lorenz Richter, and Gerhard Neumann. Underdamped diffusion  
 559 bridges with applications to sampling. In *The Thirteenth International Conference on Learning  
 560 Representations*, 2025. URL <https://openreview.net/forum?id=Q1QTxFm0Is>.

561

562 Nicolas Brosse, Alain Durmus, and   ric Moulines. Normalizing constants of log-concave densities.  
 563 *Electronic Journal of Statistics*, 12(1):851 – 889, 2018. doi: 10.1214/18-EJS1411. URL <https://doi.org/10.1214/18-EJS1411>.

564

565 Davide Carbone, Mengjian Hua, Simon Coste, and Eric Vanden-Eijnden. Efficient  
 566 training of energy-based models using Jarzynski equality. In A. Oh, T. Naumann,  
 567 A. Globerson, K. Saenko, M. Hardt, and S. Levine (eds.), *Advances in Neural In-  
 568 formation Processing Systems*, volume 36, pp. 52583–52614. Curran Associates, Inc.,  
 569 2023. URL [https://proceedings.neurips.cc/paper\\_files/paper/2023/file/a4ddb865e0a8ca3cca43fd7387b4b0da-Paper-Conference.pdf](https://proceedings.neurips.cc/paper_files/paper/2023/file/a4ddb865e0a8ca3cca43fd7387b4b0da-Paper-Conference.pdf).

570

571 Sourav Chatterjee and Persi Diaconis. The sample size required in importance sampling. *The  
 572 Annals of Applied Probability*, 28(2):1099 – 1135, 2018. doi: 10.1214/17-AAP1326. URL  
 573 <https://doi.org/10.1214/17-AAP1326>.

574

575 Omar Chehab, Aapo Hyv  inen, and Andrej Risteski. Provable benefits of annealing for es-  
 576 timating normalizing constants: Importance sampling, noise-contrastive estimation, and be-  
 577 yond. In *Thirty-seventh Conference on Neural Information Processing Systems*, 2023. URL  
 578 <https://openreview.net/forum?id=iWGC0Nsq9i>.

579

580 Omar Chehab, Anna Korba, Austin J Stromme, and Adrien Vacher. Provable convergence and  
 581 limitations of geometric tempering for Langevin dynamics. In *The Thirteenth International  
 582 Conference on Learning Representations*, 2025. URL <https://openreview.net/forum?id=DZcmz9wU0i>.

583

584 Jannis Chemeddine, Christian Wald, Richard Duong, and Gabriele Steidl. Neural sampling from  
 585 Boltzmann densities: Fisher-Rao curves in the Wasserstein geometry. In *The Thirteenth Interna-  
 586 tional Conference on Learning Representations*, 2025. URL <https://openreview.net/forum/?id=TUvg5uwdeG>.

587

588 Haoxuan Chen and Lexing Ying. Ensemble-based annealed importance sampling. *arXiv preprint  
 589 arXiv:2401.15645*, 2024.

590

591 Junhua Chen, Lorenz Richter, Julius Berner, Denis Blessing, Gerhard Neumann, and Anima Anand-  
 592 kumar. Sequential controlled Langevin Diffusions. In *The Thirteenth International Confer-  
 593 ence on Learning Representations*, 2025. URL <https://openreview.net/forum?id=dImD2sgy86>.

594 Ming-Hui Chen and Qi-Man Shao. On Monte Carlo methods for estimating ratios of normalizing  
 595 constants. *The Annals of Statistics*, 25(4):1563 – 1594, 1997. doi: 10.1214/aos/1031594732. URL  
 596 <https://doi.org/10.1214/aos/1031594732>.

597

598 Sitan Chen, Sinho Chewi, Jerry Li, Yuanzhi Li, Adil Salim, and Anru Zhang. Sampling is as easy as  
 599 learning the score: theory for diffusion models with minimal data assumptions. In *The Eleventh*  
 600 *International Conference on Learning Representations*, 2023. URL [https://openreview.net/forum?id=zyLVMgsZOU\\_](https://openreview.net/forum?id=zyLVMgsZOU_).

601

602 Yongxin Chen, Tryphon T Georgiou, and Michele Pavon. On the relation between optimal transport  
 603 and Schrödinger bridges: A stochastic control viewpoint. *Journal of Optimization Theory and*  
 604 *Applications*, 169:671–691, 2016. doi: 10.1007/s10957-015-0803-z.

605

606 Yongxin Chen, Tryphon T. Georgiou, and Allen Tannenbaum. Stochastic control and nonequilibrium  
 607 thermodynamics: Fundamental limits. *IEEE Transactions on Automatic Control*, 65(7):2979–2991,  
 608 2020. doi: 10.1109/TAC.2019.2939625.

609

610 Yongxin Chen, Tryphon T. Georgiou, and Michele Pavon. Stochastic control liaisons: Richard  
 611 Sinkhorn meets Gaspard Monge on a Schrödinger bridge. *SIAM Review*, 63(2):249–313, 2021.  
 612 doi: 10.1137/20M1339982. URL <https://doi.org/10.1137/20M1339982>.

613

614 Xiang Cheng, Niladri S. Chatterji, Peter L. Bartlett, and Michael I. Jordan. Underdamped  
 615 Langevin MCMC: A non-asymptotic analysis. In Sébastien Bubeck, Vianney Perchet, and  
 616 Philippe Rigollet (eds.), *Proceedings of the 31st Conference On Learning Theory*, volume 75  
 617 of *Proceedings of Machine Learning Research*, pp. 300–323. PMLR, 06–09 Jul 2018. URL  
 618 <https://proceedings.mlr.press/v75/cheng18a.html>.

619

620 Xiang Cheng, Bohan Wang, Jingzhao Zhang, and Yusong Zhu. Fast conditional mix-  
 621 ing of MCMC algorithms for non-log-concave distributions. In A. Oh, T. Neumann,  
 622 A. Globerson, K. Saenko, M. Hardt, and S. Levine (eds.), *Advances in Neural In-  
 623 formation Processing Systems*, volume 36, pp. 13374–13394. Curran Associates, Inc.,  
 624 2023. URL [https://proceedings.neurips.cc/paper\\_files/paper/2023/file/2b00b3331bd0f5fbfdd966ac06338f6d-Paper-Conference.pdf](https://proceedings.neurips.cc/paper_files/paper/2023/file/2b00b3331bd0f5fbfdd966ac06338f6d-Paper-Conference.pdf).

625

626 Sinho Chewi. *Log-Concave Sampling*. Book draft, in preparation, 2022. URL <https://chewisinho.github.io>.

627

628 Sinho Chewi, Murat A Erdogdu, Mufan Li, Ruoqi Shen, and Shunshi Zhang. Analysis of  
 629 Langevin Monte Carlo from Poincaré to log-Sobolev. In Po-Ling Loh and Maxim Ragin-  
 630 sky (eds.), *Proceedings of Thirty Fifth Conference on Learning Theory*, volume 178 of *Pro-  
 631 ceedings of Machine Learning Research*, pp. 1–2. PMLR, 02–05 Jul 2022. URL <https://proceedings.mlr.press/v178/chewi22a.html>.

632

633 Christophe Chipot and Andrew Pohorille (eds.). *Free Energy Calculations: Theory and Applications  
 634 in Chemistry and Biology*. Springer Series in Chemical Physics. Springer Berlin, Heidelberg, 2007.  
 635 doi: 10.1007/978-3-540-38448-9.

636

637 Giovanni Conforti and Luca Tamanini. A formula for the time derivative of the entropic cost  
 638 and applications. *Journal of Functional Analysis*, 280(11):108964, 2021. ISSN 0022-1236.  
 639 doi: 10.1016/j.jfa.2021.108964. URL <https://www.sciencedirect.com/science/article/pii/S002212362100046X>.

640

641 Ben Cousins and Santosh Vempala. Gaussian cooling and  $O^*(n^3)$  algorithms for volume and Gaussian  
 642 volume. *SIAM Journal on Computing*, 47(3):1237–1273, 2018. doi: 10.1137/15M1054250. URL  
 643 <https://doi.org/10.1137/15M1054250>.

644

645 Gavin E. Crooks. Nonequilibrium measurements of free energy differences for microscopically  
 646 reversible Markovian systems. *Journal of Statistical Physics*, 90:1481–1487, 1998. doi: 10.1023/A:  
 647 1023208217925.

648

649 Gavin E. Crooks. Entropy production fluctuation theorem and the nonequilibrium work relation for  
 650 free energy differences. *Phys. Rev. E*, 60:2721–2726, Sep 1999. doi: 10.1103/PhysRevE.60.2721.  
 651 URL <https://link.aps.org/doi/10.1103/PhysRevE.60.2721>.

648 Pierre Del Moral, Arnaud Doucet, and Ajay Jasra. Sequential Monte Carlo samplers. *Journal of the*  
 649 *Royal Statistical Society Series B: Statistical Methodology*, 68(3):411–436, 5 2006.  
 650

651 Arnaud Doucet, Simon Godsill, and Christophe Andrieu. On sequential Monte Carlo sampling  
 652 methods for bayesian filtering. *Statistics and computing*, 10:197–208, 2000. doi: 10.1023/A:  
 653 1008935410038.

654 Arnaud Doucet, Will Grathwohl, Alexander G Matthews, and Heiko Strathmann. Score-  
 655 based diffusion meets annealed importance sampling. In S. Koyejo, S. Mohamed,  
 656 A. Agarwal, D. Belgrave, K. Cho, and A. Oh (eds.), *Advances in Neural Infor-*  
 657 *mation Processing Systems*, volume 35, pp. 21482–21494. Curran Associates, Inc.,  
 658 2022. URL [https://proceedings.neurips.cc/paper\\_files/paper/2022/file/86b7128efa3950df7c0f6c0342e6dcc1-Paper-Conference.pdf](https://proceedings.neurips.cc/paper_files/paper/2022/file/86b7128efa3950df7c0f6c0342e6dcc1-Paper-Conference.pdf).

659

660 Yuanqi Du, Jiajun He, Francisco Vargas, Yuanqing Wang, Carla P Gomes, José Miguel Hernández-  
 661 Lobato, and Eric Vanden-Eijnden. FEAT: Free energy estimators with adaptive transport. In  
 662 *The Thirty-ninth Annual Conference on Neural Information Processing Systems*, 2025. URL  
 663 <https://openreview.net/forum?id=GQXeLGYMda>.  
 664

665 Martin Dyer, Alan Frieze, and Ravi Kannan. A random polynomial-time algorithm for approximating  
 666 the volume of convex bodies. *J. ACM*, 38(1):1–17, January 1991. ISSN 0004-5411. doi: 10.1145/  
 667 102782.102783. URL <https://doi.org/10.1145/102782.102783>.

668

669 Ignacia Echeverria and L. Mario Amzel. Estimation of free-energy differences from computed work  
 670 distributions: An application of Jarzynski’s equality. *The Journal of Physical Chemistry B*, 116  
 671 (36):10977–11396, 2012. doi: 10.1021/jp300527q.

672 Rémi Flamary, Nicolas Courty, Alexandre Gramfort, Mokhtar Z. Alaya, Aurélie Boisbunon, Stanislas  
 673 Chambon, Laetitia Chapel, Adrien Corenflos, Kilian Fatras, Nemo Fournier, Léo Gautheron,  
 674 Nathalie T.H. Gayraud, Hicham Janati, Alain Rakotomamonjy, Ievgen Redko, Antoine Rolet,  
 675 Antony Schutz, Vivien Seguy, Danica J. Sutherland, Romain Tavenard, Alexander Tong, and  
 676 Titouan Vayer. POT: Python optimal transport. *Journal of Machine Learning Research*, 22(78):  
 677 1–8, 2021. URL <http://jmlr.org/papers/v22/20-451.html>.

678

679 Hao Ge and Da-Quan Jiang. Generalized Jarzynski’s equality of inhomogeneous multidimensional  
 680 diffusion processes. *Journal of Statistical Physics*, 131:675–689, 3 2008. ISSN 1572-9613. doi:  
 681 10.1007/s10955-008-9520-4.

682 Rong Ge, Holden Lee, and Andrej Risteski. Beyond log-concavity: Provable guarantees  
 683 for sampling multi-modal distributions using simulated tempering Langevin Monte Carlo.  
 684 In S. Bengio, H. Wallach, H. Larochelle, K. Grauman, N. Cesa-Bianchi, and R. Gar-  
 685 nett (eds.), *Advances in Neural Information Processing Systems*, volume 31. Curran Asso-  
 686 ciates, Inc., 2018. URL [https://proceedings.neurips.cc/paper\\_files/paper/2018/file/c6ede20e6f597abf4b3f6bb30ceel6c7-Paper.pdf](https://proceedings.neurips.cc/paper_files/paper/2018/file/c6ede20e6f597abf4b3f6bb30ceel6c7-Paper.pdf).

687

688 Rong Ge, Holden Lee, and Jianfeng Lu. Estimating normalizing constants for log-concave dis-  
 689 tributions: Algorithms and lower bounds. In *Proceedings of the 52nd Annual ACM SIGACT*  
 690 *Symposium on Theory of Computing*, STOC 2020, pp. 579–586, New York, NY, USA, 2020.  
 691 Association for Computing Machinery. ISBN 9781450369794. doi: 10.1145/3357713.3384289.  
 692 URL <https://doi.org/10.1145/3357713.3384289>.

693

694 Andrew Gelman and Xiao-Li Meng. Simulating normalizing constants: from importance sampling to  
 695 bridge sampling to path sampling. *Statistical Science*, 13(2):163 – 185, 1998. doi: 10.1214/ss/  
 696 1028905934. URL <https://doi.org/10.1214/ss/1028905934>.

697

698 Andrew Gelman, John B. Carlin, Hal S. Stern, and Donald B. Rubin. *Bayesian data analysis*.  
 699 Chapman and Hall/CRC, 3 edition, 2013.

700 Wei Guo, Molei Tao, and Yongxin Chen. Provable benefit of annealed Langevin Monte Carlo for non-  
 701 log-concave sampling. In *The Thirteenth International Conference on Learning Representations*,  
 2025. URL <https://openreview.net/forum?id=P6IVIOGRRg>.

702 Carsten Hartmann and Lorenz Richter. Nonasymptotic bounds for suboptimal importance sam-  
 703 pling. *SIAM/ASA Journal on Uncertainty Quantification*, 12(2):309–346, 2024. doi: 10.1137/  
 704 21M1427760. URL <https://doi.org/10.1137/21M1427760>.

705 Carsten Hartmann, Lorenz Richter, Christof Schütte, and Wei Zhang. Variational characterization  
 706 of free energy: Theory and algorithms. *Entropy*, 19(11), 2017. ISSN 1099-4300. doi: 10.3390/  
 708 e19110626. URL <https://www.mdpi.com/1099-4300/19/11/626>.

709 Carsten Hartmann, Christof Schütte, and Wei Zhang. Jarzynski’s equality, fluctuation theorems,  
 710 and variance reduction: Mathematical analysis and numerical algorithms. *Journal of Statistical  
 711 Physics*, 175:1214–1261, 2019. doi: 10.1007/s10955-019-02286-4. URL <https://doi.org/10.1007/s10955-019-02286-4>.

712 Aaron J Havens, Benjamin Kurt Miller, Bing Yan, Carles Domingo-Enrich, Anuroop Sriram,  
 713 Daniel S. Levine, Brandon M Wood, Bin Hu, Brandon Amos, Brian Karrer, Xiang Fu, Guan-  
 714 Horng Liu, and Ricky T. Q. Chen. Adjoint sampling: Highly scalable diffusion samplers via  
 715 adjoint matching. In *Forty-second International Conference on Machine Learning*, 2025. URL  
 716 <https://openreview.net/forum?id=6Eg1OrHmg2>.

717 Ye He, Kevin Rojas, and Molei Tao. Zeroth-order sampling methods for non-log-concave distributions:  
 718 Alleviating metastability by denoising diffusion. In *The Thirty-eighth Annual Conference on  
 719 Neural Information Processing Systems*, 2024. URL <https://openreview.net/forum?id=X3A1julsw5>.

720 Yuchen He and Chihao Zhang. On the query complexity of sampling from non-log-concave distri-  
 721 butions (extended abstract). In Nika Haghtalab and Ankur Moitra (eds.), *Proceedings of Thirty  
 722 Eighth Conference on Learning Theory*, volume 291 of *Proceedings of Machine Learning Research*,  
 723 pp. 2786–2787. PMLR, 30 Jun–04 Jul 2025. URL <https://proceedings.mlr.press/v291/he25a.html>.

724 Xunpeng Huang, Hanze Dong, Yifan Hao, Yian Ma, and Tong Zhang. Reverse diffusion Monte  
 725 Carlo. In *The Twelfth International Conference on Learning Representations*, 2024a. URL  
 726 <https://openreview.net/forum?id=kIPEyMSdFV>.

727 Xunpeng Huang, Difan Zou, Hanze Dong, Yi-An Ma, and Tong Zhang. Faster sampling with-  
 728 out isoperimetry via diffusion-based Monte Carlo. In Shipra Agrawal and Aaron Roth (eds.),  
 729 *Proceedings of Thirty Seventh Conference on Learning Theory*, volume 247 of *Proceedings  
 730 of Machine Learning Research*, pp. 2438–2493. PMLR, 30 Jun–03 Jul 2024b. URL <https://proceedings.mlr.press/v247/huang24a.html>.

731 Mark Huber. Approximation algorithms for the normalizing constant of Gibbs distributions. *The  
 732 Annals of Applied Probability*, 25(2):974 – 985, 2015. doi: 10.1214/14-AAP1015. URL <https://doi.org/10.1214/14-AAP1015>.

733 Christopher Jarzynski. Nonequilibrium equality for free energy differences. *Phys. Rev. Lett.*, 78:  
 734 2690–2693, Apr 1997. doi: 10.1103/PhysRevLett.78.2690. URL <https://link.aps.org/doi/10.1103/PhysRevLett.78.2690>.

735 Ajay Jasra, Kengo Kamatani, Prince Peprah Osei, and Yan Zhou. Multilevel particle filters:  
 736 normalizing constant estimation. *Statistics and Computing*, 28:47–60, 2018. doi: 10.1007/  
 737 s11222-016-9715-5.

738 Mark R. Jerrum, Leslie G. Valiant, and Vijay V. Vazirani. Random generation of combinatorial  
 739 structures from a uniform distribution. *Theoretical Computer Science*, 43:169–188, 1986. ISSN  
 740 0304-3975. doi: 10.1016/0304-3975(86)90174-X. URL <https://www.sciencedirect.com/science/article/pii/030439758690174X>.

741 Ioannis Karatzas and Steven E. Shreve. *Brownian Motion and Stochastic Calculus*. Graduate Texts  
 742 in Mathematics. Springer New York, NY, 2 edition, 1991. doi: 10.1007/978-1-4612-0949-2.

743 Diederik P Kingma and Max Welling. Auto-encoding variational Bayes. *arXiv preprint  
 744 arXiv:1312.6114*, 2013.

756 John G. Kirkwood. Statistical mechanics of fluid mixtures. *The Journal of Chemical Physics*, 3(5):  
 757 300–313, 05 1935. ISSN 0021-9606. doi: 10.1063/1.1749657. URL <https://doi.org/10.1063/1.1749657>.

759

760 Yunbum Kook and Santosh S. Vempala. Sampling and integration of logconcave functions by  
 761 algorithmic diffusion. In *Proceedings of the 57th Annual ACM Symposium on Theory of Computing*,  
 762 STOC '25, pp. 924–932, New York, NY, USA, 2025. Association for Computing Machinery.  
 763 ISBN 9798400715105. doi: 10.1145/3717823.3718202. URL <https://doi.org/10.1145/3717823.3718202>.

764

765 Yunbum Kook, Santosh Vempala, and Matthew Shunshi Zhang. In-and-Out: Algorithmic diffusion  
 766 for sampling convex bodies. In *The Thirty-eighth Annual Conference on Neural Information  
 767 Processing Systems*, 2024. URL <https://openreview.net/forum?id=aNQWRHyh15>.

768

769 Svetoslav Kostov and Nick Whiteley. An algorithm for approximating the second moment of the  
 770 normalizing constant estimate from a particle filter. *Methodology and Computing in Applied  
 771 Probability*, 19:799–818, 2017. doi: 10.1007/s11009-016-9513-8.

772

773 Oswin Krause, Asja Fischer, and Christian Igel. Algorithms for estimating the partition function  
 774 of restricted Boltzmann machines. *Artificial Intelligence*, 278:103195, 2020. ISSN 0004-3702.  
 775 doi: 10.1016/j.artint.2019.103195. URL <https://www.sciencedirect.com/science/article/pii/S0004370219301948>.

776

777 C. Le Bris and P.-L. Lions. Existence and uniqueness of solutions to Fokker–Planck type equa-  
 778 tions with irregular coefficients. *Communications in Partial Differential Equations*, 33(7):  
 779 1272–1317, 2008. doi: 10.1080/03605300801970952. URL <https://doi.org/10.1080/03605300801970952>.

780

781 Holden Lee, Jianfeng Lu, and Yixin Tan. Convergence of score-based generative modeling for general  
 782 data distributions. In Shipra Agrawal and Francesco Orabona (eds.), *Proceedings of The 34th  
 783 International Conference on Algorithmic Learning Theory*, volume 201 of *Proceedings of Machine  
 784 Learning Research*, pp. 946–985. PMLR, 20 Feb–23 Feb 2023. URL <https://proceedings.mlr.press/v201/lee23a.html>.

785

786 Tony Lelièvre, Mathias Rousset, and Gabriel Stoltz. *Free Energy Computations: A Mathematical  
 787 Perspective*. Imperial College Press, 2010. doi: 10.1142/p579.

788

789 Christian Léonard. A survey of the Schrödinger problem and some of its connections with optimal  
 790 transport. *Discrete and Continuous Dynamical Systems - Series A*, 34(4):1533–1574, 2014. URL  
 791 <https://hal.science/hal-00849930>.

792

793 Jianzhu Ma, Jin Peng, Sheng Wang, and Jinbo Xu. Estimating the partition function of graphical  
 794 models using langevin importance sampling. In Carlos M. Carvalho and Pradeep Ravikumar (eds.),  
 795 *Proceedings of the Sixteenth International Conference on Artificial Intelligence and Statistics*,  
 796 volume 31 of *Proceedings of Machine Learning Research*, pp. 433–441, Scottsdale, Arizona, USA,  
 797 29 Apr–01 May 2013. PMLR. URL <https://proceedings.mlr.press/v31/ma13a.html>.

798

799 Bálint Máté and François Fleuret. Learning interpolations between Boltzmann densities. *Transactions  
 800 on Machine Learning Research*, 2023. ISSN 2835-8856. URL <https://openreview.net/forum?id=TH6YrEcbth>.

801

802 Bálint Máté, François Fleuret, and Tristan Bereau. Neural thermodynamic integration: Free energies  
 803 from energy-based diffusion models. *The Journal of Physical Chemistry Letters*, 15(45):11395–  
 804 11404, 2024. doi: 10.1021/acs.jpclett.4c01958. URL <https://doi.org/10.1021/acs.jpclett.4c01958>. PMID: 39503734.

805

806 O Mazonka and C Jarzynski. Exactly solvable model illustrating far-from-equilibrium predictions.  
 807 *arXiv preprint cond-mat/9912121*, 1999.

808

809 Ferran Mazzanti and Enrique Romero. Efficient evaluation of the partition function of RBMs with  
 annealed importance sampling. *arXiv preprint arXiv:2007.11926*, 2020.

810 Xiao-Li Meng and Wing Hung Wong. Simulating ratios of normalizing constants via a simple identity:  
 811 a theoretical exploration. *Statistica Sinica*, 6(4):831–860, 1996. ISSN 10170405, 19968507. URL  
 812 <http://www.jstor.org/stable/24306045>.

813 Alireza Mousavi-Hosseini, Tyler K. Farghly, Ye He, Krishna Balasubramanian, and Murat A. Erdogdu.  
 814 Towards a complete analysis of Langevin Monte Carlo: Beyond Poincaré inequality. In Gergely  
 815 Neu and Lorenzo Rosasco (eds.), *Proceedings of Thirty Sixth Conference on Learning Theory*,  
 816 volume 195 of *Proceedings of Machine Learning Research*, pp. 1–35. PMLR, 12–15 Jul 2023.  
 817 URL <https://proceedings.mlr.press/v195/mousavi-hosseini23a.html>.

818 Radford M. Neal. Annealed importance sampling. *Statistics and Computing*, 11(2):125–139, April  
 819 2001. ISSN 1573-1375. doi: 10.1023/A:1008923215028. URL <https://doi.org/10.1023/A:1008923215028>.

820 Edward Nelson. *Dynamical Theories of Brownian Motion*. Princeton University Press, 1967. ISBN  
 821 9780691079509. URL <http://www.jstor.org/stable/j.ctv15r57jg>.

822 Nikolas Nüsken and Lorenz Richter. Solving high-dimensional Hamilton–Jacobi–Bellman PDEs  
 823 using neural networks: perspectives from the theory of controlled diffusions and measures  
 824 on path space. *Partial differential equations and applications*, 2(4):48, 2021. doi: 10.1007/  
 825 s42985-021-00102-x.

826 Andrew Pohorille, Christopher Jarzynski, and Christophe Chipot. Good practices in free-energy  
 827 calculations. *The Journal of Physical Chemistry B*, 114(32):10235–10253, 2010. ISSN 1520-6106.  
 828 doi: 10.1021/jp102971x. URL <https://doi.org/10.1021/jp102971x>.

829 Yinuo Ren, Haoxuan Chen, Grant M. Rotskoff, and Lexing Ying. How discrete and continuous  
 830 diffusion meet: Comprehensive analysis of discrete diffusion models via a stochastic integral  
 831 framework. In *The Thirteenth International Conference on Learning Representations*, 2025a. URL  
 832 <https://openreview.net/forum?id=6awxwQEi82>.

833 Yinuo Ren, Haoxuan Chen, Yuchen Zhu, Wei Guo, Yongxin Chen, Grant M. Rotskoff, Molei Tao,  
 834 and Lexing Ying. Fast solvers for discrete diffusion models: Theory and applications of high-order  
 835 algorithms. In *The Thirty-ninth Annual Conference on Neural Information Processing Systems*,  
 836 2025b. URL <https://openreview.net/forum?id=Ouk1L6Q3sO>.

837 Lorenz Richter and Julius Berner. Improved sampling via learned diffusions. In *The Twelfth  
 838 International Conference on Learning Representations*, 2024. URL <https://openreview.net/forum?id=h4pNROsO06>.

839 Herbert E. Robbins. *An Empirical Bayes Approach to Statistics*, pp. 388–394. Springer New York,  
 840 New York, NY, 1992. ISBN 978-1-4612-0919-5. doi: 10.1007/978-1-4612-0919-5\_26. URL  
 841 [https://doi.org/10.1007/978-1-4612-0919-5\\_26](https://doi.org/10.1007/978-1-4612-0919-5_26).

842 Hamza Ruzayqat, Neil K Chada, and Ajay Jasra. Multilevel estimation of normalization constants  
 843 using ensemble Kalman–Bucy filters. *Statistics and Computing*, 32(3):38, 2022. doi: 10.1007/  
 844 s11222-022-10094-2.

845 Michael Eli Sander, Vincent Roulet, Tianlin Liu, and Mathieu Blondel. Joint learning of energy-  
 846 based models and their partition function. In *Forty-second International Conference on Machine  
 847 Learning*, 2025. URL <https://openreview.net/forum?id=uPgr7MzPKI>.

848 Filippo Santambrogio. *Optimal Transport for Applied Mathematicians*. Birkhäuser Cham, 2015. doi:  
 849 10.1007/978-3-319-20828-2.

850 Christoph Schönle, Marylou Gabrié, Tony Lelièvre, and Gabriel Stoltz. Sampling metastable systems  
 851 using collective variables and Jarzynski–Crooks paths. *Journal of Computational Physics*, 527:  
 852 113806, 2025. ISSN 0021-9991. doi: <https://doi.org/10.1016/j.jcp.2025.113806>. URL <https://www.sciencedirect.com/science/article/pii/S0021999125000890>.

853 Udo Seifert. Stochastic thermodynamics, fluctuation theorems and molecular machines. *Reports  
 854 on Progress in Physics*, 75(12):126001, nov 2012. doi: 10.1088/0034-4885/75/12/126001. URL  
 855 <https://dx.doi.org/10.1088/0034-4885/75/12/126001>.

864 Ken Sekimoto. *Stochastic Energetics*. Lecture Notes in Physics. Springer, 1 edition, 2010. doi:  
 865 10.1007/978-3-642-05411-2.  
 866

867 Jascha Sohl-Dickstein and Benjamin J Culpepper. Hamiltonian annealed importance sampling  
 868 for partition function estimation. Technical report, Redwood Technical Report, 2012. URL  
 869 <http://arxiv.org/abs/1205.1925>.

870 Yang Song and Diederik P Kingma. How to train your energy-based models. *arXiv preprint*  
 871 *arXiv:2101.03288*, 2021.  
 872

873 Yang Song, Jascha Sohl-Dickstein, Diederik P Kingma, Abhishek Kumar, Stefano Ermon, and Ben  
 874 Poole. Score-based generative modeling through stochastic differential equations. In *International*  
 875 *Conference on Learning Representations*, 2021. URL <https://openreview.net/forum?id=PxTIG12RRHS>.

876 Jingtong Sun, Julius Berner, Lorenz Richter, Marius Zeinhofer, Johannes Müller, Kamyar Aziz-  
 877 zadenesheli, and Anima Anandkumar. Dynamical measure transport and neural PDE solvers for  
 878 sampling. *arXiv preprint arXiv:2407.07873*, 2024.  
 879

880 Saifuddin Syed, Alexandre Bouchard-Côté, George Deligiannidis, and Arnaud Doucet. Non-  
 881 reversible parallel tempering: A scalable highly parallel MCMC scheme. *Journal of the Royal*  
 882 *Statistical Society Series B: Statistical Methodology*, 84(2):321–350, 12 2021. ISSN 1369-7412.  
 883 doi: 10.1111/rssb.12464. URL <https://doi.org/10.1111/rssb.12464>.  
 884

885 Saifuddin Syed, Alexandre Bouchard-Côté, Kevin Chern, and Arnaud Doucet. Optimised annealed  
 886 sequential Monte Carlo samplers. *arXiv preprint arXiv:2408.12057*, 2024.  
 887

888 Nicholas G Tawn, Gareth O Roberts, and Jeffrey S Rosenthal. Weight-preserving simulated tempering.  
 889 *Statistics and Computing*, 30(1):27–41, 2020. doi: 10.1007/s11222-019-09863-3.  
 890

891 Ali Süleyman Üstünel and Moshe Zakai. *Transformation of Measure on Wiener Space*. Springer  
 892 Monographs in Mathematics. Springer Berlin, Heidelberg, 1 edition, 2013. doi: 10.1007/  
 893 978-3-662-13225-8.

894 Adrien Vacher, Omar Chehab, and Anna Korba. Sampling from multi-modal distributions with  
 895 polynomial query complexity in fixed dimension via reverse diffusion. In *The Thirty-ninth Annual*  
 896 *Conference on Neural Information Processing Systems*, 2025. URL <https://openreview.net/forum?id=Ex72DkOeNS>.  
 897

898 Suriyanarayanan Vaikuntanathan and Christopher Jarzynski. Escorted free energy simulations:  
 899 Improving convergence by reducing dissipation. *Phys. Rev. Lett.*, 100:190601, May 2008.  
 900 doi: 10.1103/PhysRevLett.100.190601. URL <https://link.aps.org/doi/10.1103/PhysRevLett.100.190601>.  
 901

902 Francisco Vargas, Shreyas Padhy, Denis Blessing, and Nikolas Nüsken. Transport meets variational  
 903 inference: Controlled Monte Carlo diffusions. In *The Twelfth International Conference on Learning*  
 904 *Representations*, 2024. URL <https://openreview.net/forum?id=PP1rudnxiW>.  
 905

906 Cédric Villani. *Topics in optimal transportation*, volume 58. American Mathematical Society, 2003.

907 Cédric Villani. *Optimal Transport: Old and New*. Grundlehren der mathematischen Wissenschaften.  
 908 Springer Berlin, Heidelberg, 1 edition, 2008. doi: 10.1007/978-3-540-71050-9. URL <https://link.springer.com/book/10.1007/978-3-540-71050-9>.  
 909

910 Dawn Woodard, Scott Schmidler, and Mark Huber. Sufficient conditions for torpid mixing of parallel  
 911 and simulated tempering. *Electronic Journal of Probability*, 14(none):780 – 804, 2009. doi:  
 912 10.1214/EJP.v14-638. URL <https://doi.org/10.1214/EJP.v14-638>.  
 913

914 Muneki Yasuda and Chako Takahashi. Free energy evaluation using marginalized annealed importance  
 915 sampling. *Phys. Rev. E*, 106:024127, Aug 2022. doi: 10.1103/PhysRevE.106.024127. URL  
 916 <https://link.aps.org/doi/10.1103/PhysRevE.106.024127>.  
 917

918 Qinsheng Zhang and Yongxin Chen. Path integral sampler: A stochastic control approach for  
 919 sampling. In *International Conference on Learning Representations*, 2022. URL [https://openreview.net/forum?id=\\_uCb2ynRu7Y](https://openreview.net/forum?id=_uCb2ynRu7Y).

920

921 Qinsheng Zhang and Yongxin Chen. Fast sampling of diffusion models with exponential integrator.  
 922 In *The Eleventh International Conference on Learning Representations*, 2023. URL <https://openreview.net/forum?id=Loek7hfb46P>.

923

924 Qinsheng Zhang, Jiaming Song, and Yongxin Chen. Improved order analysis and design of exponential  
 925 integrator for diffusion models sampling. *arXiv preprint arXiv:2308.02157*, 2023a.

926

927 Qinsheng Zhang, Molei Tao, and Yongxin Chen. gDDIM: Generalized denoising diffusion implicit  
 928 models. In *The Eleventh International Conference on Learning Representations*, 2023b. URL  
 929 <https://openreview.net/forum?id=1hKE9qjvz->.

930

931 Daniel M. Zuckerman and Thomas B. Woolf. Theory of a systematic computational error in free  
 932 energy differences. *Phys. Rev. Lett.*, 89:180602, Oct 2002. doi: 10.1103/PhysRevLett.89.180602.  
 933 URL <https://link.aps.org/doi/10.1103/PhysRevLett.89.180602>.

934

935 Daniel M. Zuckerman and Thomas B. Woolf. Systematic finite-sampling inaccuracy in free energy  
 936 differences and other nonlinear quantities. *Journal of Statistical Physics*, 114:1303–1323, 3 2004.  
 937 doi: 10.1023/B:JOSS.0000013961.84860.5b.

938

939

940

941

942

943

944

945

946

947

948

949

950

951

952

953

954

955

956

957

958

959

960

961

962

963

964

965

966

967

968

969

970

971

972	CONTENTS	
973		
974		
975	<b>1</b> <b>Introduction</b>	<b>1</b>
976		
977	<b>2</b> <b>Preliminaries and Problem Setting</b>	<b>3</b>
978		
979	<b>3</b> <b>Analysis of the Jarzynski Equality</b>	<b>4</b>
980		
981	<b>4</b> <b>Analysis of the Annealed Importance Sampling</b>	<b>6</b>
982		
983	<b>5</b> <b>Normalizing Constant Estimation via Denoising Diffusion</b>	<b>8</b>
984		
985	<b>6</b> <b>Conclusion, Limitations, and Future Directions</b>	<b>10</b>
986		
987		
988	<b>A</b> <b>Preliminaries</b>	<b>21</b>
989		
990	A.1 Stochastic Analysis: Forward-backward SDEs and Girsanov's Theorem . . . . .	21
991	A.2 Optimal Transport: Wasserstein Geometry and Metric Derivative . . . . .	24
992		
993	<b>B</b> <b>Pseudo-codes of the Algorithms</b>	<b>24</b>
994		
995	<b>C</b> <b>Proofs for Sec. 3</b>	<b>24</b>
996		
997	C.1 A Complete Proof of Thm. 1 . . . . .	24
998	C.2 Proof of Thm. 2 . . . . .	25
999		
1000	<b>D</b> <b>Proof of Thm. 4</b>	<b>27</b>
1001		
1002	<b>E</b> <b>Proofs for Sec. 5</b>	<b>33</b>
1003		
1004	E.1 Proof of Prop. 1 . . . . .	33
1005	E.2 Proof of Prop. 2 . . . . .	36
1006	E.3 Proof of Thm. 5 . . . . .	36
1007	E.4 An Upper Bound of the TV Distance along the OU Process . . . . .	37
1008	E.5 Discussion on the Overall Complexity of RDS . . . . .	38
1009		
1010	<b>F</b> <b>Supplementary Lemmas</b>	<b>39</b>
1011		
1012	<b>G</b> <b>Review and Discussion on the Error Guarantee (1)</b>	<b>41</b>
1013		
1014	G.1 Literature Review of Existing Bounds . . . . .	41
1015	G.2 Equivalence in Complexities for Estimating $Z$ and $F$ . . . . .	42
1016	G.3 (1) is Weaker than Bias and Variance . . . . .	42
1017	G.4 An Upper Bound on the Normalized Variance of $\hat{Z}$ in Jarzynski Equality . . . . .	42
1018		
1019	<b>H</b> <b>Related Works</b>	<b>43</b>
1020		
1021	H.1 Thermodynamic Integration . . . . .	43
1022	H.2 Path Integral Sampler and Controlled Monte Carlo Diffusion . . . . .	45
1023		

1026	<b>I Details of Experimental Results</b>	<b>46</b>
1027		
1028	I.1 Modified Müller Brown distribution . . . . .	46
1029	I.2 Gaussian Mixture Distribution . . . . .	47
1030	I.3 Implementation Details . . . . .	47
1031		
1032		
1033		
1034		
1035		
1036		
1037		
1038		
1039		
1040		
1041		
1042		
1043		
1044		
1045		
1046		
1047		
1048		
1049		
1050		
1051		
1052		
1053		
1054		
1055		
1056		
1057		
1058		
1059		
1060		
1061		
1062		
1063		
1064		
1065		
1066		
1067		
1068		
1069		
1070		
1071		
1072		
1073		
1074		
1075		
1076		
1077		
1078		
1079		

1080 **A PRELIMINARIES**  
 1081

1082 **A.1 STOCHASTIC ANALYSIS: FORWARD-BACKWARD SDES AND GIRSANOV'S THEOREM**  
 1083

1084 For a stochastic differential equation (SDE)  $X = (X_t)_{t \in [0, T]}$  defined on  $\Omega = C([0, T]; \mathbb{R}^d)$ , the  
 1085 distribution of  $X$  over  $\Omega$  is called the **path measure** of  $X$ , defined by  $\mathbb{P}^X$ : measurable  $A \subset \Omega \mapsto$   
 1086  $\Pr(X \in A)$ . The following lemma, as a corollary of the **Girsanov's theorem** (Üstünel & Zakai, 2013,  
 1087 Prop. 2.3.1 & Cor. 2.3.1), provides a method for computing the Radon-Nikodým (RN) derivative and  
 1088 KL divergence between two path measures, which serves as a key technical tool in our proof.

1089 **Lemma 1.** *Assume we have the following two SDEs with  $t \in [0, T]$ :*

1090 
$$dX_t = a_t(X_t)dt + \sigma dB_t, \quad X_0 \sim \mu; \quad dY_t = b_t(Y_t)dt + \sigma dB_t, \quad Y_0 \sim \nu.$$
  
 1091

1092 Denote the path measures of  $X$  and  $Y$  as  $\mathbb{P}^X$  and  $\mathbb{P}^Y$ , respectively. Then for any trajectory  $\xi \in \Omega$ ,

1093 
$$\log \frac{d\mathbb{P}^X}{d\mathbb{P}^Y}(\xi) = \log \frac{d\mu}{d\nu}(\xi_0) + \frac{1}{\sigma^2} \int_0^T \langle a_t(\xi_t) - b_t(\xi_t), d\xi_t \rangle - \frac{1}{2\sigma^2} \int_0^T (\|a_t(\xi_t)\|^2 - \|b_t(\xi_t)\|^2) dt.$$
  
 1094

1095 In particular, plugging in  $\xi \leftarrow X \sim \mathbb{P}^X$ , we can compute the KL divergence:

1096 
$$\text{KL}(\mathbb{P}^X \parallel \mathbb{P}^Y) = \text{KL}(\mu \parallel \nu) + \frac{1}{2\sigma^2} \int_0^T \mathbb{E}_{\mathbb{P}^X} \|a_t(X_t) - b_t(X_t)\|^2 dt.$$
  
 1097

1098 **Remark 3.** The Girsanov's theorem requires a technical condition ensuring that a local martingale  
 1099 is a true martingale, typically verified via the Novikov condition (Karatzas & Shreve, 1991, Chap. 3,  
 1100 Cor. 5.13), which can be challenging to establish. However, when only an upper bound of the KL  
 1101 divergence is needed, the approximation argument from Chen et al. (2023, App. B.2) circumvents  
 1102 the verification of the Novikov condition. For additional context, see Chewi (2022, Sec. 3.2). In this  
 1103 paper, we omit these technical details and always assume that the Novikov condition holds.

1104 We now present the theory of backward stochastic integral and the Girsanov's theorem, which  
 1105 are adapted from Vargas et al. (2024). Here, we include relevant results and proofs to ensure a  
 1106 self-contained presentation.

1107 The backward SDE can be perceived as the time-reversal of a forward SDE:

1108 **Definition 1** (Backward SDE). *Given a BM  $(B_t)_{t \in [0, T]}$ , let its time-reversal be  $(B_t^\leftarrow :=$   
 1109  $B_{T-t})_{t \in [0, T]}$ . We say that a process  $(X_t^\leftarrow)_{t \in [0, T]}$  satisfies the **backward SDE***

1110 
$$dX_t^\leftarrow = a_t(X_t^\leftarrow)dt + \sigma dB_t^\leftarrow, \quad t \in [0, T]; \quad X_T^\leftarrow \sim \nu$$
  
 1111

1112 if its time-reversal  $(X_t = X_{T-t}^\leftarrow)_{t \in [0, T]}$  satisfies the following forward SDE:

1113 
$$dX_t = -a_{T-t}(X_t)dt + \sigma dB_t, \quad t \in [0, T]; \quad X_0 \sim \nu.$$
  
 1114

1115 **Remark 4.** Intuitively, one can understand the backward SDE through the following Euler-Maruyama  
 1116 discretization: with  $\Delta t > 0$ :

1117 
$$\begin{aligned} X_{t-\Delta t}^\leftarrow &\approx X_t^\leftarrow + a_t(X_t^\leftarrow)(-\Delta t) + \sigma(B_{t-\Delta t}^\leftarrow - B_t^\leftarrow) \\ \iff X_{T-t+\Delta t} &\approx X_{T-t} - a_t(X_{T-t})\Delta t + \sigma(B_{T-t+\Delta t} - B_{T-t}). \end{aligned}$$
  
 1118

1119 where  $B_{t-\Delta t}^\leftarrow - B_t^\leftarrow \sim \mathcal{N}(0, \Delta t I)$  and is independent of  $(X_s^\leftarrow)_{s \in [t, T]}$ .

1120 The forward and backward SDEs are related through the following Nelson's relation:

1121 **Lemma 2** (Nelson's relation (Nelson, 1967; Anderson, 1982)). *Given a BM  $(B_t)_{t \in [0, T]}$  and its  
 1122 time-reversal  $(B_t^\leftarrow = B_{T-t})_{t \in [0, T]}$ , the following two SDEs*

1123 
$$dX_t = a_t(X_t)dt + \sigma dB_t, \quad X_0 \sim p_0; \quad \text{and} \quad dY_t = b_t(Y_t)dt + \sigma dB_t^\leftarrow, \quad Y_T \sim q$$
  
 1124

1125 have the same path measure if and only if

1126 
$$q = p_T, \quad \text{and} \quad b_t = a_t - \sigma^2 \nabla \log p_t, \quad \forall t \in [0, T],$$
  
 1127

1128 where  $p_t$  is the p.d.f. of  $X_t$ .

1134 *Proof.* The proof is by verifying the Fokker-Planck equation. For  $X$ , we have  
 1135

$$1136 \quad \partial_t p_t = -\nabla \cdot (a_t p_t) + \frac{\sigma^2}{2} \Delta p_t.$$

1138 Let  $\star_t^\leftarrow := \star_{T-t}$ . Then  $p_t^\leftarrow$  satisfies  
 1139

$$1140 \quad \partial_t p_t^\leftarrow = \nabla \cdot (a_t^\leftarrow p_t^\leftarrow) - \frac{\sigma^2}{2} \Delta p_t^\leftarrow = -\nabla \cdot ((-a_t^\leftarrow + \sigma^2 \nabla \log p_t^\leftarrow) p_t^\leftarrow) + \frac{\sigma^2}{2} \Delta p_t^\leftarrow,$$

1141 which means  $(X_t^\leftarrow)_{t \in [0, T]}$  has the same path measure as the following SDE:  
 1142

$$1143 \quad dZ_t = -(a_t^\leftarrow - \sigma^2 \nabla \log p_t^\leftarrow)(Z_t) dt + \sigma dB_t, \quad Z_t \sim p_t^\leftarrow.$$

1144 On the other hand, by definition,  $(Y_t^\leftarrow)_{t \in [0, T]}$  satisfies the forward SDE  
 1145

$$1146 \quad dY_t^\leftarrow = -b_t^\leftarrow(Y_t^\leftarrow) dt + \sigma dB_t, \quad Y_0 \sim q,$$

1147 and thus the claim is evident.  $\square$   
 1148

1149 We now introduce the concept of backward stochastic integral, which allows us to represent the RN  
 1150 derivative between path measures of forward and backward SDEs.  
 1151

1152 **Definition 2** (Backward stochastic integral). *For two continuous stochastic processes  $X$  and  $Y$  on  
 1153  $C([0, T]; \mathbb{R}^d)$ , the **backward stochastic integral** of  $Y$  with respect to  $X$  is defined as*

$$1154 \quad \int_0^T \langle Y_t, *dX_t \rangle := \Pr - \lim_{\|\Pi\| \rightarrow 0} \sum_{i=0}^{n-1} \langle Y_{t_{i+1}}, X_{t_{i+1}} - X_{t_i} \rangle,$$

1155 where  $\Pi = \{0 = t_0 < t_1 < \dots < t_n = T\}$  is a partition of  $[0, T]$ ,  $\|\Pi\| := \max_{i \in [1, n]} (t_{i+1} - t_i)$ , and  
 1156 the convergence is in the probability sense. When both  $X$  and  $Y$  are continuous semi-martingales,  
 1157 one can equivalently define  
 1158

$$1159 \quad \int_0^T \langle Y_t, *dX_t \rangle := \int_0^T \langle Y_t, dX_t \rangle + [X, Y]_T, \quad (15)$$

1160 where  $[X, Y]$  is the cross quadratic variation process<sup>6</sup> of the local martingale parts of  $X$  and  $Y$ .  
 1161

1162 **Remark 5.** Although rarely used in practice, the backward stochastic integral is sometimes referred  
 1163 to as the Hänggi-Klimontovich integral in the literature. Recall that the Itô integral is defined as the  
 1164 limit of Riemann sums when the leftmost point of each interval is used, while the Stratonovich integral  
 1165 is based on the midpoint and the backward integral uses the rightmost point. The equivalence in (15)  
 1166 can be justified in Karatzas & Shreve (1991, Chap. 3.3).  
 1167

1168 **Lemma 3** (Continuation of Lem. 1). **1.** *If we replace the SDEs in Lem. 1 with*

$$1169 \quad dX_t = a_t(X_t) dt + \sigma dB_t^\leftarrow, \quad X_T \sim \mu; \quad dY_t = b_t(Y_t) dt + \sigma dB_t^\leftarrow, \quad Y_T \sim \nu,$$

1170 while keeping other assumptions and notations unchanged, then for any trajectory  $\xi \in \Omega$ ,

$$1171 \quad \log \frac{d\mathbb{P}^X}{d\mathbb{P}^Y}(\xi) = \log \frac{d\mu}{d\nu}(\xi_T) + \frac{1}{\sigma^2} \int_0^T \langle a_t(\xi_t) - b_t(\xi_t), *d\xi_t \rangle - \frac{1}{2\sigma^2} \int_0^T (\|a_t(\xi_t)\|^2 - \|b_t(\xi_t)\|^2) dt,$$

1172 and consequently,

$$1173 \quad \text{KL}(\mathbb{P}^X \| \mathbb{P}^Y) = \text{KL}(\mu \| \nu) + \frac{1}{2\sigma^2} \int_0^T \mathbb{E}_{\mathbb{P}^X} \|a_t(X_t) - b_t(X_t)\|^2 dt.$$

1174 **2.** *Define the following two SDEs from 0 to  $T$ :*

$$1175 \quad dX_t = a_t(X_t) dt + \sigma dB_t, \quad X_0 \sim \mu; \quad dY_t = b_t(Y_t) dt + \sigma dB_t^\leftarrow, \quad Y_T \sim \nu.$$

1176 Denote the path measures of  $X$  and  $Y$  as  $\mathbb{P}^X$  and  $\mathbb{P}^Y$ , respectively. Then for any trajectory  $\xi \in \Omega$ ,

$$1177 \quad \log \frac{d\mathbb{P}^X}{d\mathbb{P}^Y}(\xi) = \log \frac{\mu(\xi_0)}{\nu(\xi_T)} + \frac{1}{\sigma^2} \int_0^T (\langle a_t(\xi_t), d\xi_t \rangle - \langle b_t(\xi_t), *d\xi_t \rangle) - \frac{1}{2\sigma^2} \int_0^T (\|a_t(\xi_t)\|^2 - \|b_t(\xi_t)\|^2) dt.$$

1178 <sup>6</sup>The notation used in Karatzas & Shreve (1991) is  $\langle \cdot, \cdot \rangle_.$  We use square brackets here to avoid conflict with  
 1179 the notation for inner product.

1188 *Proof. 1. Only in the proof of this theorem, we use the notation  $\star_t^\leftarrow := \star_{T-t}$  to represent the time  
1189 reversal.* We know that  
1190

$$1191 \quad dX_t^\leftarrow = -a_t^\leftarrow(X_t^\leftarrow)dt + \sigma dB_t, \quad X_0^\leftarrow \sim \mu; \quad dY_t^\leftarrow = -b_t^\leftarrow(Y_t^\leftarrow)dt + \sigma dB_t, \quad Y_0^\leftarrow \sim \nu.$$

1192 Let  $\mathbb{P}^{X^\leftarrow}$  and  $\mathbb{P}^{Y^\leftarrow}$  be the path measures of  $X^\leftarrow$  and  $Y^\leftarrow$ , respectively. From Lem. 1, we know that  
1193

$$1194 \quad \log \frac{d\mathbb{P}^{X^\leftarrow}}{d\mathbb{P}^{Y^\leftarrow}}(\xi) = \log \frac{d\mu}{d\nu}(\xi_0) - \frac{1}{\sigma^2} \int_0^T \langle a_t^\leftarrow(\xi_t) - b_t^\leftarrow(\xi_t), d\xi_t \rangle - \frac{1}{2\sigma^2} \int_0^T (\|a_t^\leftarrow(\xi_t)\|^2 - \|b_t^\leftarrow(\xi_t)\|^2)dt.$$

1197 Since  $\mathbb{P}^{X^\leftarrow}(d\xi) = \Pr(X^\leftarrow \in d\xi) = \Pr(X \in d\xi^\leftarrow) = \mathbb{P}^X(d\xi^\leftarrow)$ , we obtain  
1198

$$\begin{aligned} 1199 \quad \log \frac{d\mathbb{P}^X}{d\mathbb{P}^Y}(\xi) &= \log \frac{d\mathbb{P}^{X^\leftarrow}}{d\mathbb{P}^{Y^\leftarrow}}(\xi^\leftarrow) \\ 1200 &= \log \frac{d\mu}{d\nu}(\xi_0^\leftarrow) - \frac{1}{\sigma^2} \int_0^T \langle a_t^\leftarrow(\xi_t^\leftarrow) - b_t^\leftarrow(\xi_t^\leftarrow), d\xi_t^\leftarrow \rangle - \frac{1}{2\sigma^2} \int_0^T (\|a_t^\leftarrow(\xi_t^\leftarrow)\|^2 - \|b_t^\leftarrow(\xi_t^\leftarrow)\|^2)dt \\ 1201 &= \log \frac{d\mu}{d\nu}(\xi_T) + \frac{1}{\sigma^2} \int_0^T \langle a_t(\xi_t) - b_t(\xi_t), *d\xi_t \rangle - \frac{1}{2\sigma^2} \int_0^T (\|a_t(\xi_t)\|^2 - \|b_t(\xi_t)\|^2)dt. \end{aligned}$$

1206 To justify the last equality, if  $\xi, \eta$  are two continuous stochastic processes, then by definition,  
1207

$$\begin{aligned} 1208 \quad \int_0^T \langle \xi_t^\leftarrow, d\eta_t^\leftarrow \rangle &= \Pr \lim_{\|\Pi\| \rightarrow 0} \sum_{i=0}^{n-1} \langle \xi_{t_{i-1}}^\leftarrow, \eta_{t_i}^\leftarrow - \eta_{t_{i-1}}^\leftarrow \rangle \\ 1209 &= \Pr \lim_{\|\Pi\| \rightarrow 0} \sum_{i=0}^{n-1} \langle \xi_{T-t_{i-1}}, \eta_{T-t_i} - \eta_{T-t_{i-1}} \rangle \\ 1210 &= \Pr \lim_{\|\Pi\| \rightarrow 0} - \sum_{i=0}^{n-1} \langle \xi_{T-t_{i-1}}, \eta_{T-t_{i-1}} - \eta_{T-t_i} \rangle \\ 1211 &= - \int_0^T \langle \xi_t, *d\eta_t \rangle. \end{aligned} \tag{16}$$

1219 On the other hand,

$$1221 \quad \int_0^T \xi_t^\leftarrow dt = \int_0^T \xi_{T-t} dt = \int_0^T \xi_t dt.$$

1224 Therefore, the equality of RN derivative holds. Plugging in  $\xi \leftarrow X$ , we have  
1225

$$1226 \quad \log \frac{d\mathbb{P}^X}{d\mathbb{P}^Y}(X) = \log \frac{d\mu}{d\nu}(X_T) + \frac{1}{\sigma} \int_0^T \langle a_t(X_t) - b_t(X_t), *dB_t^\leftarrow \rangle + \frac{1}{2\sigma^2} \int_0^T \|a_t(X_t) - b_t(X_t)\|^2 dt.$$

1228 To obtain the KL divergence, it suffices to show the expectation of the second term is zero. Let  
1229

$$1230 \quad M_t := \int_t^T \langle a_r(X_r) - b_r(X_r), *dB_r^\leftarrow \rangle, \quad t \in [0, T].$$

1232 By (16), we have  
1233

$$1234 \quad M_t^\leftarrow = - \int_0^t \langle a_r^\leftarrow(X_r^\leftarrow) - b_r^\leftarrow(X_r^\leftarrow), dB_r \rangle.$$

1236 Since  $dX_t^\leftarrow = -a_t^\leftarrow(X_t^\leftarrow)dt + \sigma dB_t$ , we conclude that  $M_t^\leftarrow$  is a (forward) martingale, and thus  $M$   
1237 is a *backward* martingale with  $\mathbb{E} M_t = \mathbb{E} M_{T-t}^\leftarrow = 0$ .  
1238

1239 **2.** We present a formal proof by considering the process  $dZ_t = \sigma dB_t$  and  $Z_0 \sim \lambda$ , the Lebesgue  
1240 measure. As a result, formally  $Z_t \sim \lambda$  for all  $t$ , so it can also be written as  $dZ_t = \sigma dB_t^\leftarrow$ ,  $Z_T \sim \lambda$ .  
1241 The result follows by applying Lem. 1 to  $X$  and  $Z$  and **1.** to  $Y$  and  $Z$ .  
1242

□

1242 A.2 OPTIMAL TRANSPORT: WASSERSTEIN GEOMETRY AND METRIC DERIVATIVE  
12431244 We provide a concise overview of essential concepts in optimal transport (OT) that will be used in the  
1245 paper. See standard textbooks (Villani, 2003; 2008; Ambrosio et al., 2008; 2021) for details.1246 For two probability measures  $\mu, \nu$  on  $\mathbb{R}^d$  with finite second-order moments (i.e.,  $\mathbb{E}_\mu \|\cdot\|^2, \mathbb{E}_\nu \|\cdot\|^2 < \infty$ ), the **Wasserstein-2 (W<sub>2</sub>) distance** between  $\mu$  and  $\nu$  is defined as  $W_2(\mu, \nu) = \inf_{\gamma \in \Pi(\mu, \nu)} (\int \|x - y\|^2 \gamma(dx, dy))^{1/2}$ , where  $\Pi(\mu, \nu)$  is the set of all couplings of  $(\mu, \nu)$ . The Brenier's theorem states that when  $\mu$  has a Lebesgue density, then there exists a unique coupling  $(\text{id} \times T_{\mu \rightarrow \nu})_\# \mu$  that reaches the infimum. Here,  $\#$  stands for the push-forward of a measure (defined by  $T_\# \mu(\cdot) = \mu(\{\omega : T(\omega) \in \cdot\})$ ), and  $T_{\mu \rightarrow \nu}$  is known as the **OT map** from  $\mu$  to  $\nu$ , which can be written as the gradient of a convex function.1254 Given a vector field  $v = (v_t)_{t \in [a, b]}$  and a curve of probability measures  $\rho = (\rho_t)_{t \in [a, b]}$  with finite  
1255 second-order moment on  $\mathbb{R}^d$ , we say that  $v$  **generates**  $\rho$  if the continuity equation  $\partial_t \rho_t + \nabla \cdot (\rho_t v_t) = 0$ ,  
1256  $t \in [a, b]$  holds in the weak sense. The **metric derivative** of  $\rho$  at  $t \in [a, b]$  is defined as

1257 
$$|\dot{\rho}|_t := \lim_{\delta \rightarrow 0} \frac{W_2(\rho_{t+\delta}, \rho_t)}{|\delta|},$$
  
1258

1259 which can be interpreted as the speed of this curve. We say  $\rho$  is **absolutely continuous** if  $|\dot{\rho}|_t$  exists  
1260 and is finite for Lebesgue-a.e.  $t \in [a, b]$ . The metric derivative and the continuity equation are related  
1261 through the following fact (Ambrosio et al., 2008, Thm. 8.3.1 & Prop. 8.4.5):1262 **Lemma 4.** *For an absolutely continuous curve of probability measures  $(\rho_t)_{t \in [a, b]}$ , any vector field*  
1263  $(v_t)_{t \in [a, b]}$  *that generates  $(\rho_t)_{t \in [a, b]}$  satisfies  $|\dot{\rho}|_t \leq \|v_t\|_{L^2(\rho_t)}$  for Lebesgue-a.e.  $t \in [a, b]$ . Moreover,*  
1264 *there exists an a.s. unique vector field  $(v_t^* \in L^2(\rho_t))_{t \in [a, b]}$  that generates  $(\rho_t)_{t \in [a, b]}$  and satisfies*  
1265  $|\dot{\rho}|_t = \|v_t^*\|_{L^2(\rho_t)}$  *for Lebesgue-a.e.  $t \in [a, b]$ , which is  $v_t^* = \lim_{\delta \rightarrow 0} \frac{T_{\rho_t \rightarrow \rho_{t+\delta}} - \text{id}}{\delta}$ .*1266 Finally, we define the **action** of an absolutely continuous curve of probability measures  $(\rho_t)_{t \in [a, b]}$  as  
1267  $\int_a^b |\dot{\rho}|_t^2 dt$ , which plays a key role in characterizing the efficiency of a curve for normalizing constant  
1268 estimation. For basic properties of the action and its relation to isoperimetric inequalities such as  
1269 log-Sobolev and Poincaré inequalities (see definitions below), we refer the reader to Guo et al. (2025,  
1270 Lem. 3 & Ex. 1).1271 **Definition 3** (Isoperimetric inequalities). *A probability measure  $\pi$  on  $\mathbb{R}^d$  satisfies a **Poincaré inequality (PI)** with constant  $C$ , or **C-PI**, if for all  $f \in C_c^\infty(\mathbb{R}^d)$ ,*

1272 
$$\text{Var}_\pi f \leq C \mathbb{E}_\pi \|\nabla f\|^2.$$

1273 *It satisfies a **log-Sobolev inequality (LSI)** with constant  $C$ , or **C-LSI**, if for all  $0 \not\equiv f \in C_c^\infty(\mathbb{R}^d)$ ,*

1274 
$$\mathbb{E}_\pi f^2 \log \frac{f^2}{\mathbb{E}_\pi f^2} \leq 2C \mathbb{E}_\pi \|\nabla f\|^2.$$

1275 *Furthermore,  $\alpha$ -strong-log-concavity implies  $\frac{1}{\alpha}$ -LSI, and C-LSI implies C-PI (Bakry et al., 2014).*1281 B PSEUDO-CODES OF THE ALGORITHMS  
1282

1283 See Algs. 1 and 2 for the detailed implementation of the AIS and RDS algorithms, respectively.

1285 C PROOFS FOR SEC. 3  
12861287 C.1 A COMPLETE PROOF OF THM. 1  
12881289 *Proof.* By Girsanov's theorem (Lem. 3), we have

1290 
$$\log \frac{d\mathbb{P}^\rightarrow}{d\mathbb{P}^\leftarrow}(\xi) = \log \frac{\tilde{\pi}_0(\xi_0)}{\tilde{\pi}_T(\xi_T)} + \frac{1}{2} \int_0^T (\langle \nabla \log \tilde{\pi}_t(\xi_t), d\xi_t \rangle + \langle \nabla \log \tilde{\pi}_t(\xi_t), *d\xi_t \rangle).$$

1291 We first prove the following result (Vargas et al., 2024, Eq. (15)): if  $dx_t = a_t(x_t)dt + \sqrt{2}dB_t$ , then  
1292

1293 
$$\int_0^T \langle a_t(x_t), *dx_t \rangle = \int_0^T \langle a_t(x_t), dx_t \rangle + 2 \int_0^T \text{tr} \nabla a_t(X_t) dt.$$

---

1296 **Algorithm 1:** Normalizing constant estimation via AIS.

1297 **Input:** The target distribution  $\pi \propto e^{-V}$ , smoothness parameter  $\beta$ , total time  $T$ ; **TI** number of  
 1298 intermediate distributions  $K$ , annealing schedule  $\lambda_0 > \dots > \lambda_K = 0$ , number of particles  
 1299  $N$ ; **AIS** steps  $M$ , annealing schedule  $\lambda(\cdot)$  with  $\lambda(0) = 2\beta$ , time points  
 1300  $0 = \theta_0 < \dots < \theta_M = 1$ .

1301 **Output:**  $\hat{Z}$ , an estimation of  $Z = \int_{\mathbb{R}^d} e^{-V(x)} dx$ .

1302 1 // Phase 1: estimate  $Z_0$  via **TI**.

1303 2 Define  $V_0 := V + \beta \|\cdot\|^2$ ,  $\rho_k := \exp(-V_0 - \frac{\lambda_k}{2} \|\cdot\|^2)$ , and  $g_k := \exp\left(\frac{\lambda_k - \lambda_{k+1}}{2} \|\cdot\|^2\right)$ , for  
 1304  $k \in [0, K-1]$ ;

1305 3 Initialize  $\hat{Z}_0 \leftarrow \exp\left(-V_0(0) + \frac{\|\nabla V_0(0)\|^2}{2(3\beta + \lambda_0)}\right) \left(\frac{2\pi}{3\beta + \lambda_0}\right)^{\frac{d}{2}}$ ;

1306 4 **for**  $k = 0$  **to**  $K-1$  **do**

1307   5 Obtain  $N$  i.i.d. approximate samples  $x_1^{(k)}, \dots, x_N^{(k)}$  from  $\rho_k$  (e.g., using LMC or proximal  
 1308 sampler);

1309   6 Update  $\hat{Z}_0 \leftarrow \left(\frac{1}{N} \sum_{n=1}^N g_k(X_n^{(k)})\right) \hat{Z}_0$ ;

1310 7 **end**

1311 8 // Phase 2: estimate  $Z$  via **AIS**.

1312 9 Approximately sample  $x_0$  from  $\pi_0$  (e.g., using LMC or proximal sampler);

1313 10 Initialize  $W \leftarrow -\frac{1}{2}(\lambda(\theta_0) - \lambda(\theta_1))\|x_0\|^2$ ;

1314 11 **for**  $\ell = 1$  **to**  $M-1$  **do**

1315   12 Sample an independent  $\xi \sim \mathcal{N}(0, I_d)$ ;

1316   13 Define  $\Lambda(t) := \int_0^t \lambda\left(\theta_{\ell-1} + \frac{\tau}{T_\ell}(\theta_\ell - \theta_{\ell-1})\right) d\tau$ , where  $T_\ell := T(\theta_\ell - \theta_{\ell-1})$ ;

1317   14 Update

1318   15  $x_\ell \leftarrow e^{-\Lambda(T_\ell)} x_{\ell-1} - \left(\int_0^{T_\ell} e^{-(\Lambda(T_\ell) - \Lambda(t))} dt\right) \nabla V(x_{\ell-1}) + \left(2 \int_0^{T_\ell} e^{-2(\Lambda(T_\ell) - \Lambda(t))} dt\right)^{\frac{1}{2}} \xi$ ;  
 1319   // see Lem. 11 for the derivation.

1320   16 Update  $W \leftarrow W - \frac{1}{2}(\lambda(\theta_\ell) - \lambda(\theta_{\ell+1}))\|x_\ell\|^2$ ;

1321 17 **end**

1322 17 **return**  $\hat{Z} = \hat{Z}_0 e^{-W}$

---

1328 *Proof.* Due to (15), it suffices to calculate  $[a(X), X]_T$ . By Itô's formula, we have

1329  $da_t(x_t) = (\partial_t a_t(x_t) + \langle \nabla a_t(x_t), a_t(x_t) \rangle + \Delta a_t(x_t)) dt + \sqrt{2} \nabla a_t dB_t$ ,  
 1330 and hence

$$1331 [a(X), X]_T = \left[ \int_0^T \sqrt{2} \nabla a_t(x_t) dB_t, \int_0^T \sqrt{2} dB_t \right]_T = \text{tr} \int_0^T 2 \nabla a_t(x_t) dt.$$

1332  $\square$

1333 Therefore, for  $X \sim \mathbb{P}^{\rightarrow}$ , we have

$$1334 \log \frac{d\mathbb{P}^{\rightarrow}}{d\mathbb{P}^{\leftarrow}}(X) = \log \frac{\tilde{\pi}_0(X_0)}{\tilde{\pi}_T(X_T)} + \int_0^T (\langle \nabla \log \tilde{\pi}_t(X_t), dX_t \rangle + \Delta \log \tilde{\pi}_t(X_t) dt).$$

1335 On the other hand, by Itô's formula, we have

$$1336 d \log \tilde{\pi}_t(X_t) = \partial_t \log \tilde{\pi}_t(X_t) + \langle \nabla \log \tilde{\pi}_t(X_t), dX_t \rangle + \Delta \log \tilde{\pi}_t(X_t) dt.$$

1337 Taking the integral, we immediately obtain (4), and the proof is complete.  $\square$

## 1338 C.2 PROOF OF THM. 2

1339 *Proof.* The proof builds on the techniques developed in Guo et al. (2025, Thm. 1), yet with new  
 1340 components including backward SDE and the corresponding version of the Girsanov's theorem.

---

1350  
1351 **Algorithm 2:** Normalizing constant estimation via RDS.  
1352 **Input:** The target distribution  $\pi \propto e^{-V}$ , total time duration  $T$ , early stopping time  $\delta \geq 0$ , time  
1353 points  $0 = t_0 < t_1 < \dots < t_N = T - \delta$ ; **non-parametric score estimator**  
1354  $s_t(\cdot) \approx \nabla \log \bar{\pi}_t(\cdot)$  based on **{RDMC, RSDMC, ZODMC, or SNDMC}** algorithms.  
1355 **Output:**  $\hat{Z}$ , an estimation of  $Z = \int_{\mathbb{R}^d} e^{-V(x)} dx$ .  
1356 1 Sample  $X_0 \sim \mathcal{N}(0, I)$ , and initialize  $W := -\frac{\|X_0\|^2}{2} - \frac{d}{2} \log 2\pi$ ;  
1357 2 **for**  $k = 0$  **to**  $N - 1$  **do**  
1358 3     Sample an independent pair of  $\begin{pmatrix} \xi_1 \\ \xi_2 \end{pmatrix} \sim \mathcal{N}\left(0, \begin{pmatrix} 1 & \rho_k \\ \rho_k & 1 \end{pmatrix} \otimes I\right)$ , where the correlation is  
1359      $\rho_k = \frac{\sqrt{2}(e^{t_{k+1}-t_k} - 1)}{\sqrt{(e^{2(t_{k+1}-t_k)} - 1)(t_{k+1}-t_k)}}$ , and  $\otimes$  stands for the Kronecker product;   // this can be  
1360     done by sampling  $\xi_1, \tilde{\xi}_2 \stackrel{\text{i.i.d.}}{\sim} \mathcal{N}(0, I)$  and setting  $\xi_2 = \rho_k \xi_1 + \sqrt{1 - \rho_k^2} \tilde{\xi}_2$   
1361     4     Update  $X_{t_{k+1}} \leftarrow e^{t_{k+1}-t_k} X_{t_k} + 2(e^{t_{k+1}-t_k} - 1) s_{T-t_k}(X_{t_k}) + \sqrt{e^{2(t_{k+1}-t_k)} - 1} \xi_1$ ; // see  
1362     Lem. 12 for the derivation  
1363     5     Update  $W \leftarrow W + (t_{k+1} - t_k) \|s_{T-t_k}(X_{t_k})\|^2 + \sqrt{2(t_{k+1} - t_k)} \langle s_{T-t_k}(X_{t_k}), \xi_2 \rangle$ ; // see  
1364     Lem. 12 for the derivation  
1365     6 **end**  
1366 7     Update  $W \leftarrow W + V(X_{t_N}) - (T - \delta)d$ ;  
1367 8 **return**  $\hat{Z} = e^{-W}$ .

---

1371  
1372 We define  $\mathbb{P}$  as the path measure of the following SDE:  
1373

$$dX_t = (\nabla \log \tilde{\pi}_t + v_t)(X_t)dt + \sqrt{2}dB_t, \quad t \in [0, T]; \quad X_0 \sim \tilde{\pi}_0, \quad (17)$$

1374 where the vector field  $(v_t)_{t \in [0, T]}$  is chosen such that  $X_t \sim \tilde{\pi}_t$  under  $\mathbb{P}$  for all  $t \in [0, T]$ . According  
1375 to the Fokker-Planck equation,<sup>7</sup>  $(v_t)_{t \in [0, T]}$  must satisfy the PDE  
1376

$$\partial_t \tilde{\pi}_t = -\nabla \cdot (\tilde{\pi}_t(\nabla \log \tilde{\pi}_t + v_t)) + \Delta \tilde{\pi}_t = -\nabla \cdot (\tilde{\pi}_t v_t), \quad t \in [0, T],$$

1377 which means that  $(v_t)_{t \in [0, T]}$  generates  $(\tilde{\pi}_t)_{t \in [0, T]}$ . The Nelson's relation (Lem. 2) implies an  
1378 equivalent definition of  $\mathbb{P}$  as the path measure of the following backward SDE with an independent  
1379 time-reversed BM  $(B_t^\leftarrow)_{t \in [0, T]}$ :

$$dX_t = (-\nabla \log \tilde{\pi}_t + v_t)(X_t)dt + \sqrt{2}dB_t^\leftarrow, \quad t \in [0, T]; \quad X_T \sim \tilde{\pi}_T.$$

1380 Now we bound the probability of  $\varepsilon$  relative error:  
1381

$$\begin{aligned} \Pr\left(\left|\frac{\hat{Z}}{Z} - 1\right| \geq \varepsilon\right) &= \mathbb{P}^\rightarrow\left(\left|\frac{e^{-W}}{e^{-\Delta F}} - 1\right| \geq \varepsilon\right) = \mathbb{P}^\rightarrow\left(\left|\frac{d\mathbb{P}^\leftarrow}{d\mathbb{P}^\rightarrow} - 1\right| \geq \varepsilon\right) \\ &\leq \frac{1}{\varepsilon} \mathbb{E}_{\mathbb{P}^\rightarrow} \left| \frac{d\mathbb{P}^\leftarrow}{d\mathbb{P}^\rightarrow} - 1 \right| = \frac{2}{\varepsilon} \text{TV}(\mathbb{P}^\leftarrow, \mathbb{P}^\rightarrow) \\ &\leq \frac{2}{\varepsilon} (\text{TV}(\mathbb{P}, \mathbb{P}^\rightarrow) + \text{TV}(\mathbb{P}, \mathbb{P}^\leftarrow)) \\ &\leq \frac{\sqrt{2}}{\varepsilon} \left( \sqrt{\text{KL}(\mathbb{P} \parallel \mathbb{P}^\rightarrow)} + \sqrt{\text{KL}(\mathbb{P} \parallel \mathbb{P}^\leftarrow)} \right). \end{aligned} \quad (18)$$

1382 In the second line above, we apply Markov inequality along with an equivalent definition of the TV  
1383 distance:  $\text{TV}(\mu, \nu) = \frac{1}{2} \int \left| \frac{d\mu}{d\lambda} - \frac{d\nu}{d\lambda} \right| d\lambda$ , where  $\lambda$  is a measure that dominates both  $\mu$  and  $\nu$ . The  
1384 third line follows from the triangle inequality for TV distance, while the final line is a consequence of  
1385 Pinsker's inequality  $\text{KL} \geq 2 \text{TV}^2$ .  
1386

1387  
1388 <sup>7</sup>We assume the existence of a unique curve of probability measures solving the Fokker-Planck equation  
1389 given the drift and diffusion terms, guaranteed under mild regularity conditions (Le Bris & Lions, 2008).  
1390

1404 By Girsanov's theorem (Lems. 1 and 3), it is straightforward to see that  
 1405

$$1406 \text{KL}(\mathbb{P} \|\mathbb{P}^{\leftarrow}) = \text{KL}(\mathbb{P} \|\mathbb{P}^{\rightarrow}) = \frac{1}{4} \mathbb{E}_{\mathbb{P}} \int_0^T \|v_t(X_t)\|^2 dt = \frac{1}{4} \int_0^T \|v_t\|_{L^2(\tilde{\pi}_t)}^2 dt.$$

1408 Leveraging the relation between metric derivative and continuity equation (Lem. 4), among all vector  
 1409 fields  $(v_t)_{t \in [0, T]}$  that generate  $(\tilde{\pi}_t)_{t \in [0, T]}$ , we can choose the one that minimizes  $\|v_t\|_{L^2(\tilde{\pi}_t)}$ , thereby  
 1410 making  $\|v_t\|_{L^2(\tilde{\pi}_t)} = |\dot{\tilde{\pi}}|_t$ , the metric derivative. With the reparameterization  $\tilde{\pi}_t = \pi_{t/T}$ , we have  
 1411 the following relation by chain rule:

$$1412 |\dot{\tilde{\pi}}|_t = \lim_{\delta \rightarrow 0} \frac{W_2(\tilde{\pi}_{t+\delta}, \tilde{\pi}_t)}{|\delta|} = \lim_{\delta \rightarrow 0} \frac{W_2(\pi_{(t+\delta)/T}, \pi_{t/T})}{T|\delta/T|} = \frac{1}{T} |\dot{\pi}|_{t/T}.$$

1413 Employing the change-of-variable formula leads to  
 1414

$$1416 \text{KL}(\mathbb{P} \|\mathbb{P}^{\leftarrow}) = \text{KL}(\mathbb{P} \|\mathbb{P}^{\rightarrow}) = \frac{1}{4} \int_0^T |\dot{\pi}|_t^2 dt = \frac{1}{4T} \int_0^1 |\dot{\pi}|_\theta^2 d\theta = \frac{\mathcal{A}}{4T}.$$

1417 Therefore, it suffices to choose  $T = \frac{32\mathcal{A}}{\varepsilon^2}$  to make the r.h.s. of (18) less than  $\frac{1}{4}$ .  $\square$   
 1418

## 1420 D PROOF OF THM. 4

1421 With the forward and backward path measures  $\mathbb{P}^{\rightarrow}$  and  $\mathbb{P}^{\leftarrow}$  defined in (5) and (6), we further define  
 1422 the reference path measure  
 1423

$$1425 \mathbb{P}(x_{0:M}) = \pi_0(x_0) \prod_{\ell=1}^M F_{\ell}^*(x_{\ell-1}, x_{\ell}), \quad (19)$$

1426 where  $F_{\ell}^*$  can be an arbitrary transition kernel transporting  $\pi_{\theta_{\ell-1}}$  to  $\pi_{\theta_{\ell}}$ , i.e., it satisfies  
 1427

$$1429 \pi_{\theta_{\ell}}(y) = \int F_{\ell}^*(x, y) \pi_{\theta_{\ell-1}}(x) dx, \forall y \in \mathbb{R}^d \implies x_{\ell} \sim \pi_{\theta_{\ell}}, \forall \ell \in \llbracket 0, M \rrbracket.$$

1430 Define the backward transition kernel of  $F_{\ell}^*$  as  
 1431

$$1433 B_{\ell}^*(x, x') = \frac{\pi_{\theta_{\ell-1}}(x')}{\pi_{\theta_{\ell}}(x)} F_{\ell}^*(x', x), \ell \in \llbracket 1, M \rrbracket,$$

1434 which transports  $\pi_{\theta_{\ell}}$  to  $\pi_{\theta_{\ell-1}}$ . Equivalently, we can write  
 1435

$$1437 \mathbb{P}(x_{0:M}) = \pi_1(x_M) \prod_{\ell=1}^M B_{\ell}^*(x_{\ell}, x_{\ell-1}).$$

1438 Straightforward calculations yield  
 1439

$$1440 \text{KL}(\mathbb{P} \|\mathbb{P}^{\rightarrow}) = \sum_{\ell=1}^M \mathbb{E}_{\pi_{\theta_{\ell-1}}(x_{\ell-1})} \text{KL}(F_{\ell}^*(x_{\ell-1}, \cdot) \| F_{\ell}(x_{\ell-1}, \cdot)),$$

$$1444 \text{KL}(\mathbb{P} \|\mathbb{P}^{\leftarrow}) = \sum_{\ell=1}^M \mathbb{E}_{\pi_{\theta_{\ell}}(x_{\ell})} \text{KL}(B_{\ell}^*(x_{\ell}, \cdot) \| B_{\ell}(x_{\ell}, \cdot))$$

$$1447 = \sum_{\ell=1}^M \text{KL}(\pi_{\theta_{\ell-1}}(x_{\ell-1}) F_{\ell}^*(x_{\ell-1}, x_{\ell}) \| \pi_{\theta_{\ell}}(x_{\ell-1}) F_{\ell}(x_{\ell-1}, x_{\ell})) \quad (20)$$

$$1450 = \text{KL}(\mathbb{P} \|\mathbb{P}^{\rightarrow}) + \sum_{\ell=1}^M \text{KL}(\pi_{\theta_{\ell-1}} \| \pi_{\theta_{\ell}}). \quad (21)$$

1453 Also, recall that the sampling path measure  $\widehat{\mathbb{P}}^{\rightarrow}$  is defined in (9) starts at  $\widehat{\pi}_0$ , the distribution of an  
 1454 approximate sample of  $\pi_0$ . For convenience, we define the following path measure, which differs  
 1455 from  $\widehat{\mathbb{P}}^{\rightarrow}$  only from the initial distribution:

$$1456 \widehat{\mathbb{P}}^{\rightarrow}(x_{0:M}) = \pi_0(x_0) \prod_{\ell=1}^M \widehat{F}_{\ell}(x_{\ell-1}, x_{\ell}). \quad (22)$$

1458 Equipped with these definitions, we first prove a lemma about a necessary condition for the estimator  
 1459  $\widehat{Z}$  to satisfy the desired accuracy (1).  
 1460

1461 **Lemma 5.** Define the estimator  $\widehat{Z} := \widehat{Z}_0 e^{-W(x_{0:M})}$ , where  $x_{0:M} \sim \widehat{\mathbb{P}}^{\rightarrow}$ , and  $\widehat{Z}_0$  is independent of  
 1462  $x_{0:M}$ . To make  $\widehat{Z}$  satisfy the criterion (1), it suffices to meet the following four conditions:

$$1463 \quad \Pr \left( \left| \frac{\widehat{Z}_0}{Z_0} - 1 \right| \geq \frac{\varepsilon}{8} \right) \leq \frac{1}{8}, \quad (23)$$

$$1464 \quad \text{TV}(\widehat{\pi}_0, \pi_0) \leq 2^{-5}, \quad (24)$$

$$1465 \quad \text{KL}(\mathbb{P} \parallel \mathbb{P}^{\leftarrow}) \leq 2^{-13} \varepsilon^2, \quad (25)$$

$$1466 \quad \text{KL}(\mathbb{P} \parallel \mathbb{P}^{\rightarrow}) \leq 2^{-8}. \quad (26)$$

1471 *Proof.* Recall that  $Z = Z_0 e^{-\Delta F}$ . Using Lem. 8, we have

$$1472 \quad \Pr \left( \left| \frac{\widehat{Z}}{Z} - 1 \right| \geq \varepsilon \right) \leq \Pr \left( \left| \log \frac{\widehat{Z}}{Z} \right| \geq \frac{\varepsilon}{2} \right) = \Pr_{x_{0:M} \sim \widehat{\mathbb{P}}^{\rightarrow}} \left( \left| \log \frac{\widehat{Z}_0}{Z_0} + \log \frac{e^{-W(x_{0:M})}}{e^{-\Delta F}} \right| \geq \frac{\varepsilon}{2} \right)$$

$$1473 \quad \leq \Pr \left( \left| \log \frac{\widehat{Z}_0}{Z_0} \right| \geq \frac{\varepsilon}{4} \right) + \widehat{\mathbb{P}}^{\rightarrow} \left( \left| \log \frac{e^{-W}}{e^{-\Delta F}} \right| \geq \frac{\varepsilon}{4} \right)$$

$$1474 \quad \leq \Pr \left( \left| \frac{\widehat{Z}_0}{Z_0} - 1 \right| \geq \frac{\varepsilon}{8} \right) + \widehat{\mathbb{P}}^{\rightarrow} \left( \left| \frac{e^{-W}}{e^{-\Delta F}} - 1 \right| \geq \frac{\varepsilon}{8} \right).$$

1483 The first term is  $\leq \frac{1}{8}$  if (23) holds. To bound the second term, using the definition of TV distance and  
 1484 the triangle inequality, we have

$$1485 \quad \widehat{\mathbb{P}}^{\rightarrow} \left( \left| \frac{e^{-W}}{e^{-\Delta F}} - 1 \right| \geq \frac{\varepsilon}{8} \right)$$

$$1486 \quad \leq \text{TV}(\widehat{\mathbb{P}}^{\rightarrow}, \mathbb{P}^{\rightarrow}) + \mathbb{P}^{\rightarrow} \left( \left| \frac{e^{-W}}{e^{-\Delta F}} - 1 \right| \geq \frac{\varepsilon}{8} \right)$$

$$1487 \quad \leq \text{TV}(\widehat{\mathbb{P}}^{\rightarrow}, \mathbb{P}^{\rightarrow}) + \text{TV}(\mathbb{P}^{\rightarrow}, \mathbb{P}) + \text{TV}(\mathbb{P}, \mathbb{P}^{\rightarrow}) + \mathbb{P}^{\rightarrow} \left( \left| \frac{d\mathbb{P}^{\leftarrow}}{d\mathbb{P}^{\rightarrow}} - 1 \right| \geq \frac{\varepsilon}{8} \right).$$

1488 Recall that by definition (9) and (22), the distributions of  $x_{1:M}$  conditional on  $x_0$  are the same under  
 1489  $\widehat{\mathbb{P}}^{\rightarrow}$  and  $\mathbb{P}^{\rightarrow}$ . Hence,  $\text{TV}(\widehat{\mathbb{P}}^{\rightarrow}, \mathbb{P}^{\rightarrow}) = \text{TV}(\widehat{\pi}_0, \pi_0)$ . Applying Pinsker's inequality and leveraging  
 1490 (18), we have

$$1491 \quad \widehat{\mathbb{P}}^{\rightarrow} \left( \left| \frac{e^{-W}}{e^{-\Delta F}} - 1 \right| \geq \frac{\varepsilon}{8} \right)$$

$$1492 \quad \leq \text{TV}(\widehat{\pi}_0, \pi_0) + \sqrt{\frac{1}{2} \text{KL}(\mathbb{P} \parallel \mathbb{P}^{\rightarrow})} + \sqrt{\frac{1}{2} \text{KL}(\mathbb{P} \parallel \mathbb{P}^{\rightarrow})} + \frac{8\sqrt{2}}{\varepsilon} \left( \sqrt{\text{KL}(\mathbb{P} \parallel \mathbb{P}^{\rightarrow})} + \sqrt{\text{KL}(\mathbb{P} \parallel \mathbb{P}^{\leftarrow})} \right).$$

1502 Note that from (21) we know that  $\text{KL}(\mathbb{P} \parallel \mathbb{P}^{\rightarrow}) \leq \text{KL}(\mathbb{P} \parallel \mathbb{P}^{\leftarrow})$ , so if (24) to (26) hold, we can achieve  
 1503  $\widehat{\mathbb{P}}^{\rightarrow} \left( \left| \frac{e^{-W}}{e^{-\Delta F}} - 1 \right| \geq \frac{\varepsilon}{8} \right) \leq \frac{1}{8}$ , and therefore  $\Pr \left( \left| \frac{\widehat{Z}}{Z} - 1 \right| \geq \varepsilon \right) \leq \frac{1}{4}$ .  $\square$

1504 Next, we study how to satisfy the conditions in (25) and (26) while minimizing oracle complexity.  
 1505 Given that we already have an approximate sample from  $\pi_0$  and an accurate estimate of  $Z_0$ , we  
 1506 proceed to the next step of the AIS algorithm. Since each transition kernel requires one call to the  
 1507 oracle of  $\nabla V$ , and by plugging in  $f_{\theta} \leftarrow V + \frac{\lambda(\theta)}{2} \|\cdot\|^2$  in AIS (Thm. 3), the work function  $W(x_{0:M})$   
 1508 is independent of  $V$ , it follows that the remaining oracle complexity is  $M$ . The result is formalized in  
 1509 the following lemma.

1512     **Lemma 6.** *To minimize the oracle complexity, it suffices to find the minimal  $M$  such that there exists  
1513     a sequence  $0 = \theta_0 < \theta_1 < \dots < \theta_M = 1$  satisfying the following three constraints:*

$$1515 \quad \sum_{\ell=1}^M \int_{\theta_{\ell-1}}^{\theta_\ell} (\lambda(\theta) - \lambda(\theta_\ell))^2 d\theta \lesssim \frac{\varepsilon^4}{m^2 \mathcal{A}}, \quad (27)$$

$$1518 \quad \sum_{\ell=1}^M (\theta_\ell - \theta_{\ell-1})^2 \lesssim \frac{\varepsilon^4}{d\beta^2 \mathcal{A}^2}, \quad (28)$$

$$1521 \quad \max_{\ell \in \llbracket 1, M \rrbracket} (\theta_\ell - \theta_{\ell-1}) \lesssim \frac{\varepsilon^2}{\beta \mathcal{A}}. \quad (29)$$

1523     *Proof.* We break down the argument into two steps.

1525     **Step 1.** We first consider (25).

1527     Note that when defining the reference path measure  $\mathbb{P}$ , the only requirement for the transition kernel  
1528      $F_\ell^*$  is that it should transport  $\pi_{\theta_{\ell-1}}$  to  $\pi_{\theta_\ell}$ . Our aim is to find the “optimal”  $F_\ell^*$ ’s in order to minimize  
1529     the sum of KL divergences, which can be viewed as a *static Schrödinger bridge problem* (Léonard,  
1530     2014; Chen et al., 2016; 2021). By data-processing inequality,

$$1531 \quad C_\ell := \inf_{F_\ell^*} \text{KL}(\pi_{\theta_{\ell-1}}(x_{\ell-1}) F_\ell^*(x_{\ell-1}, x_\ell) \| \pi_{\theta_\ell}(x_{\ell-1}) F_\ell(x_{\ell-1}, x_\ell)) \leq \inf_{\mathbf{P}^\ell} \text{KL}(\mathbf{P}^\ell \| \mathbf{Q}^\ell),$$

1533     where the infimum is taken among all path measures from 0 to  $T_\ell$  with the marginal constraints  
1534      $\mathbf{P}_0^\ell = \pi_{\theta_{\ell-1}}$  and  $\mathbf{P}_{T_\ell}^\ell = \pi_{\theta_\ell}$ ;  $\mathbf{Q}^\ell$  is the path measure of (8) (i.e., LD with target distribution  $\pi_{\theta_\ell}$ )  
1535     initialized at  $X_0 \sim \pi_{\theta_0}$ .

1536     For each  $\ell \in \llbracket 1, M \rrbracket$ , define the following interpolation between  $\pi_{\theta_{\ell-1}}$  and  $\pi_{\theta_\ell}$ :

$$1538 \quad \mu_t^\ell := \pi_{\theta_{\ell-1} + \frac{t}{T_\ell}(\theta_\ell - \theta_{\ell-1})}, \quad t \in [0, T_\ell].$$

1540     Let  $\mathbf{P}^\ell$  be the path measure of

$$1542 \quad dX_t = (\nabla \log \mu_t^\ell + u_t^\ell)(X_t) dt + \sqrt{2} dB_t, \quad t \in [0, T_\ell]; \quad X_0 \sim \pi_{\theta_{\ell-1}},$$

1544     where the vector field  $(u_t^\ell)_{t \in [0, T_\ell]}$  is chosen such that  $X_t \sim \mu_t^\ell$  under  $\mathbf{P}^\ell$ , and in particular, the  
1545     marginal distributions at 0 and  $T_\ell$  are  $\pi_{\theta_{\ell-1}}$  and  $\pi_{\theta_\ell}$ , respectively. By verifying the Fokker-Planck  
1546     equation, the following PDE needs to be satisfied:

$$1547 \quad \partial_t \mu_t^\ell = -\nabla \cdot (\mu_t^\ell (\nabla \log \mu_t^\ell + u_t^\ell)) + \Delta \mu_t^\ell = -\nabla \cdot (\mu_t^\ell u_t^\ell), \quad t \in [0, T_\ell],$$

1549     meaning that  $(u_t^\ell)_{t \in [0, T_\ell]}$  generates  $(\mu_t^\ell)_{t \in [0, T_\ell]}$ . Similar to the proof of JE (Thm. 2), using the relation  
1550     between metric derivative and continuity equation (Lem. 4), among all vector fields generating  
1551      $(\mu_t^\ell)_{t \in [0, T_\ell]}$ , we choose  $(u_t^\ell)_{t \in [0, T_\ell]}$  to be the a.s.-unique vector field that satisfies  $\|u_t^\ell\|_{L^2(\mu_t^\ell)} = |\dot{\mu}_t^\ell|_t$   
1552     for Lebesgue-a.e.  $t \in [0, T_\ell]$ , which implies (using the chain rule)

$$1554 \quad \int_0^{T_\ell} \|u_t^\ell\|_{L^2(\mu_t^\ell)}^2 dt = \int_0^{T_\ell} |\dot{\mu}_t^\ell|_t^2 dt \\ 1556 \quad = \int_0^{T_\ell} \left( \frac{\theta_\ell - \theta_{\ell-1}}{T_\ell} |\dot{\pi}|_{\theta_{\ell-1} + \frac{t}{T_\ell}(\theta_\ell - \theta_{\ell-1})} \right)^2 dt = \frac{\theta_\ell - \theta_{\ell-1}}{T_\ell} \int_{\theta_{\ell-1}}^{\theta_\ell} |\dot{\pi}|_\theta^2 d\theta.$$

1559     By Lem. 2, we can equivalently write  $\mathbf{P}^\ell$  as the path measure of the following backward SDE:

$$1561 \quad dX_t = (-\nabla \log \mu_t^\ell + u_t^\ell)(X_t) dt + \sqrt{2} dB_t^\leftarrow, \quad t \in [0, T_\ell]; \quad X_T \sim \pi_{\theta_\ell}.$$

1563     Recall that  $\mathbf{Q}^\ell$  is the path measure of (8) initialized at  $X_0 \sim \pi_{\theta_\ell}$ , so  $X_t \sim \pi_{\theta_\ell}$  for all  $t \in [0, T_\ell]$ . By  
1564     Nelson’s relation (Lem. 2), we can equivalently write  $\mathbf{Q}^\ell$  as the path measure of

$$1565 \quad dX_t = -\nabla \log \pi_{\theta_\ell}(X_t) dt + \sqrt{2} dB_t^\leftarrow, \quad t \in [0, T_\ell]; \quad X_{T_\ell} \sim \pi_{\theta_\ell}.$$

The purpose of writing these two path measures in the way of backward SDEs is to avoid the extra term of the KL divergence between the initialization distributions  $\pi_{\theta_{\ell-1}}$  and  $\pi_{\theta_\ell}$  at time 0 when calculating  $\text{KL}(\mathbf{P}^\ell \|\mathbf{Q}^\ell)$ . To see this, by Girsanov's theorem (Lem. 3), the triangle inequality, and the change-of-variable formula, we have

$$\begin{aligned} C_\ell &\leq \text{KL}(\mathbf{P}^\ell \|\mathbf{Q}^\ell) = \frac{1}{4} \int_0^{T_\ell} \left\| u_t^\ell - \nabla \log \frac{\mu_t^\ell}{\pi_{\theta_\ell}} \right\|_{L^2(\mu_t^\ell)}^2 dt \\ &\lesssim \int_0^{T_\ell} \|u_t^\ell\|_{L^2(\mu_t^\ell)}^2 dt + \int_0^{T_\ell} \left\| \nabla \log \frac{\mu_t^\ell}{\pi_{\theta_\ell}} \right\|_{L^2(\mu_t^\ell)}^2 dt \\ &= \frac{\theta_\ell - \theta_{\ell-1}}{T_\ell} \int_{\theta_{\ell-1}}^{\theta_\ell} |\dot{\pi}|_\theta^2 d\theta + \frac{T_\ell}{\theta_\ell - \theta_{\ell-1}} \int_{\theta_{\ell-1}}^{\theta_\ell} \left\| \nabla \log \frac{\pi_\theta}{\pi_{\theta_\ell}} \right\|_{L^2(\pi_\theta)}^2 d\theta. \end{aligned}$$

**Remark 6.** Our bound above is based on a specific interpolation between  $\pi_{\theta_{\ell-1}}$  and  $\pi_{\theta_\ell}$  along the curve  $(\pi_\theta)_{\theta \in [\theta_{\ell-1}, \theta_\ell]}$ . This approach is inspired by, yet slightly differs from, Conforti & Tamanini (2021, Theorem 1.6), where the interpolation is based on the Wasserstein geodesic. As we will demonstrate shortly, our formulation simplifies the analysis of the second term (the Fisher divergence), making it more straightforward to bound.

Now, summing over all  $\ell \in \llbracket 1, M \rrbracket$ , we can see that in order to ensure  $\text{KL}(\mathbb{P} \|\mathbb{P}^\leftarrow) \leq \sum_{\ell=1}^M C_\ell \leq \varepsilon^2$ , we only need the following two conditions to hold:

$$\sum_{\ell=1}^M \frac{\theta_\ell - \theta_{\ell-1}}{T_\ell} \int_{\theta_{\ell-1}}^{\theta_\ell} |\dot{\pi}|_\theta^2 d\theta \lesssim \varepsilon^2, \quad (30)$$

$$\sum_{\ell=1}^M \frac{T_\ell}{\theta_\ell - \theta_{\ell-1}} \int_{\theta_{\ell-1}}^{\theta_\ell} \left\| \nabla \log \frac{\pi_\theta}{\pi_{\theta_\ell}} \right\|_{L^2(\pi_\theta)}^2 d\theta \lesssim \varepsilon^2. \quad (31)$$

Since  $\sum_{\ell=1}^M \int_{\theta_{\ell-1}}^{\theta_\ell} |\dot{\pi}|_\theta^2 d\theta = \mathcal{A}$ , it suffices to choose

$$\frac{T_\ell}{\theta_\ell - \theta_{\ell-1}} =: T \asymp \frac{\mathcal{A}}{\varepsilon^2}, \quad \forall \ell \in \llbracket 1, M \rrbracket \quad (32)$$

to make the l.h.s. of (30)  $O(\varepsilon^2)$ . Notably,  $T$  is the summation over all  $T_\ell$ 's, which has the same order as the total time  $T$  for running JE ((2)) in the continuous scenario, in Thm. 1. Plugging this  $T_\ell$  into the second summation, and noticing that by (7) and Lem. 14,

$$\left\| \nabla \log \frac{\pi_\theta}{\pi_{\theta'}} \right\|_{L^2(\pi_\theta)}^2 = \mathbb{E}_{x \sim \pi_\theta} \|(\lambda(\theta) - \lambda(\theta'))x\|^2 \leq (\lambda(\theta) - \lambda(\theta'))^2 m^2,$$

we conclude that (27) implies (31).

**Step 2.** Now consider the other constraint (26). By chain rule and data-processing inequality,

$$\text{KL}(\mathbb{P} \|\mathbb{P}^\leftarrow) = \sum_{\ell=1}^M \text{KL}(\pi_{\theta_{\ell-1}}(x_{\ell-1}) F_\ell^*(x_{\ell-1}, x_\ell) \| \pi_{\theta_{\ell-1}}(x_{\ell-1}) \widehat{F}_\ell(x_{\ell-1}, x_\ell)) \leq \sum_{\ell=1}^M \text{KL}(\mathbf{P}^\ell \|\widehat{\mathbf{Q}}^\ell),$$

where  $\mathbf{P}^\ell$  is the previously defined path measure of the SDE

$$\begin{aligned} dX_t &= (\nabla \log \mu_t^\ell + u_t^\ell)(X_t) dt + \sqrt{2} dB_t \\ &= \left( -\nabla V(X_t) - \lambda \left( \theta_{\ell-1} + \frac{t}{T_\ell} (\theta_\ell - \theta_{\ell-1}) \right) X_t + u_t^\ell(X_t) \right) dt + \sqrt{2} dB_t, \quad t \in [0, T_\ell]; X_0 \sim \pi_{\theta_{\ell-1}}, \end{aligned}$$

and  $\widehat{\mathbf{Q}}^\ell$  is the path measure of (10) initialized at  $X_0 \sim \pi_{\theta_{\ell-1}}$ , i.e.,

$$dX_t = \left( -\nabla V(X_0) - \lambda \left( \theta_{\ell-1} + \frac{t}{T_\ell} (\theta_\ell - \theta_{\ell-1}) \right) X_t \right) dt + \sqrt{2} dB_t, \quad t \in [0, T_\ell]; X_0 \sim \pi_{\theta_{\ell-1}}.$$

1620 By Lem. 1, triangle inequality, and the smoothness of  $V$ , we have  
 1621

$$\begin{aligned} 1622 \text{KL}(\mathbf{P}^\ell \|\widehat{\mathbf{Q}}^\ell) &= \frac{1}{4} \int_0^{T_\ell} \mathbb{E}_{\mathbf{P}^\ell} \|\nabla V(X_t) - \nabla V(X_0) - u_t^\ell(X_t)\|^2 dt \\ 1623 &\lesssim \int_0^{T_\ell} \mathbb{E}_{\mathbf{P}^\ell} [\|\nabla V(X_t) - \nabla V(X_0)\|^2 + \|u_t^\ell(X_t)\|^2] dt \\ 1624 &\leq \beta^2 \int_0^{T_\ell} \mathbb{E}_{\mathbf{P}^\ell} \|X_t - X_0\|^2 dt + \int_0^{T_\ell} \|u_t^\ell\|_{L^2(\mu_t^\ell)}^2 dt \\ 1625 \\ 1626 \\ 1627 \\ 1628 \\ 1629 \end{aligned}$$

1630 To bound the first part, note that under  $\mathbf{P}^\ell$ , we have  
 1631

$$1632 X_t - X_0 = \int_0^t (\nabla \log \mu_\tau^\ell + u_\tau^\ell)(X_\tau) d\tau + \sqrt{2} B_t. \\ 1633$$

1634 Thanks to the fact that  $X_t \sim \mu_t^\ell$  under  $\mathbf{P}^\ell$ ,  
 1635

$$\begin{aligned} 1636 \mathbb{E}_{\mathbf{P}^\ell} \|X_t - X_0\|^2 &\lesssim \mathbb{E}_{\mathbf{P}^\ell} \left\| \int_0^t (\nabla \log \mu_\tau^\ell + u_\tau^\ell)(X_\tau) d\tau \right\|^2 + \mathbb{E} \|\sqrt{2} B_t\|^2 \\ 1637 &\lesssim t \int_0^t \mathbb{E}_{\mathbf{P}^\ell} \|(\nabla \log \mu_\tau^\ell + u_\tau^\ell)(X_\tau)\|^2 d\tau + dt \\ 1638 &\lesssim t \int_0^t \left( \|\nabla \log \mu_\tau^\ell\|_{L^2(\mu_\tau^\ell)}^2 + \|u_\tau^\ell\|_{L^2(\mu_\tau^\ell)}^2 \right) d\tau + dt \\ 1639 &\lesssim T_\ell \int_0^{T_\ell} \left( \|\nabla \log \mu_\tau^\ell\|_{L^2(\mu_\tau^\ell)}^2 + \|u_\tau^\ell\|_{L^2(\mu_\tau^\ell)}^2 \right) d\tau + dT_\ell, \quad \forall t \in [0, T_\ell], \\ 1640 \\ 1641 \\ 1642 \\ 1643 \\ 1644 \\ 1645 \end{aligned}$$

1646 where the second inequality follows from Jensen's inequality (Cheng et al., 2018, Sec. 4):

$$1647 \left\| \int_0^t f_\tau d\tau \right\|^2 = t^2 \mathbb{E}_{\tau \sim \text{Unif}(0, t)} \|f_\tau\|^2 \leq t^2 \mathbb{E}_{\tau \sim \text{Unif}(0, t)} \|f_\tau\|^2 = t \int_0^t \|f_\tau\|^2 d\tau. \\ 1648 \\ 1649$$

1650 Therefore,  
 1651

$$\begin{aligned} 1652 \text{KL}(\mathbf{P}^\ell \|\widehat{\mathbf{Q}}^\ell) &\leq \beta^2 \int_0^{T_\ell} \mathbb{E}_{\mathbf{P}^\ell} \|X_t - X_0\|^2 dt + \int_0^{T_\ell} \|u_t^\ell\|_{L^2(\mu_t^\ell)}^2 dt \\ 1653 &\leq \beta^2 T_\ell^2 \int_0^{T_\ell} \|\nabla \log \mu_\tau^\ell\|_{L^2(\mu_\tau^\ell)}^2 d\tau + (\beta^2 T_\ell^2 + 1) \int_0^{T_\ell} \|u_\tau^\ell\|_{L^2(\mu_\tau^\ell)}^2 d\tau + d\beta^2 T_\ell^2 \\ 1654 &= \beta^2 T_\ell^2 \frac{T_\ell}{\theta_\ell - \theta_{\ell-1}} \int_{\theta_{\ell-1}}^{\theta_\ell} \|\nabla \log \pi_\theta\|_{L^2(\pi_\theta)}^2 d\theta + (\beta^2 T_\ell^2 + 1) \frac{\theta_\ell - \theta_{\ell-1}}{T_\ell} \int_{\theta_{\ell-1}}^{\theta_\ell} |\dot{\pi}|_\theta^2 d\theta + d\beta^2 T_\ell^2. \\ 1655 \\ 1656 \\ 1657 \\ 1658 \\ 1659 \\ 1660 \end{aligned}$$

1661 Recall that the potential of  $\pi_\theta$  is  $(\beta + \lambda(\theta))$ -smooth. By Lem. 13 and the monotonicity of  $\lambda(\cdot)$ ,  
 1662

$$1663 \int_{\theta_{\ell-1}}^{\theta_\ell} \|\nabla \log \pi_\theta\|_{L^2(\pi_\theta)}^2 d\theta \leq \int_{\theta_{\ell-1}}^{\theta_\ell} d(\beta + \lambda(\theta)) d\theta \leq d(\theta_\ell - \theta_{\ell-1})(\beta + \lambda(\theta_{\ell-1})). \\ 1664 \\ 1665$$

1666 Thus,  
 1667

$$\begin{aligned} 1668 \text{KL}(\mathbb{P} \|\overrightarrow{\mathbb{P}}) &\leq \sum_{\ell=1}^M \left( \beta^2 T_\ell^3 d(\beta + \lambda(\theta_{\ell-1})) + (\beta^2 T_\ell^2 + 1) \frac{\theta_\ell - \theta_{\ell-1}}{T_\ell} \int_{\theta_{\ell-1}}^{\theta_\ell} |\dot{\pi}|_\theta^2 d\theta + d\beta^2 T_\ell^2 \right) \\ 1669 &= \sum_{\ell=1}^M \left( \beta^2 dT_\ell^2 (T_\ell(\beta + \lambda(\theta_{\ell-1})) + 1) + (\beta^2 T_\ell^2 + 1) \frac{\theta_\ell - \theta_{\ell-1}}{T_\ell} \int_{\theta_{\ell-1}}^{\theta_\ell} |\dot{\pi}|_\theta^2 d\theta \right) \\ 1670 \\ 1671 \\ 1672 \\ 1673 \end{aligned}$$

1674 Assume  $\max_{\ell \in \llbracket 1, M \rrbracket} T_\ell \lesssim \frac{1}{\beta}$ , i.e., (29). so  $\max_{\ell \in \llbracket 1, M \rrbracket} T_\ell(\beta + \lambda(\theta_{\ell-1})) \lesssim 1$ , due to  $\lambda(\cdot) \leq 2\beta$ . We  
 1675 can further simplify the above expression to  
 1676

$$\begin{aligned} 1677 \text{KL}(\mathbb{P} \parallel \bar{\mathbb{P}}) &\leq \sum_{\ell=1}^M \left( \beta^2 d T_\ell^2 + \frac{\theta_\ell - \theta_{\ell-1}}{T_\ell} \int_{\theta_{\ell-1}}^{\theta_\ell} |\dot{\pi}|_\theta^2 d\theta \right) \lesssim \beta^2 d \left( \sum_{\ell=1}^M T_\ell^2 \right) + \varepsilon^2 \\ 1680 &= \beta^2 d T^2 \sum_{\ell=1}^M (\theta_\ell - \theta_{\ell-1})^2 + \varepsilon^2 \lesssim \beta^2 d \frac{\mathcal{A}^2}{\varepsilon^4} \sum_{\ell=1}^M (\theta_\ell - \theta_{\ell-1})^2 + \varepsilon^2. \\ 1682 \end{aligned}$$

1683 So (29) implies that the r.h.s. of the above equation is  $O(1)$ .  
 1684

□

1685 Finally, we have arrived at the last step of proving Thm. 4, that is to decide the schedule of  $\theta_\ell$ 's.  
 1686

1687 Define  $\vartheta_\ell := 1 - \theta_\ell$ ,  $\ell \in \llbracket 0, M \rrbracket$ . We consider the annealing schedule  $\lambda(\theta) = 2\beta(1 - \theta)^r$  for some  
 1688  $1 \leq r \lesssim 1$ , and to emphasize the dependence on  $r$ , we use  $\mathcal{A}_r$  to represent the action of  $(\pi_\theta)_{\theta \in [0, 1]}$ .  
 1689 The l.h.s. of (27) is  
 1690

$$\begin{aligned} 1691 \sum_{\ell=1}^M \int_{\theta_{\ell-1}}^{\theta_\ell} (\lambda(\theta) - \lambda(\theta_\ell))^2 d\theta &\leq \sum_{\ell=1}^M (\theta_\ell - \theta_{\ell-1}) (2\beta(1 - \theta_{\ell-1})^r - 2\beta(1 - \theta_\ell)^r)^2 \\ 1692 &= \sum_{\ell=1}^M (\vartheta_{\ell-1} - \vartheta_\ell) (2\beta\vartheta_{\ell-1}^r - 2\beta\vartheta_\ell^r)^2 \\ 1693 &\lesssim \beta^2 \sum_{\ell=1}^M (\vartheta_{\ell-1} - \vartheta_\ell) (\vartheta_{\ell-1}^r - \vartheta_\ell^r)^2 \\ 1694 &\lesssim \beta^2 \sum_{\ell=1}^M (\vartheta_{\ell-1} - \vartheta_\ell) (\vartheta_{\ell-1} - \vartheta_\ell)^2 = \beta^2 \sum_{\ell=1}^M (\vartheta_{\ell-1} - \vartheta_\ell)^3, \\ 1695 & \\ 1696 & \\ 1697 & \\ 1698 & \\ 1699 & \\ 1700 & \\ 1701 & \\ 1702 & \\ 1703 & \\ 1704 \end{aligned}$$

where the last inequality comes from Lem. 9. So to satisfy (27), it suffices to ensure

$$\sum_{\ell=1}^M (\vartheta_{\ell-1} - \vartheta_\ell)^3 \lesssim \frac{\varepsilon^4}{m^2 \beta^2 \mathcal{A}_r},$$

1708 while (28) and (29) are equivalent to  
 1709

$$\sum_{\ell=1}^M (\vartheta_{\ell-1} - \vartheta_\ell)^2 \lesssim \frac{\varepsilon^4}{d\beta^2 \mathcal{A}_r^2}, \quad \max_{\ell \in \llbracket 1, M \rrbracket} (\vartheta_{\ell-1} - \vartheta_\ell) \lesssim \frac{\varepsilon^2}{\beta \mathcal{A}_r}.$$

1710 Since we are minimizing the total number of oracle calls  $M$ , the Hölder's inequality implies that the  
 1711 optimal schedule of  $\vartheta_\ell$ 's is an arithmetic sequence, i.e.,  $\vartheta_\ell = 1 - \frac{\ell}{M}$ . We need to ensure  
 1712

$$\frac{1}{M^2} \lesssim \frac{\varepsilon^4}{m^2 \beta^2 \mathcal{A}_r}, \quad \frac{1}{M} \lesssim \frac{\varepsilon^4}{d\beta^2 \mathcal{A}_r^2}, \quad \frac{1}{M} \lesssim \frac{\varepsilon^2}{\beta \mathcal{A}_r}.$$

1713 So it suffices to choose  $\frac{1}{M} \asymp \frac{\varepsilon^2}{m\beta\mathcal{A}_r^{\frac{1}{2}}} \wedge \frac{\varepsilon^4}{d\beta^2\mathcal{A}_r^2}$ , which implies the oracle complexity  
 1714

$$M \asymp \frac{m\beta\mathcal{A}_r^{\frac{1}{2}}}{\varepsilon^2} \vee \frac{d\beta^2\mathcal{A}_r^2}{\varepsilon^4},$$

1715 and the hyperparameter  $T_\ell$  is thus  $T_\ell \asymp \frac{\mathcal{A}_r^{\frac{1}{2}}}{m\beta} \wedge \frac{\varepsilon^2}{d\beta^2\mathcal{A}_r}$  according to (32).  
 1716

□

1717 **Remark 7.** The work Guo et al. (2025) used similar methodologies to prove an  $\tilde{O}\left(\frac{d\beta^2\mathcal{A}^2}{\varepsilon^6}\right)$  oracle  
 1718 complexity for obtaining a sample that is  $\varepsilon^2$ -close in KL divergence to the target distribution. While  
 1719

our assumptions are mostly the same with Guo et al. (2025) except for some insignificant technical ones, and both proofs involve the standard discretization analysis through Girsanov's theorem, the improvement of the  $\varepsilon$ -dependency in Thm. 4 is due to the fact that Guo et al. (2025) requires  $\text{KL}(\mathbb{P} \parallel \bar{\mathbb{P}}^\rightarrow) \lesssim \varepsilon^2$  for sampling, which results in a  $\tilde{\Theta}(\varepsilon^4)$  step size in Guo et al. (2025), while our proof only needs  $\text{KL}(\mathbb{P} \parallel \bar{\mathbb{P}}^\rightarrow) \lesssim 1$  and  $\text{KL}(\mathbb{P} \parallel \mathbb{P}^\leftarrow) \lesssim \varepsilon^2$  for normalizing constant estimation, resulting in an improved  $\tilde{\Theta}(\varepsilon^2)$  step size.

## E PROOFS FOR SEC. 5

### E.1 PROOF OF PROP. 1

*Proof.* The claim of smoothness follows from Guo et al. (2025, Lem. 7). A similar approach for proving the lower bound of metric derivative was used independently in Chemseddine et al. (2025, App. B).

Throughout this proof, let  $\phi$  and  $\Phi$  denote the p.d.f. and c.d.f. of the standard normal distribution  $\mathcal{N}(0, 1)$ , respectively. Unless otherwise specified, the integration ranges are assumed to be  $(-\infty, \infty)$ .

Note that

$$\begin{aligned} \pi(x) e^{-\frac{\lambda}{2}x^2} &\propto \left( e^{-\frac{x^2}{2}} + e^{-\frac{(x-m)^2}{2}} \right) e^{-\frac{\lambda}{2}x^2} \\ &= e^{-\frac{\lambda+1}{2}x^2} + e^{-\frac{\lambda m^2}{2(\lambda+1)}} e^{-\frac{\lambda+1}{2}(x-\frac{m}{\lambda+1})^2} \\ &= \frac{1}{1 + e^{-\frac{\lambda m^2}{2(\lambda+1)}}} \mathcal{N}\left(x \middle| 0, \frac{1}{\lambda+1}\right) + \frac{e^{-\frac{\lambda m^2}{2(\lambda+1)}}}{1 + e^{-\frac{\lambda m^2}{2(\lambda+1)}}} \mathcal{N}\left(x \middle| \frac{m}{\lambda+1}, \frac{1}{\lambda+1}\right). \end{aligned}$$

Define  $S(\theta) := \frac{1}{1+m^2(1-\theta)^2}$ , and let

$$\underline{\pi}_s(x) := \pi(x) e^{-\frac{1/s-1}{2}x^2} = w(s) \mathcal{N}(x|0, s) + (1-w(s)) \mathcal{N}(x|sm, s),$$

where

$$w(s) = \frac{1}{1 + e^{-(1-s)m^2/2}}, \quad w'(s) = -\frac{e^{-(1-s)m^2/2}m^2/2}{(1 + e^{-(1-s)m^2/2})^2}.$$

By definition,  $\pi_\theta = \underline{\pi}_{S(\theta)}$ . The p.d.f. of  $\underline{\pi}_s$  is

$$f_s(x) = \frac{w(s)}{\sqrt{s}} \phi\left(\frac{x}{\sqrt{s}}\right) + \frac{1-w(s)}{\sqrt{s}} \phi\left(\frac{x-sm}{\sqrt{s}}\right),$$

and the c.d.f. of  $\underline{\pi}_s$  is

$$F_s(x) = w(s) \Phi\left(\frac{x}{\sqrt{s}}\right) + (1-w(s)) \Phi\left(\frac{x-sm}{\sqrt{s}}\right).$$

We now derive a formula for calculating the metric derivative. From Villani (2003, Thm. 2.18),  $\text{W}_2^2(\mu, \nu) = \int_0^1 (F_\mu^{-1}(y) - F_\nu^{-1}(y))^2 dy$ , where  $F_\mu, F_\nu$  stand for the c.d.f.s of  $\mu, \nu$ . Assuming regularity conditions hold, we have

$$\lim_{\delta \rightarrow 0} \frac{\text{W}_2^2(\underline{\pi}_s, \underline{\pi}_{s+\delta})}{\delta^2} = \lim_{\delta \rightarrow 0} \int_0^1 \left( \frac{F_{s+\delta}^{-1}(y) - F_s^{-1}(y)}{\delta} \right)^2 dy = \int_0^1 (\partial_s F_s^{-1}(y))^2 dy.$$

Consider change of variable  $y = F_s(x)$ , then  $\frac{dy}{dx} = f_s(x)$ . As  $x = F_s^{-1}(y)$ ,  $(F_s^{-1})'(y) = \frac{dx}{dy} = \frac{1}{f_s(x)}$ . Taking the derivative of  $s$  on both sides of the equation  $x = F_s^{-1}(F_s(x))$  yields

$$0 = \partial_s F_s^{-1}(F_s(x)) + (F_s^{-1})'(F_s(x)) \partial_s F_s(x) = \partial_s F_s^{-1}(y) + \frac{1}{f_s(x)} \partial_s F_s(x).$$

1782 Therefore,

1783

$$1784 \int_0^1 (\partial_s F_s^{-1}(y))^2 dy = \int \left( \frac{\partial_s F_s(x)}{f_s(x)} \right)^2 f_s(x) dx = \int \frac{(\partial_s F_s(x))^2}{f_s(x)} dx.$$

1785

1786 Consider the interval  $x \in [\frac{m}{2} - 0.1, \frac{m}{2} + 0.1]$ , and fix the range of  $s$  to be  $[0.9, 0.99]$ . We have

1787

$$\begin{cases} 1 - w(s) = \frac{1}{1 + e^{(1-s)m^2/2}} \asymp \frac{1}{e^{(1-s)m^2/2}}, & \forall m \gtrsim 1 \\ -w'(s) = \frac{e^{(1-s)m^2/2} m^2/2}{(1 + e^{(1-s)m^2/2})^2} \asymp \frac{m^2}{e^{(1-s)m^2/2}}, & \forall m \gtrsim 1 \end{cases}$$

1788

1789 First consider upper bounding  $f_s(x)$ . We have the following two bounds:

1790

1791

$$\frac{w(s)}{\sqrt{s}} \phi\left(\frac{x}{\sqrt{s}}\right) \lesssim e^{-\frac{x^2}{2s}} \leq e^{-\frac{(m/2-0.1)^2}{2 \times 0.99}} \leq e^{-\frac{m^2}{8}}, \forall m \gtrsim 1,$$

1792

1793

$$\frac{1 - w(s)}{\sqrt{s}} \phi\left(\frac{x - sm}{\sqrt{s}}\right) \lesssim \frac{1}{e^{(1-s)m^2/2}} e^{-\frac{(sm-x)^2}{2s}} = \exp\left(-\frac{1}{2} \left[ \frac{(sm-x)^2}{s} + (1-s)m^2 \right]\right).$$

1794

1795 The term in the square brackets above is

1796

1797

$$\begin{aligned} \frac{(sm-x)^2}{s} + (1-s)m^2 &\geq \frac{1}{s} \left( sm - \frac{m}{2} - 0.1 \right)^2 + (1-s)m^2 \\ &= \frac{m^2}{4s} - 0.2 \left( 1 - \frac{1}{2s} \right) m + \frac{0.01}{s} \\ &\geq \frac{m^2}{4 \times 0.99} - 0.1m + 0.1 \geq \frac{m^2}{4}, \forall m \gtrsim 1. \end{aligned}$$

1798

1799 Hence, we conclude that  $f_s(x) \lesssim e^{-\frac{m^2}{8}}$ .

1800

1801 Next, we consider lower bounding the term  $(\partial_s F_s(x))^2$ . Note that

1802

1803

$$\begin{aligned} -\partial_s F_s(x) &= -w'(s) \left( \Phi\left(\frac{x}{\sqrt{s}}\right) - \Phi\left(\frac{x - sm}{\sqrt{s}}\right) \right) \\ &\quad + w(s) \phi\left(\frac{x}{\sqrt{s}}\right) \frac{x}{2s^{3/2}} + (1 - w(s)) \phi\left(\frac{x - sm}{\sqrt{s}}\right) \left( \frac{x}{2s^{3/2}} + \frac{m}{2s^{1/2}} \right). \end{aligned}$$

1804

1805 As  $x \in [\frac{m}{2} - 0.1, \frac{m}{2} + 0.1]$  and  $s \in [0.9, 0.99]$ , all these three terms are positive. We only focus on the first term. Note the following two bounds:

1806

1807

$$\begin{cases} \Phi\left(\frac{x}{\sqrt{s}}\right) \geq \Phi\left(\frac{m}{2} - 0.1\right) \geq \frac{3}{4}, & \forall m \gtrsim 1, \\ \Phi\left(\frac{x - sm}{\sqrt{s}}\right) \leq \Phi\left(\frac{m/2 + 0.1 - sm}{\sqrt{s}}\right) \leq \Phi(-0.4m + 0.1) \leq \frac{1}{4}, & \forall m \gtrsim 1. \end{cases}$$

1808

1809 Therefore, we have

1810

1811

$$-\partial_s F_s(x) \gtrsim \frac{m^2}{e^{(1-s)m^2/2}}.$$

1812

1813 To summarize, we derive the following lower bound on the metric derivative:

1814

1815

$$\begin{aligned} |\dot{\underline{\pi}}|_s^2 &= \int \frac{(\partial_s F_s(x))^2}{f_s(x)} dx \geq \int_{\frac{m}{2} - 0.1}^{\frac{m}{2} + 0.1} \frac{(\partial_s F_s(x))^2}{f_s(x)} dx \\ &\gtrsim \int_{\frac{m}{2} - 0.1}^{\frac{m}{2} + 0.1} \frac{m^4 e^{-(1-s)m^2}}{e^{-m^2/8}} dx \\ &\gtrsim m^4 e^{(s - \frac{7}{8})m^2} \geq m^4 e^{\frac{m^2}{40}}, \forall s \in [0.9, 0.99]. \end{aligned}$$

1816

1817 Finally, recall that  $S(\theta) := \frac{1}{1 + m^2(1-\theta)^r}$ , and  $\pi_\theta = \underline{\pi}_{S(\theta)}$ . Hence, by chain rule of derivative,

1818  $|\dot{\pi}|_\theta = |\dot{\underline{\pi}}|_{S(\theta)} |S'(\theta)|$ . Let

1819

1820

$$\Theta := \{\theta \in [0, 1] : S(\theta) \in [0.9, 0.99]\} = \left[ 1 - \left( \frac{1/0.9 - 1}{m^2} \right)^{\frac{1}{r}}, 1 - \left( \frac{1/0.99 - 1}{m^2} \right)^{\frac{1}{r}} \right].$$

1821

1836 We have

$$\begin{aligned}
 1838 \quad \mathcal{A}_r &= \int_0^1 |\dot{\pi}|_\theta^2 d\theta = \int_0^1 |\dot{\pi}|_{S(\theta)}^2 |S'(\theta)|^2 d\theta \geq \int_\Theta |\dot{\pi}|_{S(\theta)}^2 |S'(\theta)|^2 d\theta \\
 1839 \\
 1840 \quad &\geq \min_{\theta \in \Theta} |S'(\theta)| \cdot \int_\Theta |\dot{\pi}|_{S(\theta)}^2 |S'(\theta)| d\theta = \min_{\theta \in \Theta} |S'(\theta)| \cdot \int_{0.9}^{0.99} |\dot{\pi}|_s^2 ds. \\
 1841 \\
 1842
 \end{aligned}$$

1843 For any  $\theta \in \Theta$ ,

$$\begin{aligned}
 1844 \\
 1845 \quad |S'(\theta)| &= \frac{m^2 r (1 - \theta)^{r-1}}{(1 + m^2 (1 - \theta)^r)^2} \geq \frac{m^2 r \left(\frac{1/0.99-1}{m^2}\right)^{1-1/r}}{\left(1 + m^2 \left(\frac{1/0.9-1}{m^2}\right)\right)^2} = \frac{m^{2/r} r (1/99)^{1-1/r}}{(1/0.9)^2} \gtrsim m^{2/r} \gtrsim 1, \\
 1846 \\
 1847 \\
 1848
 \end{aligned}$$

1849 where in the first “ $\gtrsim$ ” we used the inequality  $r \left(\frac{1}{99}\right)^{1-\frac{1}{r}} \geq \frac{1}{e^4}$  that holds for all  $r \geq 1$ . Thus, the  
 1850 proof is complete.  $\square$

1851 **Remark 8.** In the above theorem, we established an exponential lower bound on the metric derivative  
 1852 of the  $W_2$  distance, given by  $\lim_{\delta \rightarrow 0} \frac{W_2(\pi_s, \pi_{s+\delta})}{|\delta|}$ . In OT, another useful distance, the **Wasserstein-1**  
 1853 ( **$W_1$  distance**), defined as  $W_1(\mu, \nu) = \inf_{\gamma \in \Pi(\mu, \nu)} \int \|x - y\| \gamma(dx, dy)$ , is a lower bound of the  $W_2$   
 1854 distance. Below, we present a surprising result regarding the metric derivative of  $W_1$  distance on the  
 1855 same curve of probability distributions. This result reveals an exponentially large gap between the  
 1856  $W_1$  and  $W_2$  metric derivatives on the same curve, which is of independent interest.

1857 **Theorem 6.** Define the probability distributions  $\pi_s$  as in the proof of Prop. 1, for some large enough  
 1858  $m \gtrsim 1$ . Then, for all  $s \in [0.9, 0.99]$ , we have

$$\begin{aligned}
 1859 \quad \lim_{\delta \rightarrow 0} \frac{W_1(\pi_s, \pi_{s+\delta})}{|\delta|} &\lesssim 1. \\
 1860 \\
 1861 \\
 1862
 \end{aligned}$$

1863 *Proof.* Since  $W_1(\mu, \nu) = \int |F_\mu(x) - F_\nu(x)| dx$  (Villani, 2003, Thm. 2.18), by assuming regularity  
 1864 conditions, we have

$$\begin{aligned}
 1865 \quad \lim_{\delta \rightarrow 0} \frac{W_1(\pi_s, \pi_{s+\delta})}{|\delta|} &= \int |\partial_s F_s(x)| dx \\
 1866 \\
 1867 \quad &\leq \int \left| w'(s) \left( \Phi\left(\frac{x}{\sqrt{s}}\right) - \Phi\left(\frac{x-sm}{\sqrt{s}}\right) \right) \right| dx \\
 1868 \\
 1869 \quad &+ \int \left| w(s) \phi\left(\frac{x}{\sqrt{s}}\right) \frac{x}{2s^{3/2}} \right| dx \\
 1870 \\
 1871 \quad &+ \int \left| (1 - w(s)) \phi\left(\frac{x-sm}{\sqrt{s}}\right) \left( \frac{x}{2s^{3/2}} + \frac{m}{2s^{1/2}} \right) \right| dx. \\
 1872 \\
 1873 \\
 1874 \\
 1875 \\
 1876 \\
 1877
 \end{aligned}$$

1878 To bound the first term, notice that for any  $\lambda > 0$ ,

$$\Phi\left(\frac{x}{\sqrt{s}}\right) - \Phi\left(\frac{x-sm}{\sqrt{s}}\right) \lesssim \begin{cases} \sqrt{s}m e^{-\frac{(x-sm)^2}{2s}}, & \frac{x-sm}{\sqrt{s}} \geq \lambda; \\ \sqrt{s}m e^{-\frac{x^2}{2s}}, & \frac{x}{\sqrt{s}} \leq -\lambda; \\ 1, & \text{otherwise.} \end{cases}$$

1879 Therefore, using Gaussian tail bound  $1 - \Phi(\lambda) \leq \frac{1}{2} e^{-\frac{\lambda^2}{2}}$ , the first term is bounded by

$$\begin{aligned}
 1880 \quad &\lesssim \frac{m^2}{e^{(1-s)m^2/2}} [2\sqrt{s}\lambda + sm + sm(1 - \Phi(\lambda)) + sm\Phi(-\lambda)] \\
 1881 \\
 1882 \quad &\lesssim \frac{m^2}{e^{(1-s)m^2/2}} [\lambda + m + e^{-\frac{\lambda^2}{2}}] \stackrel{\lambda \leftarrow \Theta(m)}{\lesssim} \frac{m^3}{e^{(1-s)m^2/2}} = o(1). \\
 1883 \\
 1884 \\
 1885
 \end{aligned}$$

1890 The second term is bounded by  
 1891

$$1892 \lesssim \int \phi\left(\frac{x}{\sqrt{s}}\right) |x| dx = s \int \phi(u) |u| du \lesssim 1.$$

1893  
 1894 Finally, the third term is bounded by  
 1895

$$1896 \lesssim \frac{1}{e^{(1-s)m^2/2}} \int \phi\left(\frac{x-sm}{\sqrt{s}}\right) (|x|+m) dx \\ 1897 \lesssim \frac{1}{e^{(1-s)m^2/2}} \int \phi(u) (|u|+m) du \lesssim \frac{m}{e^{(1-s)m^2/2}} = o(1).$$

□

1901  
 1902  
 1903 **E.2 PROOF OF PROP. 2**

1904 *Proof.* We first prove a more general result with  $\phi$  being *any* distribution with weak regularity  
 1905 condition, and then focus on the special case where  $\phi = \mathcal{N}(0, I)$ .

1906  
 1907 Note that the LD with target distribution  $\phi$ ,

$$1908 dY_t = \nabla \log \phi(Y_t) dt + \sqrt{2} dB_t, \quad Y_t \sim \bar{\pi}_t,$$

1909 can be perceived as the Wasserstein gradient flow of  $\text{KL}(\cdot \parallel \phi)$ .  $\bar{\pi}_t$  satisfies the Fokker-Planck equation  
 1910  $\partial_t \bar{\pi}_t = \nabla \cdot \left( \bar{\pi}_t \nabla \log \frac{\bar{\pi}_t}{\phi} \right)$ . Hence, the vector field  $\left( v_t := -\nabla \log \frac{\bar{\pi}_t}{\phi} \right)_{t \in [0, \infty)}$  generates  $(\bar{\pi}_t)_{t \in [0, \infty)}$ ,  
 1911 and each  $v_t$  can be written as a gradient field of a potential function. Thus, by the uniqueness result  
 1912 in Lem. 4, we conclude that  
 1913

$$1914 |\dot{\bar{\pi}}|_t^2 = \left\| \nabla \log \frac{\bar{\pi}_t}{\phi} \right\|_{L^2(\bar{\pi}_t)}^2 = \text{FI}(\bar{\pi}_t \parallel \phi) = -\partial_t \text{KL}(\bar{\pi}_t \parallel \phi) \implies \int_0^\infty |\dot{\bar{\pi}}|_t^2 dt = \text{KL}(\pi \parallel \phi),$$

1915 where FI is the Fisher divergence.  
 1916

1917 For the special case where  $\phi = \mathcal{N}(0, I)$ , using the log-Sobolev equality (Def. 3), the smoothness of  
 1918  $V$ , and Lem. 13, we can further bound the KL divergence as follows:

$$1919 \text{KL}(\pi \parallel \phi) \leq \frac{1}{2} \text{FI}(\pi \parallel \phi) = \frac{1}{2} \mathbb{E}_{\pi(x)} \| -\nabla V(x) + x \|^2 \leq \mathbb{E}_\pi \|\nabla V\|^2 + \mathbb{E}_\pi \|\cdot\|^2 \leq d\beta + m^2.$$

□

1920  
 1921  
 1922  
 1923 **E.3 PROOF OF THM. 5**

1924 *Proof.* By Nelson's relation (Lem. 2),  $\mathbb{Q}$  is equivalent to the path measure of the following SDE:  
 1925

$$1926 dX_t = X_t dt + \sqrt{2} dB_t^\leftarrow, \quad t \in [0, T-\delta]; \quad X_{T-\delta} \sim \bar{\pi}_\delta.$$

1927 Leveraging Girsanov's theorem (Lem. 3), we know that for a.s.  $X \sim \mathbb{Q}^\dagger$ :

$$1928 \log \frac{d\mathbb{Q}^\dagger}{d\mathbb{Q}}(X) = \log \frac{\phi(X_0)}{\bar{\pi}_\delta(X_{T-\delta})} + \frac{1}{2} \int_0^{T-\delta} (\langle X_t + 2s_{T-t-}(X_{t-}), dX_t \rangle - \langle X_t, *dX_t \rangle) \\ 1929 - \frac{1}{4} \int_0^{T-\delta} (\|X_t + 2s_{T-t-}(X_{t-})\|^2 - \|X_t\|^2) dt.$$

1930 Note that for  $X \sim \mathbb{Q}^\dagger$ ,  $\int_0^{T-\delta} \langle X_t, *dX_t \rangle = \int_0^{T-\delta} \langle X_t, dX_t \rangle + [X, X]_{T-\delta}$  and  $[X, X]_{T-\delta} =$   
 1931  $[\sqrt{2}B, \sqrt{2}B]_{T-\delta} = 2(T-\delta)d$ . Some simple calculations yield

$$1932 \log \frac{d\mathbb{Q}^\dagger}{d\mathbb{Q}}(X) = \log \frac{\phi(X_0)}{\bar{\pi}_\delta(X_{T-\delta})} - (T-\delta)d + \int_0^{T-\delta} (\|s_{T-t-}(X_{t-})\|^2 dt + \sqrt{2} \langle s_{T-t-}(X_{t-}), dB_t \rangle) \\ 1933 = \log Z + W(X) + \log \frac{d\pi}{d\bar{\pi}_\delta}(X_{T-\delta}).$$

1944 Thus, the equation  $\mathbb{E}_{\mathbb{Q}^\dagger} \frac{d\mathbb{Q}}{d\mathbb{Q}^\dagger} = 1$  implies  
 1945

1946 
$$Z = \mathbb{E}_{\mathbb{Q}^\dagger(X)} e^{-W(X)} \frac{d\bar{\pi}_\delta}{d\pi}(X_{T-\delta}) \approx \mathbb{E}_{\mathbb{Q}^\dagger(X)} e^{-W(X)} = \mathbb{E} \hat{Z}.$$
  
 1947

1948 Since  $\frac{\hat{Z}}{Z} = \frac{d\mathbb{Q}}{d\mathbb{Q}^\dagger}(X) \frac{d\pi}{d\bar{\pi}_\delta}(X_{T-\delta})$ , we have  
 1949

1950 
$$\begin{aligned} \Pr \left( \left| \frac{\hat{Z}}{Z} - 1 \right| \geq \varepsilon \right) &= \Pr_{X \sim \mathbb{Q}^\dagger} \left( \left| \frac{d\mathbb{Q}}{d\mathbb{Q}^\dagger}(X) \frac{d\pi}{d\bar{\pi}_\delta}(X_{T-\delta}) - 1 \right| \geq \varepsilon \right) \\ &\leq \Pr_{X \sim \mathbb{Q}^\dagger} \left( \left| \frac{d\mathbb{Q}}{d\mathbb{Q}^\dagger}(X) - 1 \right| \gtrsim \varepsilon \right) + \Pr_{X \sim \mathbb{Q}^\dagger} \left( \left| \frac{d\pi}{d\bar{\pi}_\delta}(X_{T-\delta}) - 1 \right| \gtrsim \varepsilon \right). \end{aligned}$$
  
 1951

1952 The inequality is due to the fact that  $|ab - 1| \geq \varepsilon$  implies  $|a - 1| \geq \frac{\varepsilon}{3}$  or  $|b - 1| \geq \frac{\varepsilon}{3}$  for  $\varepsilon \in [0, 1]$ . It  
 1953 suffices to make both terms above  $O(1)$ . To bound the first term, we use the similar approach as in  
 1954 the proof of (18) in Thm. 2:  
 1955

1956 
$$\Pr_{X \sim \mathbb{Q}^\dagger} \left( \left| \frac{d\mathbb{Q}}{d\mathbb{Q}^\dagger}(X) - 1 \right| \gtrsim \varepsilon \right) = \mathbb{Q}^\dagger \left( \left| \frac{d\mathbb{Q}}{d\mathbb{Q}^\dagger} - 1 \right| \gtrsim \varepsilon \right) \lesssim \frac{\text{TV}(\mathbb{Q}, \mathbb{Q}^\dagger)}{\varepsilon} \lesssim \frac{\sqrt{\text{KL}(\mathbb{Q} \parallel \mathbb{Q}^\dagger)}}{\varepsilon}.$$
  
 1957

1958 Hence, it suffices to let  $\text{TV}(\mathbb{Q}, \mathbb{Q}^\dagger)^2 \lesssim \text{KL}(\mathbb{Q} \parallel \mathbb{Q}^\dagger) \lesssim \varepsilon^2$ . To bound the second term, we have  
 1959

1960 
$$\begin{aligned} \Pr_{X \sim \mathbb{Q}^\dagger} \left( \left| \frac{d\pi}{d\bar{\pi}_\delta}(X_{T-\delta}) - 1 \right| \gtrsim \varepsilon \right) &\leq \Pr_{X \sim \mathbb{Q}} \left( \left| \frac{d\pi}{d\bar{\pi}_\delta}(X_{T-\delta}) - 1 \right| \gtrsim \varepsilon \right) + \text{TV}(\mathbb{Q}, \mathbb{Q}^\dagger) \\ &\leq \bar{\pi}_\delta \left( \left| \frac{d\pi}{d\bar{\pi}_\delta} - 1 \right| \gtrsim \varepsilon \right) + \text{TV}(\mathbb{Q}, \mathbb{Q}^\dagger) \\ &\lesssim \frac{\text{TV}(\bar{\pi}_\delta, \pi)}{\varepsilon} + \varepsilon. \end{aligned}$$
  
 1961

1962 Therefore, it suffices to make  $\text{TV}(\bar{\pi}_\delta, \pi) \lesssim \varepsilon$ . □  
 1963

#### 1964 E.4 AN UPPER BOUND OF THE TV DISTANCE ALONG THE OU PROCESS

1965 **Lemma 7.** Assume that the target distribution  $\pi \propto e^{-V}$  satisfies Assump. 2. Let  $\bar{\pi}_\delta$  be the distribution  
 1966 of  $Y_\delta$  in the OU process (12) initialized at  $Y_0 \sim \pi$ , for some  $\delta \lesssim 1$ . Then,  
 1967

1968 
$$\text{TV}(\pi, \bar{\pi}_\delta) \lesssim \delta(\beta m^2 + d + \beta d) + \delta^{\frac{1}{2}} d^{\frac{1}{2}} \beta m.$$
  
 1969

1970 **Remark 9.** Consider a simplified case where  $\beta \gtrsim 1$  and  $m^2 \asymp d$ . Then it suffices to choose  $\delta \lesssim \frac{\varepsilon^2}{\beta^2 d^2}$   
 1971 in order to guarantee  $\text{TV}(\pi, \bar{\pi}_\delta) \lesssim \varepsilon$ .  
 1972

1973 *Proof.* Our proof is inspired by Lee et al. (2023, Lem. 6.4), which addresses the case where  $V$  is  
 1974 Lipschitz.  
 1975

1976 Without loss of generality, suppose  $\pi = e^{-V}$ . Let  $\phi$  be the p.d.f. of  $\mathcal{N}(0, I)$ , and define  $\sigma^2 :=$   
 1977  $1 - e^{-2\delta} \asymp \delta$ . We will use the following inequality:  $|e^a - e^b| \leq (e^a + e^b)|a - b|$ , which is due to the  
 1978 convexity of the exponential function. By the smoothness of  $V$ ,  $\|\nabla V(x)\| = \|\nabla V(x) - \nabla V(0)\| \leq$   
 1979  $\beta\|x\|$ .  
 1980

1981 Define  $\pi'(x) = e^{d\delta} \pi(e^\delta x)$ , and thus  $\bar{\pi}_\delta(x) = \int \pi'(x + \sigma u) \phi(u) du$ . Using triangle inequality, we  
 1982 bound  $\text{TV}(\pi, \pi')$  and  $\text{TV}(\pi', \bar{\pi}_\delta)$  separately. First,  
 1983

1984 
$$\begin{aligned} \text{TV}(\pi, \pi') &= \frac{1}{2} \int |e^{-V(x)} - e^{-V(e^\delta x) + d\delta}| dx \\ &\lesssim \int (\pi(x) + \pi'(x)) (|V(e^\delta x) - V(x)| + d\delta) dx. \end{aligned}$$
  
 1985

1998  
1999

By the smoothness,

2000  
2001  
2002  
2003  
2004  
2005

$$\begin{aligned} |V(e^\delta x) - V(x)| &\leq \|\nabla V(x)\|(e^\delta - 1)\|x\| + \frac{\beta}{2}(e^\delta - 1)^2\|x\|^2 \\ &\lesssim \beta\|x\|\delta\|x\| + \beta\delta^2\|x\|^2 \lesssim \beta\delta\|x\|^2. \\ \implies \text{TV}(\pi, \pi') &\lesssim \delta \int (\pi(x) + \pi'(x))(\beta\|x\|^2 + d)dx. \end{aligned}$$

2006  
2007  
2008  
2009

Note that  $\int \pi(x)(\beta\|x\|^2 + d)dx = \beta m^2 + d$ . Since  $\mathbb{E}_{\pi'} \varphi = \mathbb{E}_\pi \varphi(e^{-\delta}\cdot)$ , we also have

$$\int \pi'(x)(\beta\|x\|^2 + d)dx = e^{-2\delta}\beta m^2 + d \leq \beta m^2 + d.$$

2010  
2011  
2012  
2013

We thus conclude that

$$\text{TV}(\pi, \pi') \lesssim \delta(\beta m^2 + d).$$

2014  
2015  
2016  
2017  
2018  
2019  
2020

Next,

$$\begin{aligned} \text{TV}(\pi', \bar{\pi}_\delta) &= \frac{1}{2} \int \left| \int (\pi'(x + \sigma u) - \pi'(x))\phi(u)du \right| dx \\ &\lesssim \iint |\pi'(x + \sigma u) - \pi'(x)|\phi(u)dudx \\ &\lesssim \iint (\pi'(x + \sigma u) + \pi'(x))|V(e^\delta(x + \sigma u)) - V(e^\delta x)|\phi(u)dudx. \end{aligned}$$

2021  
2022

Again, by smoothness,

$$\begin{aligned} V(e^\delta(x + \sigma u)) - V(e^\delta x) &\leq \|\nabla V(e^\delta x)\|e^\delta\sigma\|u\| + \frac{\beta}{2}e^{2\delta}\sigma^2\|u\|^2 \\ &\lesssim \beta e^\delta\|x\|e^\delta\sigma\|u\| + \beta e^{2\delta}\sigma^2\|u\|^2 \\ &\lesssim \beta\|x\|\delta^{\frac{1}{2}}\|u\| + \beta\delta\|u\|^2. \end{aligned}$$

2027  
2028

Therefore,

$$\text{TV}(\pi', \bar{\pi}_\delta) \lesssim \beta\delta^{\frac{1}{2}} \iint (\pi'(x + \sigma u) + \pi'(x))(\|u\|\|x\| + \delta^{\frac{1}{2}}\|u\|^2)\phi(u)dudx.$$

2031  
2032

Note that, first,

$$\iint \pi'(x)(\|u\|\|x\| + \delta^{\frac{1}{2}}\|u\|^2)\phi(u)dudx \lesssim \mathbb{E}_{\pi'} \|\cdot\|d^{\frac{1}{2}} + \delta^{\frac{1}{2}}d \leq md^{\frac{1}{2}} + \delta^{\frac{1}{2}}d;$$

2035  
2036

second,

$$\begin{aligned} &\iint \pi'(x + \sigma u)(\|u\|\|x\| + \delta^{\frac{1}{2}}\|u\|^2)\phi(u)dudx \\ &= \iint \pi'(y)(\|u\|\|y - \sigma u\| + \delta^{\frac{1}{2}}\|u\|^2)\phi(u)dudy \\ &\lesssim \iint \pi'(y)(\|u\|\|y\| + \delta^{\frac{1}{2}}\|u\|^2)\phi(u)dudy \lesssim md^{\frac{1}{2}} + \delta^{\frac{1}{2}}d. \end{aligned}$$

2044  
2045

Therefore,  $\text{TV}(\pi', \bar{\pi}_\delta) \lesssim \beta\delta^{\frac{1}{2}}d^{\frac{1}{2}}(m + \delta^{\frac{1}{2}}d^{\frac{1}{2}})$ . The proof is complete.  $\square$

2046  
2047

## E.5 DISCUSSION ON THE OVERALL COMPLEXITY OF RDS

2048  
2049  
2050  
2051

In RDS, an accurate score estimate  $s \approx \nabla \log \bar{\pi}$  is critical for the algorithmic efficiency. Existing methods estimate scores through different ways. Here, we review the existing methods and their complexity guarantees for sampling, and leverage Thm. 5 to derive the complexity of normalizing constant estimation. Throughout this section, we always assume that the target distribution  $\pi \propto e^{-V}$  satisfies  $m^2 := \mathbb{E}_\pi \|\cdot\|^2 < \infty$  and that  $V$  is  $\beta$ -smooth.

2052 (I) **Reverse diffusion Monte Carlo.** The seminal work directly leveraged the following Tweedie's  
 2053 formula (Robbins, 1992) to estimate the score:  
 2054

$$2055 \quad \nabla \log \bar{\pi}_t(x) = \mathbb{E}_{\bar{\pi}_{0|t}(x_0|x)} \frac{e^{-t}x_0 - x}{1 - e^{-2t}}, \quad (33)$$

2056 where

$$2057 \quad \bar{\pi}_{0|t}(x_0|x) \propto_{x_0} \exp \left( -V(x_0) - \frac{\|x_0 - e^t x\|^2}{2(e^{2t} - 1)} \right) \quad (34)$$

2058 is the posterior distribution of  $Y_0$  conditional on  $Y_t = x$  in the OU process (12). The paper proposed  
 2059 to sample from  $\bar{\pi}_{0|t}(\cdot|x)$  by LMC and estimate the score via empirical mean, which has a provably  
 2060 better LSI constant than the target distribution  $\pi$  (see Huang et al. (2024a, Lem. 2)). They show  
 2061 that if the scores  $\nabla \log \bar{\pi}_t$  are uniformly  $\beta$ -Lipschitz, and assume that there exists some  $c > 0$  and  
 2062  $n > 0$  such that for any  $r > 0$ ,  $V + r\|\cdot\|^2$  is convex for  $\|x\| \geq \frac{c}{r^n}$ , then w.p.  $\geq 1 - \zeta$ , the overall  
 2063 complexity for guaranteeing  $\text{KL}(\mathbb{Q} \parallel \mathbb{Q}^\dagger) \lesssim \varepsilon^2$  is  
 2064

$$2065 \quad O \left( \text{poly} \left( d, \frac{1}{\zeta} \right) \exp \left( \frac{1}{\varepsilon} \right)^{O(n)} \right),$$

2066 which is also the complexity of obtaining a  $\hat{Z}$  satisfying (1).  
 2067

2068 (II) **Recursive score diffusion-based Monte Carlo.** A second work Huang et al. (2024b) proposed  
 2069 to estimate the scores in a recursive scheme. Assuming the scores  $\nabla \log \bar{\pi}_t$  are uniformly  $\beta$ -Lipschitz,  
 2070 they established a complexity  
 2071

$$2072 \quad \exp \left( \beta^3 \log^3 \text{poly} \left( \beta, d, m^2, \frac{1}{\zeta} \right) \right)$$

2073 in order to guarantee  $\text{KL}(\mathbb{Q} \parallel \mathbb{Q}^\dagger) \lesssim \varepsilon^2$  w.p.  $\geq 1 - \zeta$ .  
 2074

2075 (III) **Zeroth-order diffusion Monte Carlo.** The following work He et al. (2024) proposed a  
 2076 zeroth-order method that leverages rejection sampling to sample from  $\bar{\pi}_{0|t}(\cdot|x)$ . When  $V$  is  $\beta$ -  
 2077 smooth, they showed that with a small early stopping time  $\delta$ , the overall complexity for guaranteeing  
 2078  $\text{KL}(\mathbb{Q} \parallel \mathbb{Q}^\dagger) \lesssim \varepsilon^2$  is  
 2079

$$2080 \quad \exp \left( \tilde{O}(d) \log \beta \log \frac{1}{\varepsilon} \right).$$

2081 (IV) **Self-normalized estimator.** Finally, a recent work Vacher et al. (2025) proposed to estimate  
 2082 the scores in a different approach:  
 2083

$$2084 \quad \nabla \log \bar{\pi}_t(x) = -\frac{1}{1 - e^{-2t}} \frac{\mathbb{E}[\xi e^{-V(e^t(x-\xi))}]}{\mathbb{E}[e^{-V(e^t(x-\xi))}]}, \quad \text{where } \xi \sim \mathcal{N}(0, (1 - e^{-2t})I).$$

2085 Assume that  $V$  is  $\beta$ -smooth, and the distributions along the OU process starting from  $\pi \propto e^{-V}$   
 2086 and  $\pi' \propto e^{-2V}$  have potentials whose Hessians are uniformly  $\succeq -\beta I$ , then the complexity for  
 2087 guaranteeing  $\mathbb{E} \text{KL}(\mathbb{Q} \parallel \mathbb{Q}^\dagger) \lesssim \varepsilon^2$  is  
 2088

$$2089 \quad O \left( \left( \frac{\beta(m^2 \vee d)}{\varepsilon} \right)^{O(d)} \right).$$

## F SUPPLEMENTARY LEMMAS

2100 **Lemma 8.** For  $x > 0$  and  $\varepsilon \in (0, \frac{1}{2})$ , define  $x_0 := |\log x|$  and  $x_1 := |x - 1|$ . Then  $x_i \geq \varepsilon$  implies  
 2101  $x_{1-i} \geq \frac{\varepsilon}{2}$ , and  $x_i \leq \varepsilon$  implies  $x_{1-i} \leq 2\varepsilon$ , for both  $i = 0, 1$ .  
 2102

2103 This follows from the standard calculus approximation  $\log x \approx x - 1$  when  $x \approx 1$ . The proof is  
 2104 straightforward and is left as an exercise for the reader.  
 2105

**Lemma 9.** For any  $0 \leq a \leq b \leq 1$  and  $r \geq 1$ ,  $b^r - a^r \leq r(b - a)$ .

2106 *Proof.* This is immediate from the decreasing property of the function  $\varphi(x) := x^r - rx$ ,  $x \in [0, 1]$ ,  
 2107 since  $\varphi'(x) = r(x^{r-1} - 1) \leq 0$ .  $\square$   
 2108

2109 **Lemma 10** (The median trick (Jerrum et al., 1986)). *Let  $\widehat{Z}_1, \dots, \widehat{Z}_N$  be  $N(\geq 3)$  i.i.d. random  
 2110 variables satisfying*

$$2111 \quad \Pr \left( \left| \frac{\widehat{Z}_n}{Z} - 1 \right| \leq \varepsilon \right) \geq \frac{3}{4}, \quad \forall n \in \llbracket 1, N \rrbracket,$$

2114 and let  $\widehat{Z}_*$  be the median of  $\widehat{Z}_1, \dots, \widehat{Z}_N$ . Then

$$2115 \quad \Pr \left( \left| \frac{\widehat{Z}_*}{Z} - 1 \right| \leq \varepsilon \right) \geq 1 - e^{-\frac{N}{72}}.$$

2118 In particular, for any  $\zeta \in (0, \frac{1}{4})$ , choosing  $N = \lceil 72 \log \frac{1}{\zeta} \rceil$ , the probability is at least  $1 - \zeta$ .  
 2119

2120 *Proof.* Let  $A_n := \left\{ \left| \frac{\widehat{Z}_n}{Z} - 1 \right| > \varepsilon \right\}$ , which are i.i.d. events happening w.p.  $p \leq \frac{1}{4}$ . If  $\left| \frac{\widehat{Z}_*}{Z} - 1 \right| > \varepsilon$ ,  
 2121 then there are at least  $\lfloor \frac{N}{2} \rfloor$   $A_n$ 's happening, i.e.,  $S_N := \sum_{n=1}^N 1_{A_n} \geq \lfloor \frac{N}{2} \rfloor$ . Then,

$$2124 \quad \Pr \left( \left| \frac{\widehat{Z}_*}{Z} - 1 \right| > \varepsilon \right) \leq \Pr \left( S_N \geq \left\lfloor \frac{N}{2} \right\rfloor \right) = \Pr \left( S_N - \mathbb{E} S_N \geq \left\lfloor \frac{N}{2} \right\rfloor - pN \right) \\ 2125 \quad \leq \Pr \left( S_N - \mathbb{E} S_N \geq \frac{N}{12} \right) \leq e^{-\frac{N}{72}},$$

2129 where the first inequality on the second line follows from the fact that  $\lfloor \frac{N}{2} \rfloor \geq \frac{N-1}{2} \geq \frac{N}{3}$  for all  
 2130  $N \geq 3$ , and the last inequality is due to the Hoeffding's inequality.  $\square$

2131 **Lemma 11.** *The update rule of AIS (10) is:*

$$2133 \quad X_{T_\ell} = e^{-\Lambda(T_\ell)} X_0 - \left( \int_0^{T_\ell} e^{-(\Lambda(T_\ell) - \Lambda(t))} dt \right) \nabla V(X_0) + \left( 2 \int_0^{T_\ell} e^{-2(\Lambda(T_\ell) - \Lambda(t))} dt \right)^{\frac{1}{2}} \xi,$$

2136 where  $\Lambda(t) := \int_0^t \lambda \left( \theta_{\ell-1} + \frac{\tau}{T_\ell} (\theta_\ell - \theta_{\ell-1}) \right) d\tau$ , and  $\xi \sim \mathcal{N}(0, I)$  is independent of  $X_0$ .  
 2137

2138 *Proof.* By Itô's formula, we have

$$2140 \quad d(e^{\Lambda(t)} X_t) = e^{\Lambda(t)} (\Lambda'(t) X_t dt + dX_t) = e^{\Lambda(t)} (-\nabla V(X_0) dt + \sqrt{2} dB_t).$$

2141 Integrating over  $t \in [0, T_\ell]$ , we obtain

$$2143 \quad e^{\Lambda(T_\ell)} X_{T_\ell} - X_0 = - \left( \int_0^{T_\ell} e^{\Lambda(t)} dt \right) \nabla V(X_0) + \sqrt{2} \int_0^{T_\ell} e^{\Lambda(t)} dB_t, \\ 2144 \quad \implies X_{T_\ell} = e^{-\Lambda(T_\ell)} X_0 - \left( \int_0^{T_\ell} e^{-(\Lambda(T_\ell) - \Lambda(t))} dt \right) \nabla V(X_0) + \sqrt{2} \int_0^{T_\ell} e^{-(\Lambda(T_\ell) - \Lambda(t))} dB_t,$$

2149 and  $\sqrt{2} \int_0^{T_\ell} e^{-(\Lambda(T_\ell) - \Lambda(t))} dB_t \sim \mathcal{N} \left( 0, \left( 2 \int_0^{T_\ell} e^{-2(\Lambda(T_\ell) - \Lambda(t))} dt \right) I \right)$  by Itô isometry.  $\square$   
 2150

2151 **Lemma 12.** *The update rule of the RDS (14) is*

$$2152 \quad X_{t_{k+1}} = e^{t_{k+1} - t_k} X_{t_k} + 2(e^{t_{k+1} - t_k} - 1) s_{T-t_k}(X_{t_k}) + \Xi_k,$$

2153 where

$$2154 \quad \Xi_k := \int_{t_k}^{t_{k+1}} \sqrt{2} e^{-(t-t_{k+1})} dB_t \sim \mathcal{N} \left( 0, (e^{2(t_{k+1} - t_k)} - 1) I \right),$$

2156 and the correlation matrix between  $\Xi_k$  and  $B_{t_{k+1}} - B_{t_k}$  is

$$2158 \quad \text{Corr}(\Xi_k, B_{t_{k+1}} - B_{t_k}) = \frac{\sqrt{2}(e^{t_{k+1} - t_k} - 1)}{\sqrt{(e^{2(t_{k+1} - t_k)} - 1)(t_{k+1} - t_k)}} I.$$

2160 *Proof.* By applying Itô’s formula to (14) for  $t \in [t_k, t_{k+1}]$ , we have  
 2161

$$\begin{aligned} 2162 \quad d(e^{-t} X_t) &= e^{-t}(-X_t dt + dX_t) = e^{-t}(2s_{T-t_k}(X_{t_k})dt + \sqrt{2}dB_t) \\ 2163 \\ 2164 \quad \implies e^{-t_{k+1}} X_{t_{k+1}} - e^{-t_k} X_{t_k} &= 2(e^{-t_k} - e^{-t_{k+1}})s_{T-t_k}(X_{t_k}) + \int_{t_k}^{t_{k+1}} \sqrt{2}e^{-t} dB_t. \\ 2165 \end{aligned}$$

2166 The covariance between two zero-mean Gaussian random variables  $\Xi_k$  and  $B_{t_{k+1}} - B_{t_k}$  is  
 2167

$$\begin{aligned} 2168 \quad \text{Cov}(\Xi_k, B_{t_{k+1}} - B_{t_k}) &= \mathbb{E}[\Xi_k (B_{t_{k+1}} - B_{t_k})^T] \\ 2169 \\ 2170 \quad &= \mathbb{E}\left[\left(\int_{t_k}^{t_{k+1}} \sqrt{2}e^{-(t-t_{k+1})} dB_t\right) \left(\int_{t_k}^{t_{k+1}} dB_t\right)^T\right] \\ 2171 \\ 2172 \quad &= \int_{t_k}^{t_{k+1}} \sqrt{2}e^{-(t-t_{k+1})} dt \cdot I = \sqrt{2}(e^{t_{k+1}-t_k} - 1)I. \\ 2173 \\ 2174 \end{aligned}$$

2175 Finally,  $\text{Corr}(u, v) = \text{diag}(\text{Cov } u)^{-\frac{1}{2}} \text{Cov}(u, v) \text{diag}(\text{Cov } v)^{-\frac{1}{2}}$  yields the correlation.  $\square$   
 2176

2177 **Lemma 13** (Chewi (2022, Lemma 4.E.1)). *Consider a probability measure  $\mu \propto e^{-U}$  on  $\mathbb{R}^d$ .*

2178 **1.** *If  $\nabla^2 U \succeq \alpha I$  for some  $\alpha > 0$  and  $x_\star$  is the global minimizer of  $U$ , then  $\mathbb{E}_\mu \|\cdot - x_\star\|^2 \leq \frac{d}{\alpha}$ .*  
 2179 **2.** *If  $\nabla^2 U \preceq \beta I$  for some  $\beta > 0$ , then  $\mathbb{E}_\mu \|\nabla U\|^2 \leq \beta d$ .*

2180 **Lemma 14.** *Define  $\hat{\pi}_\lambda \propto \exp(-V - \frac{\lambda}{2}\|\cdot\|^2)$ ,  $\lambda \geq 0$ . Then under Assump. 2,  $\mathbb{E}_{\hat{\pi}_\lambda} \|\cdot\|^2 \leq m^2$  for  
 2181 all  $\lambda \geq 0$ .*

2182 *Proof.* Let  $V_\lambda := V + \frac{\lambda}{2}\|\cdot\|^2$ , and  $Z_\lambda = \int e^{-V_\lambda} dx$ , so  $\hat{\pi}_\lambda = e^{-V_\lambda - \log Z_\lambda}$ . We have  
 2183

$$\begin{aligned} 2184 \quad \frac{d}{d\lambda} \log Z_\lambda &= \frac{Z'_\lambda}{Z_\lambda} = -\frac{1}{Z_\lambda} \int e^{-V_\lambda} V'_\lambda dx = -\frac{1}{2} \mathbb{E}_{\hat{\pi}_\lambda} \|\cdot\|^2, \\ 2185 \\ 2186 \quad \implies \frac{d}{d\lambda} \log \hat{\pi}_\lambda &= -V'_\lambda - \frac{d}{d\lambda} \log Z_\lambda = \frac{1}{2} (\mathbb{E}_{\hat{\pi}_\lambda} \|\cdot\|^2 - \|\cdot\|^2), \\ 2187 \\ 2188 \quad \implies \frac{d}{d\lambda} \mathbb{E}_{\hat{\pi}_\lambda} \|\cdot\|^2 &= \int \|\cdot\|^2 \left( \frac{d}{d\lambda} \log \hat{\pi}_\lambda \right) d\hat{\pi}_\lambda = \frac{1}{2} \left( (\mathbb{E}_{\hat{\pi}_\lambda} \|\cdot\|^2)^2 - \mathbb{E}_{\hat{\pi}_\lambda} \|\cdot\|^4 \right) \leq 0. \\ 2189 \\ 2190 \end{aligned}$$

2191  $\square$   
 2192

## 2194 G REVIEW AND DISCUSSION ON THE ERROR GUARANTEE (1)

### 2196 G.1 LITERATURE REVIEW OF EXISTING BOUNDS

2197 **Estimation of  $Z$ .** Traditionally, the statistical properties of an estimator are typically analyzed  
 2198 through its bias and variance. However, deriving closed-form expressions of the variance of  $\hat{Z}$  and  $\hat{F}$   
 2199 in JE remains challenging. Recall that the estimator  $\hat{Z} = Z_0 e^{-W(X)}$ ,  $X \sim \mathbb{P}^\rightarrow$  for  $Z = Z_0 e^{-\Delta F}$ ,  
 2200 and that JE implies  $\text{Bias } \hat{Z} = 0$ . For general (sub-optimally) controlled SDEs, Hartmann & Richter  
 2201 (2024) established both upper and lower bounds of the relative error of the importance sampling  
 2202 estimator, yet bounds tailored for JE are not well-studied. Inspired by this, we establish an upper  
 2203 bound on the *normalized variance*  $\text{Var } \frac{\hat{Z}}{Z}$  in Prop. 3 at the end of this section using techniques in  
 2204 Rényi divergence. However, we remark that connecting this upper bound to the properties of the  
 2205 curve (e.g., action) is non-trivial, which we leave for future work.  
 2206

2207 **Estimation of  $F$ .** Turning to the estimator  $\hat{F} = -\log \hat{Z}$  for  $F = -\log Z$ , we have  
 2208

$$\text{Bias } \hat{F} = \mathbb{E}_{\mathbb{P}^\rightarrow} W - \Delta F = \mathcal{W} - \Delta F = \mathcal{W}_{\text{diss}}.$$

2209 Bounding the average dissipated work  $\mathcal{W}_{\text{diss}} = \text{KL}(\mathbb{P}^\rightarrow \|\mathbb{P}^\leftarrow) = -\mathbb{E}_{\mathbb{P}^\rightarrow} \int_0^T (\partial_t \log \tilde{\pi}_t)(X_t) dt$  re-  
 2210 mains challenging as well, as the law of  $X_t$  under  $\mathbb{P}^\rightarrow$  is unknown, thus complicating the bounding of  
 2211 the expectation. To the best of our knowledge, Chen et al. (2020) established a lower bound in terms  
 2212 of the action function  $\mathcal{A}$ .

of  $W_2(\pi_0, \pi_1)$  via the Wasserstein gradient flow, but an upper bound remains elusive. Furthermore,  $\mathbb{E} \widehat{F}^2 = \mathbb{E}_{\mathbb{P}^{\rightarrow}(X)} (\log Z_0 - W(X))^2$  is similarly intractable to analyze.

For multiple estimators, i.e.,  $\widehat{F}_K := -\log \left( Z_0 \frac{1}{M} \sum_{k=1}^K e^{-W(X^{(k)})} \right)$  where  $X^{(1)}, \dots, X^{(K)} \stackrel{\text{i.i.d.}}{\sim} \mathbb{P}^{\rightarrow}$ , Zuckerman & Woolf (2002; 2004) (see also Lelièvre et al. (2010, Sec. 4.1.5)) derived approximate asymptotic bounds on Bias  $\widehat{F}_K$  and Var  $\widehat{F}_K$  via the delta method (or equivalently, the central limit theorem and Taylor expansions). Precise and non-asymptotic bounds remain elusive to date.

## G.2 EQUIVALENCE IN COMPLEXITIES FOR ESTIMATING $Z$ AND $F$

We prove the claim in Rmk. 1 that estimating  $Z$  with  $O(\varepsilon)$  relative error and estimating  $F$  with  $O(\varepsilon)$  absolute error share the same complexity up to absolute constants. This follows directly from Lem. 8: for any  $\varepsilon \in (0, \frac{1}{2})$ ,

$$(1) \implies \Pr(|\widehat{F} - F| \leq 2\varepsilon) \geq \frac{3}{4}, \quad \text{and} \quad (1) \iff \Pr(|\widehat{F} - F| \leq \frac{\varepsilon}{2}) \geq \frac{3}{4}.$$

## G.3 (1) IS WEAKER THAN BIAS AND VARIANCE

We demonstrate that (1) is a weaker criterion than controlling bias and variance, which is an immediate result from the Chebyshev inequality:

$$\Pr\left(\left|\frac{\widehat{Z}}{Z} - 1\right| \geq \varepsilon\right) \leq \frac{1}{\varepsilon^2} \mathbb{E}\left(\left(\frac{\widehat{Z}}{Z} - 1\right)^2\right) = \frac{\text{Bias}^2 \widehat{Z} + \text{Var} \widehat{Z}}{\varepsilon^2 Z^2},$$

$$\Pr(|\widehat{F} - F| \geq \varepsilon) \leq \frac{\mathbb{E}(\widehat{F} - F)^2}{\varepsilon^2} = \frac{\text{Bias}^2 \widehat{F} + \text{Var} \widehat{F}}{\varepsilon^2}.$$

On the other hand, suppose one has established a bound in the following form:

$$\Pr\left(\left|\frac{\widehat{Z}}{Z} - 1\right| \geq \varepsilon\right) \leq p(\varepsilon), \quad \text{for some } p : [0, \infty) \rightarrow [0, 1],$$

and assume that  $\widehat{Z}$  is unbiased. Then this implies

$$\text{Var} \frac{\widehat{Z}}{Z} = \mathbb{E}\left(\left(\frac{\widehat{Z}}{Z} - 1\right)^2\right) = \int_0^\infty \Pr\left(\left(\frac{\widehat{Z}}{Z} - 1\right)^2 \geq \varepsilon\right) d\varepsilon \leq \int_0^\infty p(\sqrt{\varepsilon}) d\varepsilon.$$

## G.4 AN UPPER BOUND ON THE NORMALIZED VARIANCE OF $\widehat{Z}$ IN JARZYNSKI EQUALITY

**Proposition 3.** *Under the setting of JE (Thm. 1), let  $(v_t)_{t \in [0, T]}$  be any vector field that generates  $(\tilde{\pi}_t)_{t \in [0, T]}$ , and define  $\mathbb{P}$  as the path measure of (17). Then,*

$$\text{Var} \frac{\widehat{Z}}{Z} \leq \left[ \mathbb{E}_{\mathbb{P}} \exp\left(14 \int_0^T \|v_t(X_t)\|^2 dt\right) \right]^{\frac{1}{2}} - 1.$$

*Proof.* The proof is inspired by Chewi et al. (2022). Note that

$$\text{Var} \frac{\widehat{Z}}{Z} = \mathbb{E}\left(\frac{\widehat{Z}}{Z}\right)^2 - 1 = \mathbb{E}_{\mathbb{P}^{\rightarrow}} \left( e^{-W(X) + \Delta F} \right)^2 - 1 = \mathbb{E}_{\mathbb{P}^{\rightarrow}} \left( \frac{d\mathbb{P}^{\leftarrow}}{d\mathbb{P}^{\rightarrow}} \right)^2 - 1,$$

which is the  $\chi^2$  divergence from  $\mathbb{P}^{\leftarrow}$  to  $\mathbb{P}^{\rightarrow}$ . Recall the  $q (> 1)$ -Rényi divergence defined as  $R_q(\mu \parallel \nu) = \frac{1}{q-1} \log \mathbb{E}_{\nu} \left( \frac{d\mu}{d\nu} \right)^q$ , and that  $\chi^2(\mathbb{P}^{\leftarrow} \parallel \mathbb{P}^{\rightarrow}) = e^{R_2(\mathbb{P}^{\leftarrow} \parallel \mathbb{P}^{\rightarrow})} - 1$ . By the weak triangle inequality of Rényi divergence (Chewi, 2022, Lem. 6.2.5):

$$R_2(\mathbb{P}^{\leftarrow} \parallel \mathbb{P}^{\rightarrow}) \leq \frac{3}{2} R_4(\mathbb{P}^{\leftarrow} \parallel \mathbb{P}) + R_3(\mathbb{P} \parallel \mathbb{P}^{\rightarrow}).$$

2268 We now bound  $\mathbb{E}_{\mathbb{P}} \left( \frac{d\mathbb{P}^{\rightarrow}}{d\mathbb{P}} \right)^q$  for any  $q \in \mathbb{R}$ . By Girsanov's theorem (Lem. 1),  
 2269

$$2270 \log \frac{d\mathbb{P}^{\rightarrow}}{d\mathbb{P}}(X) = \int_0^T \left( -\frac{1}{\sqrt{2}} \langle v_t(X_t), dB_t \rangle - \frac{1}{4} \|v_t(X_t)\|^2 dt \right), \text{ a.s. } X \sim \mathbb{P}.$$

2272 Therefore,

$$\begin{aligned} 2273 \mathbb{E}_{\mathbb{P}} \left( \frac{d\mathbb{P}^{\rightarrow}}{d\mathbb{P}} \right)^q &= \mathbb{E}_{\mathbb{P}} \exp \int_0^T \left( -\frac{q}{\sqrt{2}} \langle v_t(X_t), dB_t \rangle - \frac{q}{4} \|v_t(X_t)\|^2 dt \right) \\ 2274 &= \mathbb{E}_{\mathbb{P}} \exp \left[ \int_0^T \left( -\frac{q}{\sqrt{2}} \langle v_t(X_t), dB_t \rangle - \frac{q^2}{2} \|v_t(X_t)\|^2 dt \right) + \int_0^T \left( \frac{q^2}{2} - \frac{q}{4} \right) \|v_t(X_t)\|^2 dt \right] \\ 2275 &\leq \left( \mathbb{E}_{\mathbb{P}} \exp \left[ \int_0^T \left( -\sqrt{2}q \langle v_t(X_t), dB_t \rangle - q^2 \|v_t(X_t)\|^2 dt \right) \right] \right)^{\frac{1}{2}} \\ 2276 &\cdot \left( \mathbb{E}_{\mathbb{P}} \exp \left[ \left( q^2 - \frac{q}{2} \right) \int_0^T \|v_t(X_t)\|^2 dt \right] \right)^{\frac{1}{2}}, \end{aligned}$$

2277 where the last line is by the Cauchy-Schwarz inequality. Let  $M_t := -\sqrt{2}q \int_0^t \langle v_r(X_r), dB_r \rangle$ ,  $X \sim \mathbb{P}$   
 2278 be a continuous martingale with quadratic variation  $[M]_t = \int_0^t 2q^2 \|v_r(X_r)\|^2 dr$ . By Karatzas  
 2279 & Shreve (1991, Chap. 3.5.D), the process  $t \mapsto e^{M_t - \frac{1}{2}[M]_t}$  is a super martingale, and hence  
 2280  $\mathbb{E} e^{M_T - \frac{1}{2}[M]_T} \leq 1$ . Thus, we have  
 2281

$$2282 \mathbb{E}_{\mathbb{P}} \left( \frac{d\mathbb{P}^{\rightarrow}}{d\mathbb{P}} \right)^q \leq \left( \mathbb{E}_{\mathbb{P}} \exp \left[ \left( q^2 - \frac{q}{2} \right) \int_0^T \|v_t(X_t)\|^2 dt \right] \right)^{\frac{1}{2}}$$

2283 From Girsanov's theorem (Lem. 3), we can similarly obtain the following RN derivative:  
 2284

$$2285 \log \frac{d\mathbb{P}^{\leftarrow}}{d\mathbb{P}}(X) = \int_0^T \left( -\frac{1}{\sqrt{2}} \langle v_t(X_t), *dB_t^{\leftarrow} \rangle - \frac{1}{4} \|v_t(X_t)\|^2 dt \right), \text{ a.s. } X \sim \mathbb{P}.$$

2286 and use the same argument to show that  $\mathbb{E}_{\mathbb{P}} \left( \frac{d\mathbb{P}^{\leftarrow}}{d\mathbb{P}} \right)^q$  has exactly the same upper bound as  $\mathbb{E}_{\mathbb{P}} \left( \frac{d\mathbb{P}^{\rightarrow}}{d\mathbb{P}} \right)^q$ .  
 2287 In particular, we can use the same martingale argument, whereas now the *backward* continuous  
 2288 martingale is defined as  $M'_t := -\sqrt{2}q \int_t^T \langle v_r(X_r), *dB_r^{\leftarrow} \rangle$ ,  $X \sim \mathbb{P}$ , with quadratic variation  
 2289  $[M']_t = \int_t^T 2q^2 \|v_r(X_r)\|^2 dr$ . Therefore, we conclude that  
 2290

$$\begin{aligned} 2291 R_2(\mathbb{P}^{\leftarrow} \parallel \mathbb{P}^{\rightarrow}) &\leq \frac{1}{4} \log \mathbb{E}_{\mathbb{P}} \exp \left( 14 \int_0^T \|v_t(X_t)\|^2 dt \right) + \frac{1}{4} \log \mathbb{E}_{\mathbb{P}} \exp \left( 5 \int_0^T \|v_t(X_t)\|^2 dt \right) \\ 2292 &\leq \frac{1}{2} \log \mathbb{E}_{\mathbb{P}} \exp \left( 14 \int_0^T \|v_t(X_t)\|^2 dt \right). \end{aligned}$$

2293  $\square$   
 2294

## H RELATED WORKS

### H.1 THERMODYNAMIC INTEGRATION

2317 **(I) Review of TI.** We first briefly review the thermodynamic integration (TI) algorithm. Its essence  
 2318 is to write the free-energy difference as an integral of the derivative of free energy. Consider the  
 2319 general curve of probability measures  $(\pi_{\theta})_{\theta \in [0,1]}$  defined in (7). Then,  
 2320

$$2321 \frac{d}{d\theta} \log Z_{\theta} = -\frac{1}{Z_{\theta}} \int e^{-V_{\theta}(x)} \partial_{\theta} V_{\theta}(x) dx = -\mathbb{E}_{\pi_{\theta}} \partial_{\theta} V_{\theta} \implies \log \frac{Z}{Z_0} = -\int_0^1 \mathbb{E}_{\pi_{\theta}} \partial_{\theta} V_{\theta} d\theta. \quad (35)$$

2322 One may choose time points  $0 = \theta_0 < \dots < \theta_M = 1$  and approximate (35) by a Riemann sum:  
 2323

$$2324 \log \frac{Z}{Z_0} \approx - \sum_{\ell=0}^{M-1} (\theta_{\ell+1} - \theta_\ell) \mathbb{E}_{\pi_{\theta_\ell}} \partial_\theta|_{\theta=\theta_\ell} V_\theta, \quad (36)$$

2327 where the expectation under each  $\pi_{\theta_\ell}$  can be estimated by sampling from  $\pi_{\theta_\ell}$ . Nevertheless, there is  
 2328 a way of writing the exact equality instead of the approximation in (36): since  
 2329

$$2330 \log \frac{Z_{\theta_{\ell+1}}}{Z_{\theta_\ell}} = \log \int \frac{1}{Z_{\theta_\ell}} e^{-V_{\theta_\ell}(x)} e^{-(V_{\theta_{\ell+1}}(x) - V_{\theta_\ell}(x))} dx = \log \mathbb{E}_{\pi_{\theta_\ell}} e^{-(V_{\theta_{\ell+1}} - V_{\theta_\ell})},$$

2332 by summing over  $\ell = 0, \dots, M-1$ , we have  
 2333

$$2334 \log \frac{Z}{Z_0} = \sum_{\ell=0}^{M-1} \log \mathbb{E}_{\pi_{\theta_\ell}} e^{-(V_{\theta_{\ell+1}} - V_{\theta_\ell})}, \quad (37)$$

2337 which constitutes the estimation framework used in Brosse et al. (2018); Ge et al. (2020); Chehab  
 2338 et al. (2023); Kook & Vempala (2025). Hence, we also use TI to name this algorithm.  
 2339

2340 **(II) TI as a special case of AIS.** We follow the notations used in Thm. 3 to demonstrate the  
 2341 following claim: *TI (37) is a special case of AIS with every transition kernel  $F_\ell(x, \cdot)$  chosen as the*  
 2342 *perfect proposal  $\pi_{\theta_\ell}$ .*

2344 *Proof.* In AIS, with  $F_\ell(x, \cdot) = \pi_{\theta_\ell}$  in the forward path  $\mathbb{P}^\rightarrow$ , we have  $\mathbb{P}^\rightarrow(x_{0:M}) = \prod_{\ell=0}^M \pi_{\theta_\ell}(x_\ell)$ .  
 2345 In this special case,

$$2346 W(x_{0:M}) = \log \prod_{\ell=0}^{M-1} \frac{e^{-V_{\theta_\ell}(x_\ell)}}{e^{-V_{\theta_{\ell+1}}(x_\ell)}},$$

2349 and hence the AIS equality becomes the following identity, exactly the same as (35):  
 2350

$$2351 \frac{Z}{Z_0} = e^{-\Delta \mathcal{F}} = \mathbb{E}_{\mathbb{P}^\rightarrow} e^{-W} = \prod_{\ell=0}^{M-1} \mathbb{E}_{\pi_{\theta_\ell}} e^{-(V_{\theta_{\ell+1}} - V_{\theta_\ell})}. \quad (38)$$

2354  $\square$   
 2355

2356 **(III) The distinction between *equilibrium* and *non-equilibrium* methods.** In our AIS framework,  
 2358 the distinction lies in the choice of the transition kernels  $F_\ell(x, \cdot)$  within the AIS framework.

2359 In equilibrium methods, the transition kernels are ideally set to the perfect proposal  $\pi_{\theta_\ell}$ . However, in  
 2360 practice, exact sampling from  $\pi_{\theta_\ell}$  is generally infeasible. Instead, one can apply multiple MCMC  
 2361 iterations targeting  $\pi_{\theta_\ell}$ , leveraging the mixing properties of MCMC algorithms to gradually approach  
 2362 the desired distribution  $\pi_{\theta_\ell}$ . Nonetheless, unless using exact sampling methods such as rejection  
 2363 sampling – which is exponentially expensive in high dimensions – the resulting sample distribution  
 2364 inevitably remains biased with a finite number of MCMC iterations.

2365 In contrast, non-equilibrium methods employ transition kernels specifically designed to transport  $\pi_{\ell-1}$   
 2366 toward  $\pi_\ell$ , often following a curve of probability measures. This distinguishes them as inherently  
 2367 non-equilibrium. A key advantage of this approach over the equilibrium one is its ability to provide  
 2368 unbiased estimates, as demonstrated in JE and AIS.

2369 **(IV) Complexity bounds for TI.** For the TI algorithm in Alg. 1 used to estimate  $Z_0 = \int e^{-V - \beta \|\cdot\|^2} dx$ , the analysis Ge et al. (2020) indicates that it suffices to choose  $K = \tilde{\Theta}(\sqrt{d})$   
 2371 intermediate distributions and  $N = \tilde{\Theta}\left(\frac{\sqrt{d}}{\varepsilon^2}\right)$  particles with multilevel estimation, which leads to a  
 2372 total complexity of  $\tilde{O}\left(\frac{d^{\frac{4}{3}}}{\varepsilon^2}\right)$  to achieve the requirement in (23) (note that the condition number of  
 2373 the potential  $V + \beta \|\cdot\|^2$  is  $O(1)$ ).

2376 H.2 PATH INTEGRAL SAMPLER AND CONTROLLED MONTE CARLO DIFFUSION  
2377

2378 In this section, we briefly discuss two learning-based samplers used for normalizing constant estimation  
2379 and refer readers to the original papers for detailed derivations. The path integral sampler (PIS)  
2380 shares structural similarities with the RDS framework discussed in Thm. 5, using the time-reversal  
2381 of a universal noising process that transforms any distribution into a prior – such as the OU process  
2382 in RDS that converges to the standard normal or the Brownian bridge in PIS that converges to the  
2383 delta distribution at zero. In contrast, the controlled Monte Carlo diffusion (CMCD) extends the  
2384 JE framework from Sec. 3, focusing on learning the compensatory drift term along an arbitrary  
2385 interpolating curve  $(\pi_\theta)_{\theta \in [0,1]}$ , as long as the density of each intermediate distribution  $\pi_\theta$  is known  
2386 up to a constant.

2387 **Path integral sampler (PIS, Zhang & Chen (2022)).** The PIS learns the drift term of a reference  
2388 SDE that interpolates the delta distribution at 0 and the target distribution  $\pi$ , which is closely  
2389 connected with the Brownian bridge and the Föllmer drift (Chewi, 2022).

2390 Fix a time horizon  $T > 0$ . For any drift term  $(u_t)_{t \in [0,T]}$ , let  $\mathcal{Q}^u$  be the path measure of the following  
2391 SDE:

$$2392 \quad dX_t = u_t(X_t)dt + dB_t, \quad t \in [0, T]; \quad X_0 \stackrel{\text{a.s.}}{=} 0.$$

2393 In particular, when  $u \equiv 0$ , the marginal distribution of  $X_T$  under  $\mathcal{Q}^0$  is  $\mathcal{N}(0, TI) =: \phi_T$ . Define  
2394 another path measure  $\mathcal{Q}^*$  by

$$2395 \quad \mathcal{Q}^*(d\xi_{[0,T]}) := \mathcal{Q}^0(d\xi_{[0,T]}|\xi_T)\pi(d\xi_T) = \mathcal{Q}^0(d\xi_{[0,T]}) \frac{d\pi}{d\phi_T}(\xi_T), \quad \forall \xi \in C([0, T]; \mathbb{R}^d)$$

2396 and consider the problem

$$2397 \quad u^* = \operatorname{argmin}_u \text{KL}(\mathcal{Q}^u \parallel \mathcal{Q}^*) \implies \mathcal{Q}^{u^*} = \mathcal{Q}^*.$$

2398 One can calculate the KL divergence between these path measures via Girsanov's theorem (Lem. 1):

$$2400 \quad \log \frac{d\mathcal{Q}^u}{d\mathcal{Q}^*}(X) = W^u(X) + \log Z, \quad \text{a.s. } X \sim \mathcal{Q}^u, \text{ where}$$

$$2401 \quad W^u(X) = \int_0^T \langle u_t(X_t), dB_t \rangle + \frac{1}{2} \int_0^T \|u_t(X_t)\|^2 dt - \frac{\|X_T\|^2}{2T} + V(X_T) - \frac{d}{2} \log 2\pi T,$$

2402 which implies  $Z = \mathbb{E}_{\mathcal{Q}^u} e^{-W^u}$ , and  $\text{KL}(\mathcal{Q}^u \parallel \mathcal{Q}^*) = \mathbb{E}_{\mathcal{Q}^u} W^u + \log Z$ . On the other hand, directly  
2403 applying Lem. 1 gives

$$2404 \quad \text{KL}(\mathcal{Q}^u \parallel \mathcal{Q}^*) = \frac{1}{2} \int_0^T \mathbb{E}_{\mathcal{Q}^u} \|u_t(X_t) - u_t^*(X_t)\|^2 dt.$$

2405 In Zhang & Chen (2022, Theorem 3), the authors considered the effective sample size (ESS) defined  
2406 by  $\text{ESS}^{-1} = \mathbb{E}_{\mathcal{Q}^u} \left( \frac{d\mathcal{Q}^*}{d\mathcal{Q}^u} \right)^2$  as the convergence criterion, and stated that  $\text{ESS} \geq 1 - \varepsilon$  as long as  
2407  $\sup_{t \in [0,T]} \|u_t - u_t^*\|_{L^\infty}^2 \leq \frac{\varepsilon}{T}$ . However, this condition is generally hard to verify since the closed-  
2408 form expression of  $u^*$  is unknown, and the  $L^\infty$  bound might be too strong. Using the criterion ((1))  
2409 and the same methodology in proving the convergence of JE (Thm. 2), we can establish an improved  
2410 result on the convergence guarantee of this estimator, relating the relative error to the training loss of  
2411  $u$ , which is defined as

$$2412 \quad \min_u L(u) := \mathbb{E}_{\mathcal{Q}^u} \left[ \frac{1}{2} \int_0^T \|u_t(X_t)\|^2 dt - \frac{\|X_T\|^2}{2T} + V(X_T) \right] = \text{KL}(\mathcal{Q}^u \parallel \mathcal{Q}^*) - \log Z + \frac{d}{2} \log 2\pi T$$

2413 **Proposition 4.** Consider the estimator  $\hat{Z} := e^{-W^u(X)}$ ,  $X \sim \mathcal{Q}^u$  for  $Z$ . To achieve both  
2414  $\text{KL}(\mathcal{Q}_T^u \parallel \pi) \lesssim \varepsilon^2$  (with  $\mathcal{Q}_T^u$  representing the law of  $X_T$  in the sampled trajectory  $X \sim \mathcal{Q}^u$ ) and  
2415  $\Pr \left( \left| \frac{\hat{Z}}{Z} - 1 \right| \leq \varepsilon \right) \geq \frac{3}{4}$ , it suffices to choose  $u$  that satisfies

$$2416 \quad L(u) = -\log Z + \frac{d}{2} \log 2\pi T + O(\varepsilon^2).$$

2430 *Proof.*

2431

$$2432 \Pr \left( \left| \frac{\widehat{Z}}{Z} - 1 \right| \geq \varepsilon \right) = \mathcal{Q}^u \left( \left| \frac{d\mathcal{Q}^*}{d\mathcal{Q}^u} - 1 \right| \geq \varepsilon \right) \lesssim \frac{\text{TV}(\mathcal{Q}^u, \mathcal{Q}^*)}{\varepsilon} \lesssim \frac{\sqrt{\text{KL}(\mathcal{Q}^u \parallel \mathcal{Q}^*)}}{\varepsilon}.$$

2433

2434 Therefore, ensuring  $\text{KL}(\mathcal{Q}^u \parallel \mathcal{Q}^*) \lesssim \varepsilon^2$  up to some sufficiently small constant guarantees that the above probability remains bounded by  $\frac{1}{4}$ . Furthermore, by the data-processing inequality,  $\text{KL}(\mathcal{Q}_T^u \parallel \pi) \leq \text{KL}(\mathcal{Q}^u \parallel \mathcal{Q}^*) \lesssim \varepsilon^2$ .  $\square$

2435

2436 **Controlled Monte Carlo Diffusion (CMCD, Vargas et al. (2024)).** We borrow the notations from Sec. 3 due to its similarity with JE.

2437 Given  $(\tilde{\pi}_t)_{t \in [0, T]}$  and the ALD (2), we know from the proof of Thm. 1 that to make  $X_t \sim \tilde{\pi}_t$  for all  $t$ , the compensatory drift term  $(v_t)_{t \in [0, T]}$  must generate  $(\tilde{\pi}_t)_{t \in [0, T]}$ . Now, consider the task of learning such a vector field  $(u_t)_{t \in [0, T]}$  by matching the following forward and backward SDEs:

2438

$$\mathcal{P}^\rightarrow : dX_t = (\nabla \log \tilde{\pi}_t + u_t)(X_t)dt + \sqrt{2}dB_t, \quad X_0 \sim \tilde{\pi}_0,$$

2439

$$\mathcal{P}^\leftarrow : dX_t = (-\nabla \log \tilde{\pi}_t + u_t)(X_t)dt + \sqrt{2}dB_t^\leftarrow, \quad X_T \sim \tilde{\pi}_T,$$

2440

2441 where the loss is  $\text{KL}(\mathcal{P}^\rightarrow \parallel \mathcal{P}^\leftarrow)$ , discretized in training. Obviously, when trained to optimality, both  $\mathcal{P}^\rightarrow$  and  $\mathcal{P}^\leftarrow$  share the marginal distribution  $\tilde{\pi}_t$  at every time  $t$ . By Girsanov's theorem (Lem. 3), one can prove the following identity for a.s.  $X \sim \mathcal{P}^\rightarrow$ :  $\log \frac{d\mathcal{P}^\rightarrow}{d\mathcal{P}^\leftarrow}(X) = W(X) + C^u(X) - \Delta F$ , where  $\Delta F$  and  $W(X)$  are defined as in Thm. 1, and

2442

$$C^u(X) := - \int_0^T (\langle u_t(X_t), \nabla \log \tilde{\pi}_t(X_t) \rangle + \nabla \cdot u_t(X_t))dt.$$

2443

2444 We refer readers to Vargas et al. (2024, Prop. 3.3) for the detailed derivation. By  $\mathbb{E}_{\mathcal{P}^\rightarrow} \frac{d\mathcal{P}^\leftarrow}{d\mathcal{P}^\rightarrow} = 1$ , we know that  $\mathbb{E}_{\mathcal{P}^\rightarrow} e^{-W(X) - C^u(X)} = e^{-\Delta F}$ . As the paper has not established inference-time performance guarantee given the training loss, we prove the following result characterizing the relationship between the training loss and the accuracy of the sampled distribution as well as the estimated normalizing constant.

2445 **Proposition 5.** Let  $\widehat{Z} = Z_0 e^{-W(X) - C^u(X)}$ ,  $X \sim \mathcal{P}^\rightarrow$  be an unbiased estimator of  $Z = Z_0 e^{-\Delta F}$ . Then, to achieve both  $\text{KL}(\mathcal{P}_T^\rightarrow \parallel \pi) \lesssim \varepsilon^2$  (where  $\mathcal{P}_T^\rightarrow$  is the law of  $X_T$  in the sampled trajectory  $X \sim \mathcal{P}^\rightarrow$ ) and  $\Pr \left( \left| \frac{\widehat{Z}}{Z} - 1 \right| \leq \varepsilon \right) \geq \frac{3}{4}$ , it suffices to choose  $u$  that satisfies  $\text{KL}(\mathcal{P}^\rightarrow \parallel \mathcal{P}^\leftarrow) \lesssim \varepsilon^2$ .

2446

2447 *Proof.* The proof of this theorem follows the same reasoning as that of Prop. 4. For normalizing constant estimation,

2448

$$\Pr \left( \left| \frac{\widehat{Z}}{Z} - 1 \right| \geq \varepsilon \right) = \mathcal{P}^\rightarrow \left( \left| \frac{d\mathcal{P}^\leftarrow}{d\mathcal{P}^\rightarrow} - 1 \right| \geq \varepsilon \right) \lesssim \frac{\text{TV}(\mathcal{P}^\rightarrow, \mathcal{P}^\leftarrow)}{\varepsilon} \lesssim \frac{\sqrt{\text{KL}(\mathcal{P}^\rightarrow \parallel \mathcal{P}^\leftarrow)}}{\varepsilon} \lesssim 1.$$

2449

2450 For sampling, the result is an immediate corollary of the data-processing inequality.  $\square$

2451

## 2452 I DETAILS OF EXPERIMENTAL RESULTS

2453

### 2454 I.1 MODIFIED MÜLLER BROWN DISTRIBUTION

2455

2456 The Müller Brown potential energy surface is a canonical example of a potential surface used in molecular dynamics. Here, we consider a modified version of this distribution as defined in He et al. (2024, App. D.5). For  $x = (x_1, x_2) \in \mathbb{R}^2$ , the target distribution is  $\pi(x) = \frac{1}{Z} \exp(-0.1(V_q(x) + V_m(x)))$ , where

2457

$$2458 \quad V_q(x) = 35.0136(\bar{x}_1 + 0.033923)^2 + 59.8399(\bar{x}_2 - 0.465694)^2,$$

2459

$$2460 \quad V_m(x) = \sum_{i=1}^4 A_i \exp(a_i(\bar{x}_1 - X_i)^2 + b_i(\bar{x}_1 - X_i)(\bar{x}_2 - Y_i) + c_i(\bar{x}_2 - Y_i)^2).$$

2461

In the above equations,  $\bar{x}_1 = 0.2(x_1 - 3.5)$ ,  $\bar{x}_2 = 0.2(x_2 + 6.5)$ ,  $A = (-200, -100, -170, 15)$ ,  $a = (-1, -1, -6.5, 0.7)$ ,  $b = (0, 0, 11, 0.6)$ ,  $c = (-10, -10, -6.5, 0.7)$ ,  $X = (1, 0, -0.5, -1)$ ,  $Y = (0, 0.5, 1.5, 1)$ . The ground truth value of the normalizing constant computed by numerical integral (`scipy.integrate dblquad`) is  $Z = 22340.9983$  with estimated absolute error 0.0001.

We run each method with approximately the same oracle complexity. Aside from the quantitative results in Tab. 1, we also visualize the samples drawn from each method against the level curves of the potential in Fig. 2. It is clear from the table and figure that TI and AIS fail to provide accurate estimates of the normalizing constant or sample from the target distribution due to the deficiency of the exploration of different modes. All four RDS-based methods provide accurate estimates of the normalizing constant, with SNDMC and ZODMC being the two best methods.

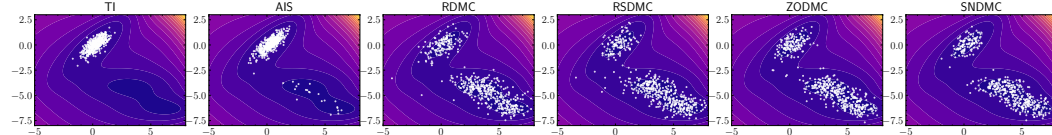


Figure 2: Visualization of the samples from the modified Müller Brown distribution. The generated samples are displayed on top of the level curves of the potential energy surface (darker color corresponds to lower potential energy, i.e., higher probability density).

## I.2 GAUSSIAN MIXTURE DISTRIBUTION

We now consider a Gaussian mixture distribution  $\pi$  in  $\mathbb{R}^2$  with 4 components, having weights 0.1, 0.2, 0.3, 0.4, means

$$\begin{pmatrix} 0 \\ 0 \end{pmatrix}, \begin{pmatrix} 0 \\ 11 \end{pmatrix}, \begin{pmatrix} 9 \\ 9 \end{pmatrix}, \begin{pmatrix} 11 \\ 0 \end{pmatrix},$$

and covariances

$$\begin{pmatrix} 1 & 0.5 \\ 0.5 & 1 \end{pmatrix}, \begin{pmatrix} 0.3 & -0.2 \\ -0.2 & 0.3 \end{pmatrix}, \begin{pmatrix} 1 & 0.3 \\ 0.3 & 1 \end{pmatrix}, \begin{pmatrix} 1.2 & -1 \\ -1 & 1.2 \end{pmatrix}.$$

As the p.d.f. is available in closed form, the ground truth value of the normalizing constant is  $Z = 1$ . Due to the separation of the modes and the imbalance of the weights, this distribution is more challenging to sample from. In the quantitative results shown in Tab. 1, we report the mean and standard deviation of  $\hat{Z}$  as well as two metrics for the quality of the samples: maximum mean discrepancy (MMD) and Wasserstein-2 distance ( $W_2$ ) between the generated samples  $\hat{\pi}_{\text{samp}}$  and ground truth samples from  $\pi$ . The visualization of the samples is shown in Fig. 3. Again, TI and AIS are confined to mode at zero where the initial samples are located, and fail to provide accurate estimates of the normalizing constant. All RDS-based methods provide accurate estimates of the normalizing constant and high quality samples.

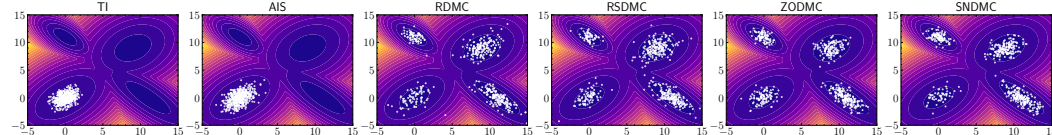


Figure 3: Visualization of the samples from the Gaussian mixture distribution. The generated samples are displayed on top of the level curves of the potential (darker color corresponds to lower potential, i.e., higher probability density).

## I.3 IMPLEMENTATION DETAILS

**General implementation details.** For both experiments, we run each method for 1024 rounds and output the mean and standard deviation of all 1024 estimates of  $\hat{Z}$ . In each round, we parallelly

2538 run 1024 i.i.d. trajectories, which produces 1024 i.i.d. samples from  $\pi$  and 1024 i.i.d. estimates  
 2539 of the normalizing constant, and we treat the average of the estimates as the final estimate of that  
 2540 round. We record the oracle complexity of each algorithm and tune the hyperparameters to make  
 2541 sure that the oracle complexity for producing *each sample* from  $\pi$  is between 50000 and 60000 for a  
 2542 fair comparison. For TI, we choose  $\lambda_0 = 100$ ,  $\lambda_{i+1} = \frac{1.45}{1+1/\sqrt{d}} \lambda_i$  until  $\lambda_i \leq \frac{1}{2\sqrt{d}}$ , and  $N = 32$  i.i.d.  
 2543 samples. For AIS, we choose  $\lambda_0 = 100$ ,  $M = 60000$  steps, and ALMC step size  $T_\ell = 0.01$ . For all  
 2544 RDS-based methods, we choose the total time duration  $T = 5$ , early stopping time  $\delta = 0.005$ , and  
 2545  $N = 50$  uniformly spaced time points  $t_n = \frac{n}{N}(T - \delta)$ . Specifically, for RDMC, we use 64 samples  
 2546 from  $\bar{\pi}_{0|t}(\cdot|x)$  to estimate the score  $\nabla \log \bar{\pi}_t(x)$ , and run LMC for 16 steps with step size 0.01,  
 2547 initialized by importance sampling from  $\bar{\pi}_{0|t}(\cdot|x) \propto e^{-V(\cdot)} \mathcal{N}(\cdot|e^t x, (e^{2t} - 1)I)$  with proposal  
 2548  $\mathcal{N}(e^t x, (e^{2t} - 1)I)$ ; for RSDMC, we choose the number of recursive steps as 2, use 16 samples  
 2549 from  $\bar{\pi}_{0|t}(\cdot|x)$  to estimate the score  $\nabla \log \bar{\pi}_t(x)$ , and run LMC for 10 steps with step size 0.01 using  
 2550 the same initialization based on importance sampling; finally, for both ZODMC and SNDMC, we use  
 2551 1024 samples from  $\bar{\pi}_{0|t}(\cdot|x)$  to estimate the score  $\nabla \log \bar{\pi}_t(x)$ .  
 2552

2553 **Evaluation metrics for sampling.** In the experiment of Gaussian mixture distribution, in each  
 2554 round, we draw 1024 samples from both the algorithm and the target distribution, and compute the  
 2555 following two metrics to evaluate the quality of the samples. For two sets of samples  $\mathcal{X} = \{x_i\}_{i=1}^n$   
 2556 and  $\mathcal{Y} = \{y_j\}_{j=1}^m$ , the MMD is defined as

$$2557 \text{MMD}(\mathcal{X}, \mathcal{Y}) := \sqrt{\frac{1}{n^2} \sum_{1 \leq i, i' \leq n} k(x_i, x_{i'}) - \frac{2}{nm} \sum_{1 \leq i \leq m, 1 \leq j \leq n} k(x_i, y_j) + \frac{1}{m^2} \sum_{1 \leq j, j' \leq m} k(y_j, y_{j'})},$$

2558 where  $k(x, y) = \frac{1}{K} \sum_{i=1}^K \exp\left(-\frac{\|x-y\|^2}{2\sigma_i^2}\right)$  is a multiscale radial basis function (RBF) kernel. Fol-  
 2559 lowing the implementation in He et al. (2024), we set  $K = 10$  and  $\{\sigma_i\}_{i=1}^{10} = \{-4, -2, 0, \dots, 12, 14\}$ .  
 2560 Second, the  $W_2$  distance is computed by `ot.emd2(a, b, M) ** 0.5` using the Python  
 2561 Optimal Transport (POT) package (Flamary et al., 2021), where  $\mathbf{a} = \frac{1}{n} \mathbf{1}_n$ ,  $\mathbf{b} = \frac{1}{m} \mathbf{1}_m$ , and  
 2562  $\mathbf{M} = (\|x_i - y_j\|^2)_{1 \leq i \leq n, 1 \leq j \leq m}$ .  $\mathbf{1}_n$  represents the vector of all ones with length  $n$ .  
 2563

2564  
 2565  
 2566  
 2567  
 2568  
 2569  
 2570  
 2571  
 2572  
 2573  
 2574  
 2575  
 2576  
 2577  
 2578  
 2579  
 2580  
 2581  
 2582  
 2583  
 2584  
 2585  
 2586  
 2587  
 2588  
 2589  
 2590  
 2591